Search for additional heavy neutral Higgs and gauge bosons in the ditau final state produced in $36\,\mathrm{fb}^{-1}$ of pp collisions at $\sqrt{s} = 13\,\mathrm{TeV}$ with the ATLAS detector

The ATLAS collaboration

E-mail: atlas.publications@cern.ch

ABSTRACT: A search for heavy neutral Higgs bosons and Z' bosons is performed using a data sample corresponding to an integrated luminosity of $36.1\,\mathrm{fb}^{-1}$ from proton-proton collisions at $\sqrt{s} = 13\,\mathrm{TeV}$ recorded by the ATLAS detector at the LHC during 2015 and 2016. The heavy resonance is assumed to decay to $\tau^+\tau^-$ with at least one tau lepton decaying to final states with hadrons and a neutrino. The search is performed in the mass range of 0.2–2.25 TeV for Higgs bosons and 0.2–4.0 TeV for Z' bosons. The data are in good agreement with the background predicted by the Standard Model. The results are interpreted in benchmark scenarios. In the context of the hMSSM scenario, the data exclude $\tan\beta > 1.0$ for $m_A = 0.25\,\mathrm{TeV}$ and $\tan\beta > 42$ for $m_A = 1.5\,\mathrm{TeV}$ at the 95% confidence level. For the Sequential Standard Model, Z'_{SSM} with $m_{Z'} < 2.42\,\mathrm{TeV}$ is excluded at 95% confidence level, while Z'_{NU} with $m_{Z'} < 2.25\,\mathrm{TeV}$ is excluded for the non-universal $G(221)$ model that exhibits enhanced couplings to third-generation fermions.

https://doi.org/10.1007/JHEP01(2018)055

Contents

1 Introduction

The discovery of a scalar particle [1, 2] at the Large Hadron Collider (LHC) [3] has provided important insight into the mechanism of electroweak symmetry breaking. Experimental studies of the new particle [4–8] demonstrate consistency with the Standard Model (SM) Higgs boson [9–14]. However, it remains possible that the discovered particle is part of an extended scalar sector, a scenario that is predicted by a number of theoretical arguments [15, 16].

The Minimal Supersymmetric Standard Model (MSSM) [15, 17, 18] is the simplest extension of the SM that includes supersymmetry. The MSSM requires two Higgs doublets of opposite hypercharge. Assuming that CP symmetry is conserved, this results in one CP-odd (A) and two CP-even (h, H) neutral Higgs bosons and two charged Higgs bosons ($H^{\pm}$). At tree level, the properties of the Higgs sector in the MSSM depend on only two non-SM parameters, which can be chosen to be the mass of the CP-odd Higgs boson, m_A, and the ratio of the vacuum expectation values of the two Higgs doublets, $\tan\beta$. Beyond tree level, a number of additional parameters affect the Higgs sector, the choice of which defines various MSSM benchmark scenarios. In the $m_h^{\mathrm{mod+}}$ scenario [19], the top-squark mixing parameter is chosen such that the mass of the lightest CP-even Higgs boson, m_h, is close to the measured mass of the Higgs boson that was discovered at the LHC. A different approach is employed in the hMSSM scenario [20, 21] in which the measured value of m_h can be used, with certain assumptions, to predict the remaining masses and couplings of the MSSM Higgs bosons without explicit reference to the soft supersymmetry-breaking parameters. The couplings of the MSSM heavy Higgs bosons to down-type fermions are enhanced with respect to the SM Higgs boson for large $\tan\beta$ values, resulting in increased branching fractions to τ-leptons and b-quarks, as well as a higher cross section for Higgs boson production in association with b-quarks. This has motivated a variety of searches for a scalar boson (generically called ϕ) in $\tau\tau$ and bb final states[1] at LEP [22], the Tevatron [23–25] and the LHC [26–29].

Heavy Z' gauge bosons appear in many extensions of the SM [30–34] and while they are typically considered to obey lepton universality, this is not necessarily a requirement. In particular, models in which the Z' boson couples preferentially to third-generation fermions may be linked to the high mass of the top quark [35–38] or to recent indications of lepton flavour universality violation in semi-tauonic B meson decays [39]. One such model is the non-universal $G(221)$ model [36–38], which contains a Z'_{NU} boson that can exhibit enhanced couplings to tau leptons. In this model the SM SU(2) gauge group is split into two parts: one coupling to fermions of the first two generations and one coupling to third generation fermions. The mixing between these groups is described by the parameter $\sin^2\phi$, with $\sin^2\phi < 0.5$ corresponding to enhanced third generation couplings. A frequently used benchmark model is the Sequential Standard Model (SSM), which contains a Z'_{SSM} boson with couplings identical to the SM Z boson. By evaluating the impact on the signal sensitivity from changing the Z'_{SSM} couplings, limits on Z'_{SSM} can be reinterpreted for a broad range of models. Indirect limits on Z' bosons with non-universal flavour couplings have been derived from measurements at LEP [40]. The most sensitive direct searches for

---

[1]The notation $\tau\tau$ and bb is used as shorthand for $\tau^+\tau^-$ and $b\bar{b}$ throughout this paper.
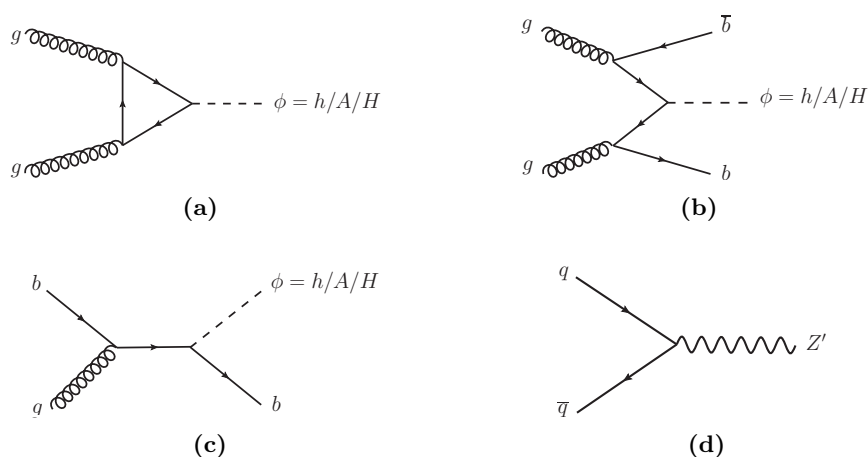
Figure 1. Lowest-order Feynman diagrams for (a) gluon-gluon fusion and b-associated production of a neutral MSSM Higgs boson in the (b) four-flavour and (c) five-flavour schemes and (d) Drell-Yan production of a Z' boson.

high-mass resonances decaying to ditau final states have been performed by the ATLAS and CMS collaborations using data collected at $\sqrt{s} = 8$ and $13\,\text{TeV}$ [29, 41, 42].

This paper presents the results of a search for neutral MSSM Higgs bosons as well as high-mass Z' resonances in the ditau decay mode using $36.1\,\text{fb}^{-1}$ of proton-proton collision data at a centre-of-mass energy of $13\,\text{TeV}$ collected with the ATLAS detector [43] in 2015 and 2016. The search is performed in the $\tau_{\text{lep}}\tau_{\text{had}}$ and $\tau_{\text{had}}\tau_{\text{had}}$ decay modes, where τ_{lep} represents the decay of a τ-lepton to an electron or a muon and neutrinos, whereas τ_{had} represents the decay to one or more hadrons and a neutrino. The search considers narrow resonances[2] with masses of 0.2–$2.25\,\text{TeV}$ and $\tan\beta$ of 1–58 for the MSSM Higgs bosons. For the Z' boson search, a mass range of 0.2–$4\,\text{TeV}$ is considered. Higgs boson production through gluon-gluon fusion and in association with b-quarks is considered (figures 1(a)–1(c)), with the latter mode dominating for high $\tan\beta$ values. Hence, both the $\tau_{\text{lep}}\tau_{\text{had}}$ and $\tau_{\text{had}}\tau_{\text{had}}$ channels are split into b-tag and b-veto categories, based on the presence or absence of jets tagged as originating from b-quarks in the final state. Since a Z' boson is expected to be predominantly produced via a Drell-Yan process (figure 1(d)), there is little gain in splitting the data into b-tag and b-veto categories. Hence, the Z' analysis uses an inclusive selection instead.

The paper is structured as follows. Section 2 provides an overview of the ATLAS detector. The event samples used in the analysis, recorded by the ATLAS detector or simulated using the ATLAS simulation framework, are reported in section 3. The event reconstruction is presented in section 4. A description of the event selection criteria is given in section 5. Section 6 explains the estimation of background contributions, followed by a description of systematic uncertainties in section 7. Results are presented in section 8, followed by concluding remarks in section 9.

---

[2]A resonance is considered "narrow" if the lineshape has no impact on experimental observables.

2 ATLAS detector

The ATLAS detector [43] at the LHC covers nearly the entire solid angle around the collision point.[3] It consists of an inner tracking detector surrounded by a thin superconducting solenoid, electromagnetic and hadronic calorimeters, and a muon spectrometer incorporating three large superconducting toroid magnets. The inner-detector system is immersed in a $2\,\mathrm{T}$ axial magnetic field and provides charged-particle tracking in the range $|\eta| < 2.5$.

The high-granularity silicon pixel detector covers the vertex region and typically provides four measurements per track. The innermost layer, known as the insertable B-Layer [44], was added in 2014 and provides high-resolution hits at small radius to improve the tracking performance. The pixel detector is surrounded by the silicon microstrip tracker, which usually provides four two-dimensional measurement points per track. These silicon detectors are complemented by the transition radiation tracker, which enables radially extended track reconstruction up to $|\eta| = 2.0$. The transition radiation tracker also provides electron identification information based on the fraction of hits (typically 30 in total) above a higher energy-deposit threshold corresponding to transition radiation.

The calorimeter system covers the pseudorapidity range $|\eta| < 4.9$. Within the region $|\eta| < 3.2$, electromagnetic calorimetry is provided by barrel and endcap high-granularity lead/liquid-argon (LAr) electromagnetic calorimeters, with an additional thin LAr presampler covering $|\eta| < 1.8$, to correct for energy loss in material upstream of the calorimeters. Hadronic calorimetry is provided by the steel/scintillator-tile calorimeter, segmented into three barrel structures within $|\eta| < 1.7$, and two copper/LAr hadronic endcap calorimeters that cover $1.5 < |\eta| < 3.2$. The solid angle coverage is completed with forward copper/LAr and tungsten/LAr calorimeter modules, optimised for electromagnetic and hadronic measurements respectively, in the region $3.1 < |\eta| < 4.9$.

The muon spectrometer comprises separate trigger and high-precision tracking chambers measuring the deflection of muons in a magnetic field generated by superconducting air-core toroids. The precision chamber system covers the region $|\eta| < 2.7$ with three layers of monitored drift tubes, complemented by cathode strip chambers in the forward region, where the background is highest. The muon trigger system covers the range $|\eta| < 2.4$ with resistive plate chambers in the barrel, and thin gap chambers in the endcap regions.

A two-level trigger system is used to select interesting events [45, 46]. The level-one trigger is implemented in hardware and uses a subset of detector information to reduce the event rate to a design value of at most $100\,\mathrm{kHz}$. This is followed by the software-based high-level trigger, which reduces the event rate to $1\,\mathrm{kHz}$.

---

[3]ATLAS uses a right-handed coordinate system with its origin at the nominal interaction point in the centre of the detector and the z-axis along the beam pipe. The x-axis points from the interaction point to the centre of the LHC ring, and the y-axis points upwards. Cylindrical coordinates (r, ϕ) are used in the transverse plane, ϕ being the azimuthal angle around the z-axis. The pseudorapidity is defined in terms of the polar angle θ as $\eta = -\ln\tan(\theta/2)$. Angular distance is measured in units of $\Delta R \equiv \sqrt{(\Delta\eta)^2 + (\Delta\phi)^2}$.

3 Data and simulated event samples

The results in this paper use proton-proton collision data at a centre-of-mass energy of $\sqrt{s} = 13\,\mathrm{TeV}$ collected by the ATLAS detector at the LHC during 2015 and 2016. The data correspond to a total integrated luminosity of $36.1\,\mathrm{fb}^{-1}$ after requiring that all relevant components of the ATLAS detector are in good working condition. Selected events must satisfy criteria designed to reduce backgrounds from cosmic rays, beam-induced events and calorimeter noise [47]. They must also contain at least one primary vertex with at least two associated tracks. The primary vertex is chosen as the proton-proton vertex candidate with the highest sum of the squared transverse momenta of the associated tracks.

Simulated events are used to estimate the signal efficiencies and some of the background contributions. The simulated event samples are normalised using their theoretical cross sections and the integrated luminosity. Simulated events with a heavy neutral MSSM Higgs boson produced via gluon-gluon fusion and in association with b-quarks were generated at next-to-leading order (NLO) with Powheg-Box v2 [48–50] and MG5_aMC@NLO 2.1.2 [51, 52] (using the four-flavour scheme), respectively. The CT10 [53] set of parton distribution functions (PDFs) was used in the generation of gluon-gluon fusion events while CT10nlo_nf4 [54] was used to produce the b-associated signal samples. Pythia 8.210 [55] with the AZNLO [56] (A14 [57]) set of tuned parameters (tune) was used together with the CTEQ6L1 [58] (NNPDF2.3LO [59]) PDF set for the parton shower calculation at leading order (LO), underlying event and hadronisation in the gluon-gluon fusion (b-associated) production. The gluon-gluon fusion sample was generated assuming SM couplings and underestimates the loop contribution from b-quarks at high $\tan\beta$, which can impact the Higgs boson p_{T} spectrum. Generator-level studies indicate this has a negligible impact on the final mass distribution and only a few percent impact on the signal acceptance, except for mass hypotheses below $400\,\mathrm{GeV}$ where the impact can be up to 10%, so the effect is neglected.

The production cross sections and branching fractions for the various MSSM scenarios are taken from ref. [60]. The cross sections for gluon-gluon fusion production are calculated using SuSHi [61], including NLO supersymmetric-QCD corrections [62–67], next-to-next-to-leading-order (NNLO) QCD corrections for the top quark [68–72], as well as light-quark electroweak effects [73, 74]. The b-associated production cross sections in the five-flavour scheme are also calculated using SuSHi based on bbh@nnlo [75], and those for b-associated production in the four-flavour scheme (where b-quarks are not considered as partons) are calculated according to refs. [76, 77]. The final b-associated production cross section is obtained by using the method described in ref. [78] to match the four-flavour and five-flavour scheme cross sections. The masses and mixing (and effective Yukawa couplings) of the Higgs bosons are computed with FeynHiggs [79–84] for all scenarios, with the exception of the hMSSM. In the case of the hMSSM scenario, Higgs masses and branching fractions are computed using HDecay [85, 86]. Branching fractions for all other scenarios use a combination of results calculated by HDecay, FeynHiggs and PROPHECY4f [87, 88].

The Z' signal events are modelled with a LO Z/γ^* sample that is reweighted with the TauSpinner algorithm [89–91], which correctly accounts for spin effects in the τ-lepton

decays. The Z/γ^* sample, enriched in events with high invariant mass, was generated with PYTHIA 8.165 [92, 93] using the NNPDF2.3LO PDF set and the A14 tune for the parton-shower and underlying-event parameters. Interference between the Z' and the SM Z/γ^* production is not included, as it is highly model dependent. Higher-order QCD corrections are applied to the simulated event samples. These corrections to the event yields are made with a mass-dependent rescaling to NNLO in the QCD coupling constant, as calculated with VRAP 0.9 [94] and the CT14NNLO PDF set. Electroweak corrections are not applied to the Z' signal samples due to the large model dependence.

The multijet background in both channels is estimated using data, while non-multijet backgrounds in which a quark- or gluon-initiated jet is misidentified as a hadronic tau decay (predominantly $W+$jets and $t\bar{t}$) are modelled using data in the $\tau_{\text{lep}}\tau_{\text{had}}$ channel and simulation with data-driven corrections in the $\tau_{\text{had}}\tau_{\text{had}}$ channel, as described in section 6. The remaining background contributions arise from Z/γ^*+jets, $W+$jets, $t\bar{t}$, single top-quark and diboson (WW, WZ and ZZ) production. These contributions are estimated using the simulated event samples described below.

Events containing Z/γ^*+jets were generated with POWHEG-BOX v2 [95] interfaced to the PYTHIA 8.186 parton shower model. The CT10 PDF set was used in the matrix element. The AZNLO tune was used, with PDF set CTEQ6L1, for the modelling of non-perturbative effects. Photon emission from electroweak vertices and charged leptons was performed with PHOTOS++ 3.52 [96]. The same setup was used to simulate $W+$jets events for background subtraction in the control regions of the $\tau_{\text{lep}}\tau_{\text{had}}$ channel. The Z/γ^*+jets samples were simulated in slices with different masses of the off-shell boson. The event yields are corrected with a mass-dependent rescaling at NNLO in the QCD coupling constant, computed with VRAP 0.9 and the CT14NNLO PDF set. Mass-dependent electroweak corrections are computed at NLO with MCSANC 1.20 [97], and these include photon-induced contributions ($\gamma\gamma \to \ell\ell$ via t- and u-channel processes) computed with the MRST2004QED PDF set [98].

The modelling of the $W+$jets process in the case of the $\tau_{\text{had}}\tau_{\text{had}}$ channel was done with the SHERPA 2.2.0 [99] event generator. Matrix elements were calculated for up to two partons at NLO and four partons at LO using COMIX [100] and OPENLOOPS [101] merged with the SHERPA parton shower [102] using the ME+PS@NLO prescription [103]. The CT10nlo PDF set was used in conjunction with dedicated parton shower tuning developed by the SHERPA authors. The $W+$jets production is normalised to the NNLO cross sections with FEWZ [94, 104, 105].

For the generation of $t\bar{t}$ or a single top quark in the Wt-channel and s-channel, the POWHEG-BOX v2 event generator was used with the CT10 PDF set in the matrix element calculation. Electroweak t-channel single-top-quark events were generated with the POWHEG-BOX v1 event generator. This event generator uses the four-flavour scheme for the NLO matrix elements calculations together with the fixed four-flavour PDF set CT10f4. For all top processes, top-quark spin correlations were preserved (for t-channel, top quarks were decayed with MADSPIN [106]). The parton shower, hadronisation, and the underlying event were simulated using PYTHIA 6.428 with the CTEQ6L1 PDF sets and the corresponding Perugia 2012 tune [107]. The top mass was set to $172.5\,\text{GeV}$. The $t\bar{t}$ production sample is normalised to the predicted production cross section as calculated with

the Top++2.0 program to NNLO in perturbative QCD, including soft-gluon resummation to next-to-next-to-leading-log (NNLL) order (ref. [108] and references therein). For the single-top-quark event samples, an approximate calculation at NLO in QCD for the s-channel and t-channel [109, 110] and an NLO+NNLL calculation for the Wt-channel [111] are used for the normalisation.

Diboson processes were modelled using the Sherpa 2.1.1 event generator and they were calculated for up to one (ZZ) or no (WW, WZ) additional partons at NLO and up to three additional partons at LO using Comix and OpenLoops merged with the Sherpa parton shower using the ME+PS@NLO prescription. The CT10 PDF set was used in conjunction with dedicated parton shower tuning developed by the Sherpa authors. The event generator cross sections are used in this case (already at NLO). In addition, the Sherpa diboson sample cross section was scaled down to account for its use of $\alpha_{\text{QED}} = 1/129$ rather than $1/132$ corresponding to the use of current PDG parameters as input to the G_μ scheme.

Properties of the bottom and charm hadron decays were set with the EvtGen v1.2.0 program [112] in samples that were not produced with Sherpa. Simulated minimum-bias events were overlaid on all simulated samples to include the effect of multiple proton-proton interactions in the same and neighbouring bunch crossings ("pile-up"). These minimum-bias events were generated with Pythia 8.186, using the A2 tune [113] and the MSTW2008LO PDF [114]. Each sample was simulated using the full Geant 4 [115, 116] simulation of the ATLAS detector, with the exception of the b-associated MSSM Higgs boson signal, for which the AtlfastII [117] fast simulation framework was used. Finally, the simulated events are processed through the same reconstruction software as the data.

4 Event reconstruction

Electron candidates are reconstructed from energy deposits in the electromagnetic calorimeter associated with a charged-particle track measured in the inner detector [118–120]. The electron candidates are required to pass a "loose" likelihood-based identification selection, to have a transverse momentum $p_{\text{T}} > 15\,\text{GeV}$ and to be in the fiducial volume of the inner detector, $|\eta| < 2.47$. The transition region between the barrel and endcap calorimeters ($1.37 < |\eta| < 1.52$) is excluded.

Muon candidates are reconstructed in the range $|\eta| < 2.5$ by matching tracks found in the muon spectrometer to tracks found in the inner detector [121]. The tracks of the muon candidates are re-fitted using the complete track information from both detector systems. They are required to have a transverse momentum $p_{\text{T}} > 7\,\text{GeV}$ and to pass a "loose" muon identification requirement.

The selected lepton (electron or muon) in the $\tau_{\text{lep}}\tau_{\text{had}}$ channel must then have $p_{\text{T}} > 30\,\text{GeV}$ and pass a "medium" identification requirement. This lepton is considered isolated if it meets p_{T}- and η-dependent isolation criteria utilising calorimetric and tracking information. The criteria correspond to an efficiency of 90% (99%) for a transverse momentum of $p_{\text{T}} = 25$ (60)$\,\text{GeV}$. The efficiency increases with lepton p_{T} as the requirements are relaxed to account for the decreased background from misidentified jets.

Jets are reconstructed from topological clusters of energy depositions [122] in the calorimeter using the anti-k_t algorithm [123, 124], with a radius parameter value $R = 0.4$. The average energy contribution from pile-up is subtracted according to the jet area and the jets are calibrated as described in ref. [125]. They are required to have $p_T > 20\,\text{GeV}$ and $|\eta| < 2.5$. To reduce the effect of pile-up, a jet vertex tagger algorithm is used for jets with $p_T < 60\,\text{GeV}$ and $|\eta| < 2.4$. It employs a multivariate technique based on jet energy, vertexing and tracking variables to determine the likelihood that the jet originates from or is heavily contaminated by pile-up [126]. In order to identify jets containing b-hadrons (b-jets), a multivariate algorithm is used, which is based on the presence of tracks with a large impact parameter with respect to the primary vertex, the presence of displaced secondary vertices and the reconstructed flight paths of b- and c-hadrons associated with the jet [127, 128]. The algorithm has an average efficiency of 70% for b-jets and rejections of approximately 13, 56 and 380 for c-jets, hadronic tau decays and jets initiated by light quarks or gluons, respectively, as determined in simulated $t\bar{t}$ events.

Hadronic tau decays are composed of a neutrino and a set of visible decay products ($\tau_{\text{had-vis}}$), typically one or three charged pions and up to two neutral pions. The reconstruction of the visible decay products is seeded by jets [129]. The $\tau_{\text{had-vis}}$ candidates must have $p_T > 25$ (45) GeV in the $\tau_{\text{lep}}\tau_{\text{had}}$ ($\tau_{\text{had}}\tau_{\text{had}}$) channel, $|\eta| < 2.5$ excluding $1.37 < |\eta| < 1.52$, one or three associated tracks and an electric charge of ± 1. The leading-p_T $\tau_{\text{had-vis}}$ candidate in the $\tau_{\text{lep}}\tau_{\text{had}}$ channel and the two leading-p_T $\tau_{\text{had-vis}}$ candidates in the $\tau_{\text{had}}\tau_{\text{had}}$ channel are then selected and all remaining candidates are considered as jets. A Boosted Decision Tree (BDT) identification procedure, based on calorimetric shower shapes and tracking information is used to reject backgrounds from jets [130, 131]. Two $\tau_{\text{had-vis}}$ identification criteria are used: "loose" and "medium", specified in section 5. The criteria correspond to efficiencies of about 60% (50%) and 55% (40%) in $Z/\gamma^* \to \tau\tau$ events and rejections of about 30 (30) and 50 (100) in multijet events, for one-track (three-track) $\tau_{\text{had-vis}}$ candidates, respectively. An additional dedicated likelihood-based veto is used to reduce the number of electrons misidentified as $\tau_{\text{had-vis}}$ in the $\tau_{\text{lep}}\tau_{\text{had}}$ channel, providing 95% efficiency and a background rejection between 20 and 200, depending on the pseudorapidity of the $\tau_{\text{had-vis}}$ candidate.

Geometrically overlapping objects are removed in the following order: (a) jets within $\Delta R = 0.2$ of selected $\tau_{\text{had-vis}}$ candidates are excluded, (b) jets within $\Delta R = 0.4$ of an electron or muon are excluded, (c) any $\tau_{\text{had-vis}}$ candidate within $\Delta R = 0.2$ of an electron or muon is excluded, (d) electrons within $\Delta R = 0.2$ of a muon are excluded.

The missing transverse momentum, $\mathbf{E}_T^{\text{miss}}$, is calculated as the negative vectorial sum of the $\mathbf{p}_T$ of all fully reconstructed and calibrated physics objects [132, 133]. This procedure includes a "soft term", which is calculated using the inner-detector tracks that originate from the hard-scattering vertex but are not associated with reconstructed objects.

5 Event selection

5.1 $\tau_{\text{had}}\tau_{\text{had}}$ channel

Events in the $\tau_{\text{had}}\tau_{\text{had}}$ channel are recorded using single-tau triggers with p_T thresholds of 80, 125 or 160 GeV, depending on the data-taking period. Events must contain at least two

$\tau_\text{had-vis}$ candidates with $p_\text{T} > 65\,\text{GeV}$ and no electrons or muons. The leading-p_T $\tau_\text{had-vis}$ candidate must be geometrically matched to the trigger signature and must exceed the trigger p_T threshold by $5\,\text{GeV}$. The leading and sub-leading $\tau_\text{had-vis}$ candidates must satisfy the "medium" and "loose" identification criteria, respectively. They must also have opposite electric charge and be back to back in the transverse plane: $|\Delta\phi(\mathbf{p}_\text{T}^{\tau_1}, \mathbf{p}_\text{T}^{\tau_2})| > 2.7\,\text{rad}$, as tau leptons from the decay of heavy neutral resonances are typically produced back to back in the transverse plane. The signal acceptance times efficiency for this selection (calculated with respect to all possible ditau final states) varies between 1% and 7% for signals with masses of $0.35\,\text{TeV}$ or higher. The maximum occurs for signals with masses of around $0.9\,\text{TeV}$, degradations occur at lower masses due to the $\tau_\text{had-vis}$ p_T thresholds and at higher masses due to the $\tau_\text{had-vis}$ reconstruction and identification efficiencies. A summary of the selection is given in table 1 of section 6.

5.2 $\tau_\text{lep}\tau_\text{had}$ channel

Events in the $\tau_\text{lep}\tau_\text{had}$ channel are recorded using single-electron and single-muon triggers with p_T thresholds ranging from 20 to $140\,\text{GeV}$ and various isolation criteria. The events must contain at least one $\tau_\text{had-vis}$ candidate passing the medium identification, exactly one isolated lepton (from here on referred to as ℓ) that is geometrically matched to the trigger signature (implying $|\eta| < 2.4$ in the $\tau_\mu\tau_\text{had}$ channel), and no additional reconstructed leptons. The identified $\tau_\text{had-vis}$ candidate must have $|\eta| < 2.3$ to reduce background from misidentified electrons. The isolated lepton and identified $\tau_\text{had-vis}$ candidate must have opposite electric charge and be back to back in the transverse plane: $|\Delta\phi(\mathbf{p}_\text{T}^{\ell}, \mathbf{p}_\text{T}^{\tau_\text{had-vis}})| > 2.4\,\text{rad}$. To reduce background from $W+$jets production, the transverse mass of the isolated lepton and the missing transverse momentum,

$$m_\text{T}(\mathbf{p}_\text{T}^{\ell}, \mathbf{E}_\text{T}^\text{miss}) \equiv \sqrt{2p_\text{T}^{\ell} E_\text{T}^\text{miss} \left[1 - \cos\Delta\phi(\mathbf{p}_\text{T}^{\ell}, \mathbf{E}_\text{T}^\text{miss})\right]}\,,$$

must be less than $40\,\text{GeV}$. To reduce background from $Z \to ee$ production in the $\tau_e\tau_\text{had}$ channel, events where the isolated lepton and identified $\tau_\text{had-vis}$ candidate have an invariant mass between 80 and $110\,\text{GeV}$ are rejected. The signal acceptance times efficiency for this selection also varies between 1% and 7%, but the maximum occurs at lower masses due to the lower p_T thresholds on the tau decay products. A summary of the selection is given in table 2 of section 6.

5.3 Event categories

Events satisfying the selection criteria in the $\tau_\text{lep}\tau_\text{had}$ and $\tau_\text{had}\tau_\text{had}$ channels are categorised to exploit the different production modes in the MSSM. Events containing at least one b-tagged jet enter the b-tag category, while events containing no b-tagged jets enter the b-veto category. The categorisation is not used for the Z' search.

5.4 Ditau mass reconstruction

The ditau mass reconstruction is important for achieving good separation between signal and background. However, ditau mass reconstruction is challenging due to the presence of

neutrinos from the τ-lepton decays. Therefore, the mass reconstruction used for both the $\tau_{\mathrm{had}}\tau_{\mathrm{had}}$ and $\tau_{\mathrm{lep}}\tau_{\mathrm{had}}$ channels is the total transverse mass, defined as:

$$m_{\mathrm{T}}^{\mathrm{tot}} \equiv \sqrt{(p_{\mathrm{T}}^{\tau_1} + p_{\mathrm{T}}^{\tau_2} + E_{\mathrm{T}}^{\mathrm{miss}})^2 - (\mathbf{p}_{\mathrm{T}}^{\tau_1} + \mathbf{p}_{\mathrm{T}}^{\tau_2} + \mathbf{E}_{\mathrm{T}}^{\mathrm{miss}})^2}\,,$$

where $\mathbf{p}_{\mathrm{T}}^{\tau_1}$ and $\mathbf{p}_{\mathrm{T}}^{\tau_2}$ are the momenta of the visible tau decay products (including τ_{had} and τ_{lep}) projected into the transverse plane. More complex mass reconstruction techniques were investigated, but they did not improve the expected sensitivity.

6 Background estimation

The dominant background contribution in the $\tau_{\mathrm{had}}\tau_{\mathrm{had}}$ channel is from multijet production, which is estimated using a data-driven technique, described in section 6.1. Other important background contributions come from $Z/\gamma^* \to \tau\tau$ production at high $m_{\mathrm{T}}^{\mathrm{tot}}$ in the b-veto category, $t\bar{t}$ production in the b-tag category, and to a lesser extent $W(\to \ell\nu)$+jets, single top-quark, diboson and $Z/\gamma^*(\to \ell\ell)$+jets production. These contributions are estimated using simulation. Corrections are applied to the simulation to account for mismodelling of the trigger, reconstruction, identification and isolation efficiencies, the electron to $\tau_{\mathrm{had\text{-}vis}}$ misidentification rate and the momentum scales and resolutions. To further improve the modelling in the $\tau_{\mathrm{had}}\tau_{\mathrm{had}}$ channel, events in the simulation that contain quark- or gluon-initiated jets (henceforth called jets) that are misidentified as $\tau_{\mathrm{had\text{-}vis}}$ candidates are weighted by fake-rates measured in W+jets and $t\bar{t}$ control regions in data.

The dominant background contribution in the $\tau_{\mathrm{lep}}\tau_{\mathrm{had}}$ channel arises from processes where the $\tau_{\mathrm{had\text{-}vis}}$ candidate originates from a jet. This contribution is estimated using a data-driven technique similar to the $\tau_{\mathrm{had}}\tau_{\mathrm{had}}$ channel, described in section 6.2. The events are divided into those where the selected lepton is correctly identified, predominantly from W+jets ($t\bar{t}$) production in the b-veto (b-tag) channel, and those where the selected lepton arises from a jet, predominantly from multijet production. Backgrounds where both the $\tau_{\mathrm{had\text{-}vis}}$ and lepton candidates originate from electrons, muons or taus (real-lepton) arise from $Z/\gamma^* \to \tau\tau$ production in the b-veto category and $t\bar{t}$ production in the b-tag category, with minor contributions from $Z/\gamma^* \to \ell\ell$, diboson and single top-quark production. These contributions are estimated using simulation. To help constrain the normalisation of the $t\bar{t}$ contribution, a control region rich in $t\bar{t}$ events (CR-T) is defined and included in the statistical fitting procedure. The other major background contributions can be adequately constrained in the signal regions. Events in this control region must pass the signal selection for the b-tag category, but the $m_{\mathrm{T}}(\mathbf{p}_{\mathrm{T}}^{\ell}, \mathbf{E}_{\mathrm{T}}^{\mathrm{miss}})$ selection is replaced by $m_{\mathrm{T}}(\mathbf{p}_{\mathrm{T}}^{\ell}, \mathbf{E}_{\mathrm{T}}^{\mathrm{miss}}) > 110\,(100)\,\mathrm{GeV}$ in the $\tau_e\tau_{\mathrm{had}}$ ($\tau_\mu\tau_{\mathrm{had}}$) channel. The tighter selection in the $\tau_e\tau_{\mathrm{had}}$ channel is used to help suppress the larger multijet contamination. The region has $\sim 90\%$ $t\bar{t}$ purity.

6.1 Jet background estimate in the $\tau_{\mathrm{had}}\tau_{\mathrm{had}}$ channel

The data-driven technique used to estimate the dominant multijet background in the $\tau_{\mathrm{had}}\tau_{\mathrm{had}}$ channel is described in section 6.1.1. The method used to weight simulated events

Region	Selection
SR	τ_1 (trigger, medium), τ_2 (loose), $q(\tau_1) \times q(\tau_2) < 0$, $|\Delta\phi(\mathbf{p}_{\mathrm{T}}^{\tau_1}, \mathbf{p}_{\mathrm{T}}^{\tau_2})| > 2.7$
CR-1	Pass SR except: τ_2 (fail loose)
DJ-FR	jet trigger, $\tau_1 + \tau_2$ (no identification), $q(\tau_1) \times q(\tau_2) < 0$, $|\Delta\phi(\mathbf{p}_{\mathrm{T}}^{\tau_1}, \mathbf{p}_{\mathrm{T}}^{\tau_2})| > 2.7$, $p_{\mathrm{T}}^{\tau_2}/p_{\mathrm{T}}^{\tau_1} > 0.3$
W-FR	μ (trigger, isolated), τ_1 (no identification), $|\Delta\phi(\mathbf{p}_{\mathrm{T}}^{\mu}, \mathbf{p}_{\mathrm{T}}^{\tau_1})| > 2.4$, $m_{\mathrm{T}}(\mathbf{p}_{\mathrm{T}}^{\mu}, \mathbf{E}_{\mathrm{T}}^{\mathrm{miss}}) > 40\,\mathrm{GeV}$
	b-veto category only
T-FR	Pass W-FR except: b-tag category only

Table 1. Definition of signal, control and fakes regions used in the $\tau_{\mathrm{had}}\tau_{\mathrm{had}}$ channel. The symbol τ_1 (τ_2) represents the leading (sub-leading) $\tau_{\mathrm{had\text{-}vis}}$ candidate.

to estimate the remaining background containing events with $\tau_{\mathrm{had\text{-}vis}}$ candidates that originate from jets is described in section 6.1.2. A summary of the signal, control and fakes regions used in these methods is provided in table 1. The associated uncertainties are discussed in section 7.2.

6.1.1 Multijet events

The contribution of multijet events in the signal region (SR) of the $\tau_{\mathrm{had}}\tau_{\mathrm{had}}$ channel is estimated using events in two control regions (CR-1 and DJ-FR). Events in CR-1 must pass the same selection as SR, but the sub-leading $\tau_{\mathrm{had\text{-}vis}}$ candidate must fail $\tau_{\mathrm{had\text{-}vis}}$ identification. The non-multijet contamination in this region, $N_{\mathrm{non-MJ}}^{\mathrm{CR-1}}$, amounts to $\sim 1.6\%$ ($\sim 7.0\%$) in the b-veto (b-tag) channel, and is subtracted using simulation. Events in DJ-FR (the dijet fakes-region) are used to measure fake-factors (f_{DJ}), which are defined as the ratio of the number of $\tau_{\mathrm{had\text{-}vis}}$ that pass to those that fail the identification. The fake-factors are used to weight the events in CR-1 to estimate the multijet contribution:

$$N_{\mathrm{multijet}}^{\mathrm{SR}} = f_{\mathrm{DJ}} \times \left(N_{\mathrm{data}}^{\mathrm{CR-1}} - N_{\mathrm{non-MJ}}^{\mathrm{CR-1}} \right).$$

The selection for the DJ-FR is designed to be as similar to the signal selection as possible, while avoiding contamination from $\tau_{\mathrm{had\text{-}vis}}$. Events are selected by single-jet triggers with p_{T} thresholds ranging from 60 to $380\,\mathrm{GeV}$, with all but the highest-threshold trigger being prescaled. They must contain at least two $\tau_{\mathrm{had\text{-}vis}}$ candidates, where the leading candidate has $p_{\mathrm{T}} > 85\,\mathrm{GeV}$ and also exceeds the trigger threshold by 10%, and the sub-leading candidate has $p_{\mathrm{T}} > 65\,\mathrm{GeV}$. The $\tau_{\mathrm{had\text{-}vis}}$ candidates must have opposite charge sign, be back to back in the transverse plane, $|\Delta\phi(\mathbf{p}_{\mathrm{T}}^{\tau_1}, \mathbf{p}_{\mathrm{T}}^{\tau_2})| > 2.7$ rad and the p_{T} of the sub-leading $\tau_{\mathrm{had\text{-}vis}}$ must be at least 30% of the leading $\tau_{\mathrm{had\text{-}vis}}$ p_{T}. The fake-factors are measured using the sub-leading $\tau_{\mathrm{had\text{-}vis}}$ candidate to avoid trigger bias and to be consistent with their application in CR-1. They are parameterised as functions of the sub-leading $\tau_{\mathrm{had\text{-}vis}}$ p_{T} and the sub-leading $\tau_{\mathrm{had\text{-}vis}}$ track multiplicity. The purity of multijet events that pass the $\tau_{\mathrm{had\text{-}vis}}$ identification is 98–99% (93–98%) for the b-veto (b-tag) categories. The non-multijet contamination is subtracted using simulation. The fake-factors are shown in figure 2.

6.1.2 Non-multijet events

In the $\tau_{\mathrm{had}}\tau_{\mathrm{had}}$ channel, backgrounds originating from jets that are misidentified as $\tau_{\mathrm{had\text{-}vis}}$ in processes other than multijet production (predominantly $W +$ jets in the b-veto and $t\bar{t}$
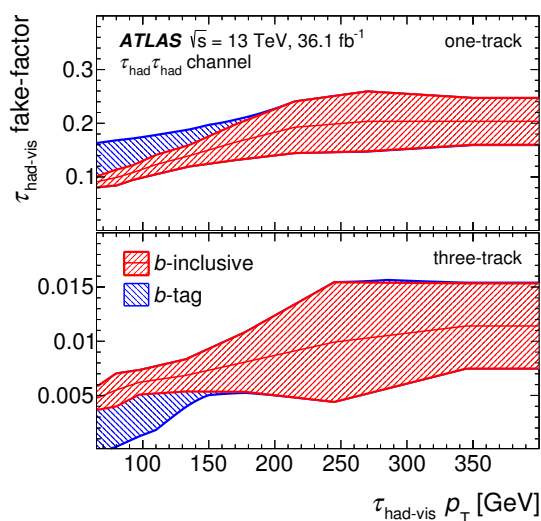
Figure 2. The $\tau_{\text{had-vis}}$ identification fake-factors in the $\tau_{\text{had}}\tau_{\text{had}}$ channel. The red band indicates the total uncertainty when used with a b-inclusive or b-veto selection. The blue band indicates the additional uncertainty when used with a b-tag selection.

in the b-tag categories) are estimated using simulation. Rather than applying the $\tau_{\text{had-vis}}$ identification to the simulated jets, they are weighted by fake-rates as in ref. [41]. This not only ensures the correct fake-rate, but also enhances the statistical precision of the estimate, as events failing the $\tau_{\text{had-vis}}$ identification are not discarded. The fake-rate for the sub-leading $\tau_{\text{had-vis}}$ candidate is defined as the ratio of the number of candidates that pass the identification to the total number of candidates. The fake-rate for the leading $\tau_{\text{had-vis}}$ candidate is defined as the ratio of the number of candidates that pass the identification and the single-tau trigger requirement to the total number of candidates.

The fake-rates applied to $t\bar{t}$ and single-top-quark events are calculated from a fakes region enriched in $t\bar{t}$ events (T-FR), while the fake-rates for all other processes are calculated in a fakes region enriched in $W+$jets events (W-FR). Both T-FR and W-FR use events selected by a single-muon trigger with a p_{T} threshold of $50\,\text{GeV}$. They must contain exactly one isolated muon with $p_{\text{T}} > 55\,\text{GeV}$ that fired the trigger, no electrons and at least one $\tau_{\text{had-vis}}$ candidate with $p_{\text{T}} > 50\,\text{GeV}$. The events must also satisfy $|\Delta\phi(\mathbf{p}_{\text{T}}^{\mu}, \mathbf{p}_{\text{T}}^{\tau_{\text{had-vis}}})| > 2.4\,\text{rad}$ and $m_{\text{T}}(\mathbf{p}_{\text{T}}^{\mu}, \mathbf{E}_{\text{T}}^{\text{miss}}) > 40\,\text{GeV}$. The events are then categorised into b-tag and b-veto categories, defining T-FR and W-FR, respectively. Backgrounds from non-$t\bar{t}$ (non-$W+$jets) processes are subtracted from T-FR (W-FR) using simulation. The fake-rates are measured using the leading-p_{T} $\tau_{\text{had-vis}}$ candidate and are parameterised as functions of the $\tau_{\text{had-vis}}$ p_{T} and track multiplicity.

6.2 Jet background estimate in the $\tau_{\text{lep}}\tau_{\text{had}}$ channel

The background contribution from events where the $\tau_{\text{had-vis}}$ candidate originates from a jet in the $\tau_{\text{lep}}\tau_{\text{had}}$ channel is estimated using a data-driven method, which is similar to the one used to estimate the multijet contribution in the $\tau_{\text{had}}\tau_{\text{had}}$ channel. Events in the control
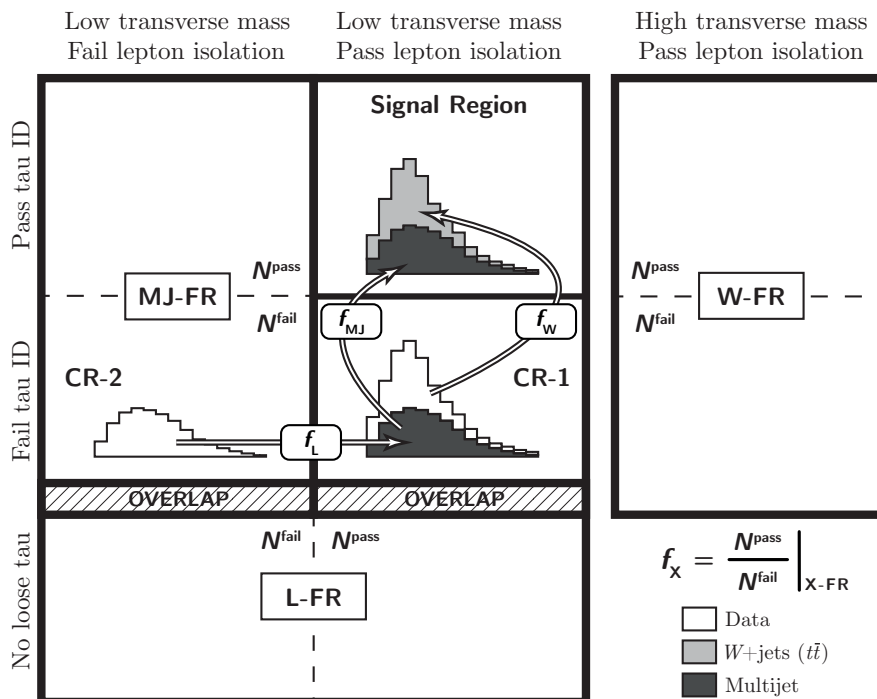
Figure 3. Schematic of the fake-factor background estimation in the $\tau_{\mathrm{lep}}\tau_{\mathrm{had}}$ channel. The fake-factors, f_{X} (X = MJ, W, L), are defined as the ratio of events in data that pass/fail the specified selection requirements, measured in the fakes-regions: MJ-FR, W-FR and L-FR, respectively. The multijet contribution is estimated by weighting events in CR-2 by the product of f_{L} and f_{MJ}. The contribution from W+jets and $t\bar{t}$ events where the $\tau_{\mathrm{had\text{-}vis}}$ candidate originates from a jet is estimated by subtracting the multijet contribution from CR-1 and then weighting by f_{W}. There is a small overlap of events between L-FR and the CR-1 and CR-2 regions. The contribution where both the selected $\tau_{\mathrm{had\text{-}vis}}$ and lepton originate from leptons is estimated using simulation (not shown here).

region CR-1 must pass the same selection as the $\tau_{\mathrm{lep}}\tau_{\mathrm{had}}$ SR, but the $\tau_{\mathrm{had\text{-}vis}}$ candidate must fail $\tau_{\mathrm{had\text{-}vis}}$ identification. These events are weighted to estimate the jet background in SR, but the weighting method must be extended to account for the fact that CR-1 contains both multijet and W+jets (or $t\bar{t}$) events, which have significantly different fake-factors. This is mainly due to a different fraction of quark-initiated jets, which are typically more narrow and produce fewer hadrons than gluon-initiated jets, and are thus more likely to pass the $\tau_{\mathrm{had\text{-}vis}}$ identification. The procedure, depicted in figure 3, is described in the following. A summary of the corresponding signal, control and fakes regions is provided in table 2. The associated uncertainties are discussed in section 7.2.

6.2.1 Multijet events

The multijet contributions in both CR-1 ($N_{\mathrm{multijet}}^{\mathrm{CR-1}}$) and SR ($N_{\mathrm{multijet}}^{\mathrm{SR}}$) are estimated from events where the $\tau_{\mathrm{had\text{-}vis}}$ fails identification and the selected lepton fails isolation (CR-2). The non-multijet background is subtracted using simulation and the events are weighted first by the lepton-isolation fake-factor (f_{L}), yielding $N_{\mathrm{multijet}}^{\mathrm{CR-1}}$, and then by the multijet

Region	Selection
SR	ℓ (trigger, isolated), τ_1 (medium), $q(\ell) \times q(\tau_1) < 0$, $|\Delta\phi(\mathbf{p}_T^\ell, \mathbf{p}_T^{\tau_1})| > 2.4$, $m_T(\mathbf{p}_T^\ell, \mathbf{E}_T^{\text{miss}}) < 40\,\text{GeV}$, veto $80 < m(\mathbf{p}^\ell, \mathbf{p}^{\tau_1}) < 110\,\text{GeV}$ ($\tau_e\tau_{\text{had}}$ channel only)
CR-1	Pass SR except: τ_1 (very-loose, fail medium)
CR-2	Pass SR except: τ_1 (very-loose, fail medium), ℓ (fail isolation)
MJ-FR	Pass SR except: τ_1 (very-loose), ℓ (fail isolation)
W-FR	Pass SR except: $70\,(60) < m_T(\mathbf{p}_T^\ell, \mathbf{E}_T^{\text{miss}}) < 150\,\text{GeV}$ in $\tau_e\tau_{\text{had}}$ ($\tau_\mu\tau_{\text{had}}$) channel
CR-T	Pass SR except: $m_T(\mathbf{p}_T^\ell, \mathbf{E}_T^{\text{miss}}) > 110\,(100)\,\text{GeV}$ in the $\tau_e\tau_{\text{had}}$ ($\tau_\mu\tau_{\text{had}}$) channel, b-tag category only
L-FR	ℓ (trigger, selected), jet (selected), no loose $\tau_{\text{had-vis}}$, $m_T(\mathbf{p}_T^\ell, \mathbf{E}_T^{\text{miss}}) < 30\,\text{GeV}$

Table 2. Definition of signal, control and fakes regions used in the $\tau_{\text{lep}}\tau_{\text{had}}$ channel. The symbol ℓ represents the selected electron or muon candidate and τ_1 represents the leading $\tau_{\text{had-vis}}$ candidate.

tau fake-factor (f_{MJ}):

$$N_{\text{multijet}}^{\text{CR}-1} = f_{\text{L}} \times \left(N_{\text{data}}^{\text{CR}-2} - N_{\text{non}-\text{MJ}}^{\text{CR}-2} \right) ,$$

$$N_{\text{multijet}}^{\text{SR}} = f_{\text{MJ}} \times N_{\text{multijet}}^{\text{CR}-1} .$$

The fake-factor f_{MJ} is measured in the multijet fakes-region (MJ-FR) defined in section 6.2.3 and the fake-factor f_{L} is measured in the lepton fakes-region (L-FR) defined in section 6.2.4.

6.2.2 Non-multijet events

The contribution from $W+$ jets (and $t\bar{t}$) events where the $\tau_{\text{had-vis}}$ candidate originates from a jet is estimated from events in CR-1 that remain after subtracting the multijet contribution and the real-lepton contribution (estimated using simulation). The events are weighted by the $W+$ jets tau fake-factor (f_{W}):

$$N_{W+\text{jets}}^{\text{SR}} = f_{\text{W}} \times \left(N_{\text{data}}^{\text{CR}-1} - N_{\text{multijet}}^{\text{CR}-1} - N_{\text{real}-\text{lepton}}^{\text{CR}-1} \right) .$$

The fake-factor f_{W} is measured in the $W+$ jets fakes-region (W-FR) defined in section 6.2.3.

6.2.3 Tau identification fake-factors

Both f_{W} and f_{MJ} are parameterised as functions of $\tau_{\text{had-vis}}$ p_T, $\tau_{\text{had-vis}}$ track multiplicity and $|\Delta\phi(\mathbf{p}_T^{\tau_{\text{had-vis}}}, \mathbf{E}_T^{\text{miss}})|$. The $|\Delta\phi(\mathbf{p}_T^{\tau_{\text{had-vis}}}, \mathbf{E}_T^{\text{miss}})|$ dependence is included to encapsulate correlations between the $\tau_{\text{had-vis}}$ identification and energy response, which impact the $\mathbf{E}_T^{\text{miss}}$ calculation. Due to the limited size of the control regions, the $|\Delta\phi(\mathbf{p}_T^{\tau_{\text{had-vis}}}, \mathbf{E}_T^{\text{miss}})|$ dependence is extracted as a sequential correction and is only applied in the b-veto channel. The selection for W-FR and MJ-FR are the same as for SR with modifications described in the following. The medium $\tau_{\text{had-vis}}$ identification criterion is replaced by a very loose
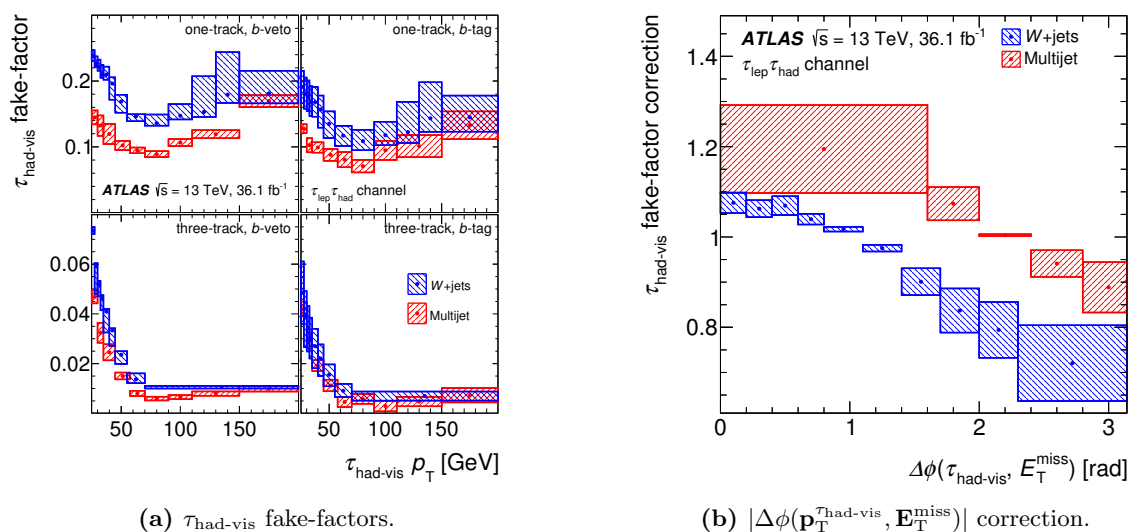
(a) $\tau_{\text{had-vis}}$ fake-factors.   **(b)** $|\Delta\phi(\mathbf{p}_T^{\tau_{\text{had-vis}}}, \mathbf{E}_T^{\text{miss}})|$ correction.

Figure 4. The $\tau_{\text{had-vis}}$ identification fake-factors and the sequential $|\Delta\phi(\mathbf{p}_T^{\tau_{\text{had-vis}}}, \mathbf{E}_T^{\text{miss}})|$ correction in the $\tau_{\text{lep}}\tau_{\text{had}}$ channel. The multijet fake-factors are for the 2016 dataset only. The bands include all uncertainties.

criterion with an efficiency of about 99% for $\tau_{\text{had-vis}}$ and a rejection of about 2 (3) for one-track (three-track) jets. Events passing the medium identification criterion enter the fake-factor numerators, while those failing enter the denominators. The very loose identification reduces differences between f_W and f_{MJ}, as it tends to reject gluon-initiated jets, enhancing the fraction of quark-initiated jets in W-FR and MJ-FR. This selection is also applied consistently to CR-1. A comparison of the two fake-factors and their respective $|\Delta\phi(\mathbf{p}_T^{\tau_{\text{had-vis}}}, \mathbf{E}_T^{\text{miss}})|$ corrections are shown in figures 4(a) and 4(b).

In MJ-FR, the selected lepton must fail isolation. The multijet purity for events that pass the $\tau_{\text{had-vis}}$ identification in this region is ~88% for the b-veto category and ~93% for the b-tag category. All non-multijet contamination is subtracted from MJ-FR using simulation. The fake-factor f_{MJ} is further split by category (b-veto, b-tag) and by data-taking period (2015, 2016) to account for changing isolation criteria in the trigger that affect MJ-FR differently to SR.

In the W-FR, the $m_T(\mathbf{p}_T^\ell, \mathbf{E}_T^{\text{miss}})$ criterion is replaced by $70(60) < m_T(\mathbf{p}_T^\ell, \mathbf{E}_T^{\text{miss}}) < 150\,\text{GeV}$ in the $\tau_e\tau_{\text{had}}$ ($\tau_\mu\tau_{\text{had}}$) channel. The purity of W+jets events that pass the $\tau_{\text{had-vis}}$ identification is ~85% in the b-veto category. The b-tag category is dominated by $t\bar{t}$ events, but the purity of events where the $\tau_{\text{had-vis}}$ candidate originates from a jet is only ~40% due to the significant fraction of $\tau_{\text{had-vis}}$ from W boson decays. The multijet and real-lepton backgrounds are subtracted from W-FR analogously to CR-1 in the W+jets estimate. Due to the large $\tau_{\text{had-vis}}$ contamination in the b-tag region, f_W is not split by category, but the b-veto parameterisation is used in the b-tag region, with a p_T-independent correction factor of 0.8 (0.66) for one-track (three-track) $\tau_{\text{had-vis}}$. The correction factor is obtained from a direct measurement of the fake-factors in b-tag events.

6.2.4 Lepton isolation fake-factor

The fake-factor f_L is measured in L-FR, which must have exactly one selected lepton, $m_\mathrm{T}(\mathbf{p}_\mathrm{T}^\ell, \mathbf{E}_\mathrm{T}^\mathrm{miss}) < 30\,\mathrm{GeV}$ and no $\tau_\mathrm{had\text{-}vis}$ candidates passing the loose identification but rather at least one selected jet (not counting the b-tagged jet in the b-tag region). The selection is designed to purify multijet events while suppressing $W+$jets and $t\bar{t}$ events. Events where the selected lepton passes (fails) isolation enter the f_L numerator (denominator). All non-multijet contributions are subtracted using simulation. The fake-factors are parameterised as a function of lepton $|\eta|$, and are further split by lepton type (electron, muon), category (b-veto, b-tag) and into two regions of muon p_T, due to differences in the isolation criteria of the low- and high-p_T triggers in the $\tau_\mu\tau_\mathrm{had}$ channel.

7 Systematic uncertainties

Uncertainties affecting the simulated signal and background contributions are discussed in section 7.1. These include uncertainties associated with the determination of the integrated luminosity, the detector simulation, the theoretical cross sections and the modelling from the event generators. Uncertainties associated with the data-driven background estimates are discussed in section 7.2.

7.1 Uncertainties in simulation estimates

The uncertainty in the combined 2015+2016 integrated luminosity is 3.2%, which affects all simulated samples. It is derived, following a methodology similar to that detailed in ref. [134], from a preliminary calibration of the luminosity scale using x–y beam-separation scans performed in August 2015 and May 2016. The uncertainty related to the overlay of pile-up events is estimated by varying the average number of interactions per bunch crossing by 9%. The uncertainties related to the detector simulation manifest themselves through the efficiency of the reconstruction, identification and triggering algorithms, and the energy scale and resolution for electrons, muons, $\tau_\mathrm{had\text{-}vis}$, ($b$-)jets and the $\mathbf{E}_\mathrm{T}^\mathrm{miss}$ soft term. These uncertainties are considered for all simulated samples; their impact is taken into account when estimating signal and background contributions and when subtracting contamination from regions in the data-driven estimates. The effects of the particle energy-scale uncertainties are propagated to $\mathbf{E}_\mathrm{T}^\mathrm{miss}$. The uncertainty in the $\tau_\mathrm{had\text{-}vis}$ identification efficiency as determined from measurements of $Z \to \tau\tau$ events is 5–6%. At high p_T, there are no abundant sources of real hadronic tau decays from which an efficiency measurement could be made. Rather, the tau identification is studied in high-p_T dijet events as a function of the jet p_T, which indicates that there is no degradation in the modelling of the detector response as a function of the p_T of tau candidates. Based on the limited precision of these studies, an additional uncertainty of 20%/TeV (25%/TeV) for one-track (three-track) $\tau_\mathrm{had\text{-}vis}$ candidates with $p_\mathrm{T} > 150\,\mathrm{GeV}$ is assigned. The $\tau_\mathrm{had\text{-}vis}$ trigger efficiency uncertainty is 3–14%. The uncertainty in the $\tau_\mathrm{had\text{-}vis}$ energy scale is 2–3%. The probability for electrons to be misidentified as $\tau_\mathrm{had\text{-}vis}$ is measured with a precision of 3–14% [131]. The electron, muon, jet and $\mathbf{E}_\mathrm{T}^\mathrm{miss}$ systematic uncertainties described above are found to have a very small impact.

Theoretical cross-section uncertainties are taken into account for all backgrounds estimated using simulation. For Z/γ^*+jets production, uncertainties are taken from ref. [135] and include variations of the PDF sets, scale, α_S, beam energy, electroweak corrections and photon-induced corrections. A single 90% CL eigenvector variation uncertainty is used, based on the CT14nnlo PDF set. The variations amount to a $\sim$5% uncertainty in the total number of Z/γ^*+jets events within the acceptance. For diboson production, an uncertainty of 10% is used [99, 136]. For $t\bar{t}$ [108] and single top-quark [109, 110] production, the assigned 6% uncertainty is based on PDF, scale and top-quark mass variations. Additional uncertainties related to initial- and final-state radiation modelling, tune and (for $t\bar{t}$ only) the choice of hdamp parameter value in POWHEG-BOX v2, which controls the amount of radiation produced by the parton shower, are also taken into account [137]. The uncertainty due to the hadronisation model is evaluated by comparing $t\bar{t}$ events generated with POWHEG-BOX v2 interfaced to either Herwig++ [138] or PYTHIA 6. To estimate the uncertainty in generating the hard scatter, the POWHEG and MG5_aMC@NLO event generators are compared, both interfaced to the Herwig++ parton shower model. The uncertainties in the W+jets cross section have a negligible impact in the $\tau_{had}\tau_{had}$ channel and the W+jets simulation is not used in the $\tau_{lep}\tau_{had}$ channel.

For MSSM Higgs boson samples, various sources of uncertainty which impact the signal acceptance are considered. The impact from varying the factorisation and renormalisation scales up and down by a factor of two, either coherently or oppositely, is taken into account. Uncertainties due to the modelling of initial- and final-state radiation, as well as multiple parton interaction are also taken into account. These uncertainties are estimated from variations of the PYTHIA 8 A14 tune [57] for the b-associated production and the AZNLO PYTHIA 8 tune [56] for the gluon-gluon fusion production. The envelope of the variations resulting from the use of the alternative PDFs in the PDF4LHC15_nlo_nf4_30 (PDF4LHC15_nlo_100) [139] set is used to estimate the PDF uncertainty for the b-associated (gluon-gluon fusion) production. The total uncertainty for the MSSM Higgs boson samples is typically 1–4%, which is dominated by variations of the radiation and multiple parton interactions, with minor impact from scale variations. The Z' signal acceptance uncertainties are expected to be negligible.

For both the MSSM Higgs boson and Z' samples, uncertainties in the integrated cross section are not included in the fitting procedure used to extract experimental cross-section limits. The uncertainty for Z' is included when overlaying model cross sections, in which case it is calculated using the same procedure as for the Z/γ^*+jets background.

7.2 Uncertainties in data-driven estimates

Uncertainties in the multijet estimate for the $\tau_{had}\tau_{had}$ channel (section 6.1.1) arise from the fake-factors f_{DJ}. These include a 10–50% uncertainty from the limited size of the DJ-FR and an uncertainty of up to 50% from the subtraction of the non-multijet contamination. An additional uncertainty is considered when applying the fake-factors in the b-tag category, which accounts for changes in the jet composition with respect to the inclusive selection of the DJ-FR. As the differences are extracted from comparisons in control regions, they are one-sided.

The uncertainty in the fake-rates used to weight simulated non-multijet events in the $\tau_{\text{had}}\tau_{\text{had}}$ channel (section 6.1.2) is dominated by the limited size of the fakes regions and can reach 40%.

Uncertainties in the multijet estimate for the $\tau_{\text{lep}}\tau_{\text{had}}$ channel (section 6.2.1) arise from the fake-factors f_{MJ} and f_{L}. The applicability of f_{MJ} measured in MJ-FR to CR-1 is investigated by studying f_{MJ} as a function of the lepton isolation and the observed differences are assigned as a systematic uncertainty. The statistical uncertainty from the limited size of MJ-FR is significant, particularly for the smaller 2015 dataset. The impact of a potential mismodelling in the subtraction of simulated non-multijet events containing non-isolated leptons is investigated by varying the subtraction by 50%, but is found to be small compared to the other sources of systematic uncertainty. A constant uncertainty of 20% in f_{MJ} is used to envelop these variations. A 50% uncertainty is assigned to the sequential $|\Delta\phi(\mathbf{p}_{\text{T}}^{\tau_{\text{had-vis}}}, \mathbf{E}_{\text{T}}^{\text{miss}})|$ correction.

The applicability of f_{L} measured in L-FR to events in MJ-FR is investigated by altering the $m_{\text{T}}(\mathbf{p}_{\text{T}}^{\ell}, \mathbf{E}_{\text{T}}^{\text{miss}})$ selection and the observed differences are assigned as a systematic uncertainty. A 20% uncertainty in the background subtraction in L-FR is considered, motivated by observations of the tau identification performance in $W+$jets events. The statistical uncertainty from the limited size of L-FR is also considered, but is relatively small. The total uncertainty in f_{L} is 5–50%.

Uncertainties in the data-driven $W+$jets and $t\bar{t}$ estimates for the $\tau_{\text{lep}}\tau_{\text{had}}$ channel (section 6.2.2) arise from the fake-factors f_{W} and the subtraction of contributions from CR-1. The applicability of f_{W} measured in W-FR to CR-1 is investigated by studying f_{W} as a function of $m_{\text{T}}(\mathbf{p}_{\text{T}}^{\ell}, \mathbf{E}_{\text{T}}^{\text{miss}})$ and the observed differences (up to $\sim$10%) are assigned as a systematic uncertainty. A 30% uncertainty is assigned to the sequential $|\Delta\phi(\mathbf{p}_{\text{T}}^{\tau_{\text{had-vis}}}, \mathbf{E}_{\text{T}}^{\text{miss}})|$ correction, based on variations observed as a function of $\tau_{\text{had-vis}}$ p_{T}. Due to the large contamination for b-tag events in W-FR, a 50% uncertainty is assigned to the correction factor applied to the b-veto parameterisation. The subtraction of the simulated samples in CR-1 is affected by experimental uncertainties and uncertainties in production cross sections, which amount to 10%. The total uncertainty in the multijet estimate in CR-1 is also propagated to the subtraction.

8 Results

The number of observed events in the signal regions of the $\tau_{\text{lep}}\tau_{\text{had}}$ and $\tau_{\text{had}}\tau_{\text{had}}$ channels together with the predicted event yields from signal and background processes are shown in table 3. In the $\tau_{\text{lep}}\tau_{\text{had}}$ channel, all events estimated using the data-driven fake-factor technique are grouped as Jet $\to \tau$ fake, while events where the $\tau_{\text{had-vis}}$ originates from a jet are removed from the other processes. In the $\tau_{\text{had}}\tau_{\text{had}}$ channel, the multijet process is estimated using the fake-factor technique while contributions from all other processes are estimated using simulation with data-driven corrections for the $\tau_{\text{had-vis}}$ candidates that originate from jets. The numbers are given before (pre-fit) and after (post-fit) applying the statistical fitting procedure described in section 8.1. The observed event yields are compatible with the

Channel	Process	b-veto		b-tag	
		pre-fit	post-fit	pre-fit	post-fit
$\tau_{\text{lep}}\tau_{\text{had}}$	$Z/\gamma^* \to \tau\tau$	$92\,000 \pm 11\,000$	$96\,400 \pm 1600$	670 ± 140	690 ± 70
	Diboson	880 ± 100	920 ± 70	6.3 ± 1.7	6.5 ± 1.4
	$t\bar{t}$ and single top-quark	1050 ± 170	1090 ± 130	2800 ± 400	2680 ± 80
	Jet $\to \tau$ fake	$83\,000 \pm 5000$	$88\,800 \pm 1700$	3000 ± 400	3390 ± 170
	$Z/\gamma^* \to \ell\ell$	$15\,800 \pm 1200$	$16\,200 \pm 700$	86 ± 21	89 ± 16
	SM Total	$193\,000 \pm 13\,000$	$203\,400 \pm 1200$	6500 ± 600	6850 ± 120
	Data		$203\,365$		6843
	A/H (300)	720 ± 80	$-$	236 ± 32	$-$
	A/H (500)	112 ± 11	$-$	39 ± 5	$-$
	A/H (800)	10.7 ± 1.1	$-$	4.8 ± 0.6	$-$
$\tau_{\text{had}}\tau_{\text{had}}$	Multijet	3040 ± 240	3040 ± 90	106 ± 32	85 ± 10
	$Z/\gamma^* \to \tau\tau$	610 ± 230	770 ± 80	7.5 ± 2.9	8.6 ± 1.3
	$W(\to \tau\nu)$+jets	178 ± 31	182 ± 15	4.0 ± 1.0	4.1 ± 0.5
	$t\bar{t}$ and single top-quark	26 ± 9	29 ± 4	60 ± 50	74 ± 15
	Others	25 ± 6	27.4 ± 2.1	1.0 ± 0.5	1.1 ± 0.4
	SM Total	3900 ± 400	4050 ± 70	180 ± 60	173 ± 16
	Data		4059		154
	A/H (300)	130 ± 50	$-$	44 ± 19	$-$
	A/H (500)	80 ± 33	$-$	28 ± 12	$-$
	A/H (800)	11 ± 4	$-$	5.1 ± 2.2	$-$

Table 3. Observed number of events and predictions of signal and background contributions in the b-veto and b-tag categories of the $\tau_{\text{lep}}\tau_{\text{had}}$ and $\tau_{\text{had}}\tau_{\text{had}}$ channels. The background predictions and uncertainties (including both the statistical and systematic components) are obtained before (pre-fit) and after (post-fit) applying the statistical fitting procedure discussed in section 8. The individual uncertainties are correlated, and do not necessarily add in quadrature to the total background uncertainty. The label "Others" refers to contributions from diboson, $Z/\gamma^*(\to \ell\ell)$+jets and $W(\to \ell\nu)$+jets production. In the $\tau_{\text{lep}}\tau_{\text{had}}$ channel, events containing a $\tau_{\text{had-vis}}$ candidate that originate from jets are removed from all processes other than Jet $\to \tau$ fake. The expected pre-fit contributions from A and H bosons with masses of 300, 500 and 800 GeV and $\tan\beta = 10$ in the hMSSM scenario are also shown.

expected event yields from SM processes, within uncertainties. The $m_{\text{T}}^{\text{tot}}$ distributions in the signal regions are shown in figures 5(a)–5(d) and in the CR-T in figure 6.

8.1 Fit model

The parameter of interest is the signal strength, μ. It is defined as the ratio of the observed to the predicted value of the cross section times branching fraction, where the prediction is evaluated at a particular point in the parameter space of the theoretical model in question (MSSM or Z' benchmark scenarios). Hence, the value $\mu = 0$ corresponds to the absence of a signal, whereas the value $\mu = 1$ indicates the presence of a signal as predicted by the
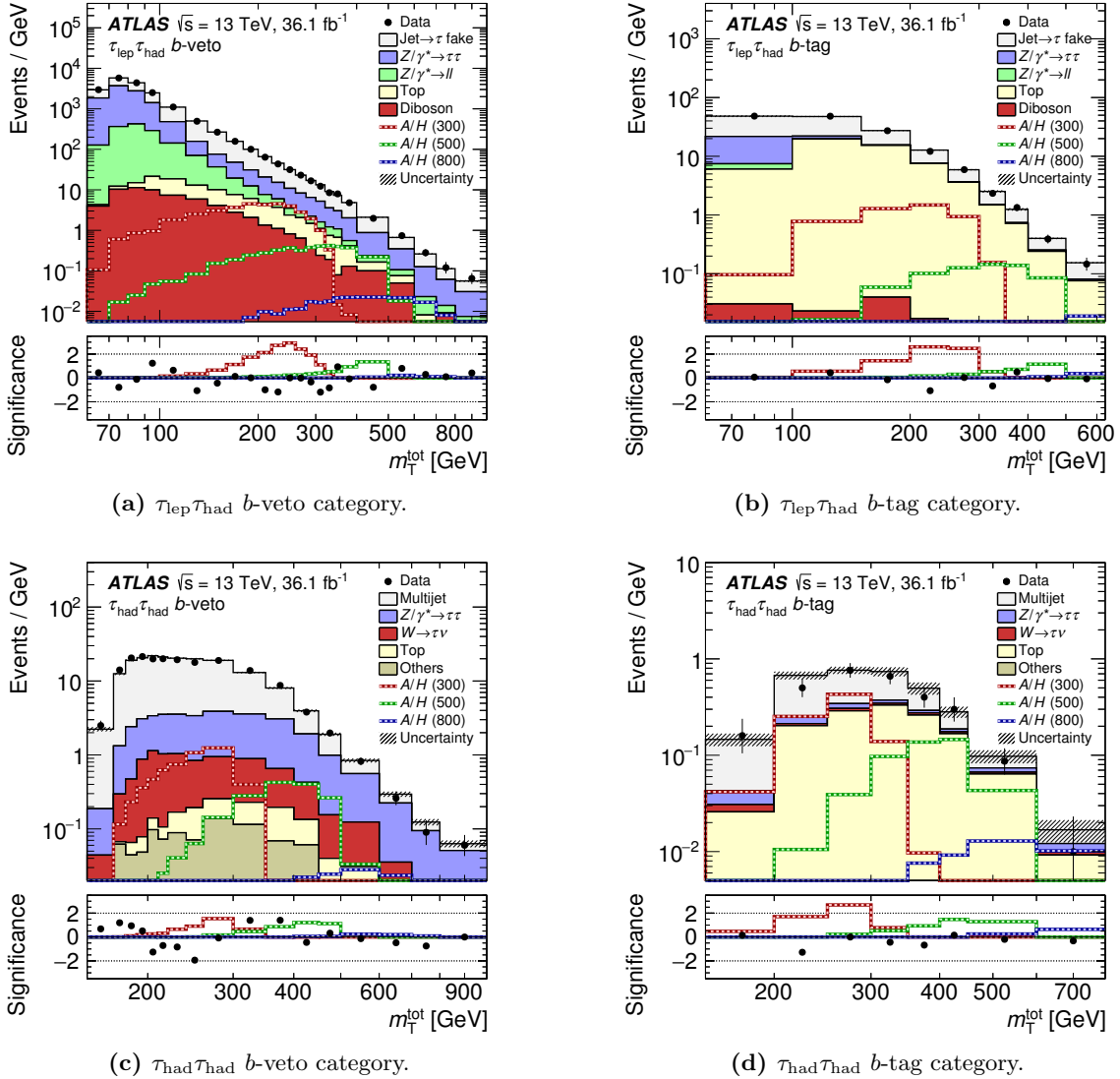
Figure 5. Distributions of m_T^{tot} for the (a) b-veto and (b) b-tag categories of the $\tau_{lep}\tau_{had}$ channel and the (c) b-veto and (d) b-tag categories of the $\tau_{had}\tau_{had}$ channel. The label "Others" refers to contributions from diboson, $Z/\gamma^*(\to \ell\ell)$+jets and $W(\to \ell\nu)$+jets production. In the $\tau_{lep}\tau_{had}$ channel, events containing $\tau_{had\text{-}vis}$ candidates that originate from jets are removed from all processes other than Jet $\to \tau$ fake. The binning displayed is that entering into the statistical fit discussed in section 8, with minor modifications needed to combine the $\tau_{lep}\tau_{had}$ channels and with underflows and overflows included in the first and last bins, respectively. The predictions and uncertainties for the background processes are obtained from the fit under the hypothesis of no signal. The combined prediction for A and H bosons with masses of 300, 500 and 800 GeV and $\tan\beta = 10$ in the hMSSM scenario are superimposed. The significance of the data given the fitted model and its uncertainty is computed in each bin following ref. [140] and is shown in the lower panels. The expected significance of the hypothetical Higgs boson signals are also overlaid.
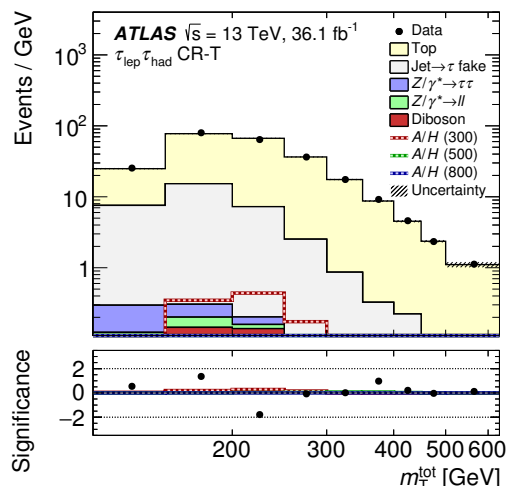
Figure 6. Distribution of m_T^{tot} in the $t\bar{t}$ enriched control region (CR-T) of the $\tau_{lep}\tau_{had}$ channel. Events containing $\tau_{had\text{-}vis}$ candidates that originate from jets are removed from all processes other than Jet $\rightarrow \tau$ fake. The binning displayed is that entering into the statistical fit discussed in section 8, with minor modifications needed to combine the $\tau_{lep}\tau_{had}$ channels and with underflows and overflows included in the first and last bins, respectively. The predictions and uncertainties for the background processes are obtained from the fit under the hypothesis of no signal. The combined prediction for A and H bosons with masses of 300, 500 and 800 GeV and $\tan\beta = 10$ in the hMSSM scenario are superimposed. The significance of the data given the fitted model and its uncertainty is computed in each bin following ref. [140] and is shown in the lower panel. The expected significance of the hypothetical Higgs boson signals are also overlaid.

model. To estimate μ, a likelihood function constructed as the product of Poisson probability terms is used. A term is included for each bin in the m_T^{tot} distributions from the $\tau_e\tau_{had}$, $\tau_\mu\tau_{had}$ and $\tau_{had}\tau_{had}$ channels. When fitting MSSM models to the data, the distributions are separated into b-tag and b-veto events to enhance sensitivity to the gluon-gluon fusion and b-associated production modes, while the inclusive distributions are used for Z' models. In all cases, the distributions in the CR-T regions of the $\tau_e\tau_{had}$ and $\tau_\mu\tau_{had}$ channels are added, which help constrain uncertainties in the $t\bar{t}$ background. Signal and background predictions depend on systematic uncertainties, which are parameterised as nuisance parameters that are constrained using Gaussian probability density functions. The asymptotic approximation is used with the test statistic $\tilde{q}_\mu$ [141] to compare the likelihoods of the null hypothesis (SM only) and the assumed signal hypothesis (SM plus signal) given the data. The bin widths are chosen to ensure a sufficient number of background events in each bin. The results from the $\tau_e\tau_{had}$, $\tau_\mu\tau_{had}$ and $\tau_{had}\tau_{had}$ channels are combined to improve the sensitivity to signal. For ditau resonance masses below about 0.6 TeV, the sensitivity is dominated by the $\tau_{lep}\tau_{had}$ channels, while the $\tau_{had}\tau_{had}$ channel is most sensitive in the higher mass range.

8.2 Cross-section limits

The data are found to be in good agreement with the predicted background yields, and the results are given in terms of exclusion limits. These are set using the modified frequentist

CL$_\text{s}$ method [142]. Upper limits on the cross section times branching fraction for ϕ and Z' bosons are set at the 95% confidence level (CL) as a function of the boson mass. They are obtained by multiplying the extracted limits on μ by the respective predicted cross sections. The ϕ boson limits assume the natural width of the boson to be negligible compared to the experimental resolution (as expected over the probed MSSM parameter space). They cover the mass range 0.2–2.25 TeV and are shown separately for gluon-gluon fusion and b-quark associated production. The limits on Z' bosons are calculated assuming an SSM Z' and extend up to 4 TeV. The limits are shown in figures 7(a)–7(c). They are in the range 0.78–0.0058 pb (0.70–0.0037 pb) for gluon-gluon fusion (b-associated) production of scalar bosons with masses of 0.2–2.25 TeV and 1.56–0.0072 pb for Drell-Yan production of Z' bosons with masses of 0.2–4 TeV. A small downward fluctuation at a mass of $\sim$0.3 TeV is observed in all limits, while a small upward fluctuation for gluon-gluon fusion and Z' bosons is seen around 0.5 TeV and a broad deficit is seen for the b-quark associated production over the entire mass range. These features arise primarily because of a deficit of events in the range 200–250 GeV followed by a mild excess in the range 300–400 GeV in figure 5(c), and by a consistent deficit of events across the whole range in figure 5(d). Modifications of the Z' chiral coupling structure can result in changes of up to 40% in the Z' cross-section limits. Reducing the Z' width can improve the limits by up to $\sim$30%, while increasing the width to 36% can degrade the limits by up to $\sim$70%. Figures 8(a) and 8(b) show the observed and expected 95% CL upper limits on the production cross section times branching fraction for $\phi \to \tau\tau$ as a function of the fractional contribution from b-associated production ($\sigma_{bb}/[\sigma_{bb} + \sigma_{gg}]$) and the scalar boson mass.

The impact of systematic uncertainties on the $\phi \to \tau\tau$ 95% CL cross section upper limits are calculated by comparing the expected upper limit in the case of no systematic uncertainties, μ_stat^{95}, with a limit calculated by introducing a group of systematic uncertainties, μ_i^{95}. The systematic uncertainty impacts are shown in figure 9(a) for gluon-gluon fusion production and figure 9(b) for b-associated production as functions of the scalar boson mass. The major uncertainties are grouped according to their origin, while minor uncertainties are collected as "Others".

In the low mass range, the sensitivity is dominated by the $\tau_\text{lep}\tau_\text{had}$ channel, and the major uncertainties arise from the estimate of the dominant $W+$ jets background. Due to the large contribution the fit is able to significantly constrain the uncertainties in this background. In the intermediate mass range the tau energy scale uncertainty becomes dominant. The fit is able to effectively constrain this conservative uncertainty due to the large contribution from $Z/\gamma^* \to \tau\tau$ and $t\bar{t}$ in each of the categories. At very high masses, the uncertainty in the identification efficiency for high-p_T $\tau_\text{had-vis}$ candidates becomes dominant, and due to the lack of significant $Z/\gamma^* \to \tau\tau$ and $t\bar{t}$ at high mass, this uncertainty remains relatively unconstrained. The addition of the CR-T region distributions to the fit allows the uncertainties in the $t\bar{t}$ modelling to be well constrained and as such, they have little impact on the sensitivity.
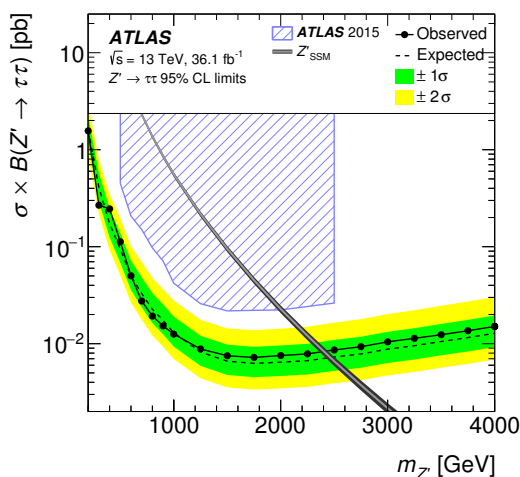
8.3 MSSM interpretations

The data are interpreted in terms of the MSSM. Figure 10 shows regions in the m_A–$\tan\beta$ plane excluded at 95% CL in the $m_\text{h}^\text{mod+}$ and hMSSM scenarios. In the MSSM
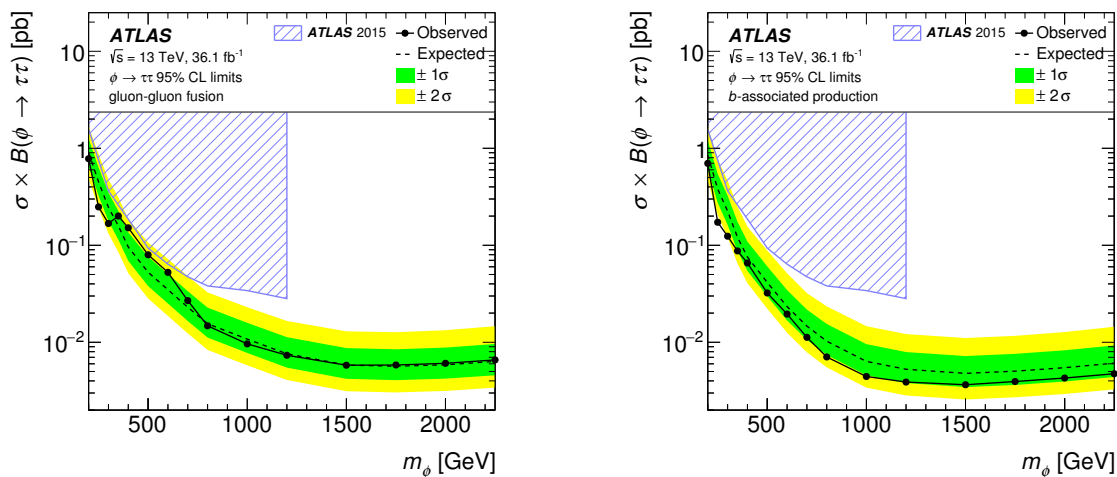
(a) $\phi \to \tau\tau$ (gluon-gluon fusion production).

(b) $\phi \to \tau\tau$ (b-associated production).

(c) $Z' \to \tau\tau$.

Figure 7. The observed and expected 95% CL upper limits on the production cross section times branching fraction for a scalar boson produced via (a) gluon-gluon fusion and (b) b-associated production, and for (c) gauge bosons. The limits are calculated from a statistical combination of the $\tau_{\mathrm{lep}}\tau_{\mathrm{had}}$ and $\tau_{\mathrm{had}}\tau_{\mathrm{had}}$ channels. The excluded regions from the 2015 data ATLAS search [29] are depicted by the hatched blue fill. The predicted cross section for a Z'_{SSM} boson is overlaid in (c), where the band depicts the total uncertainty.
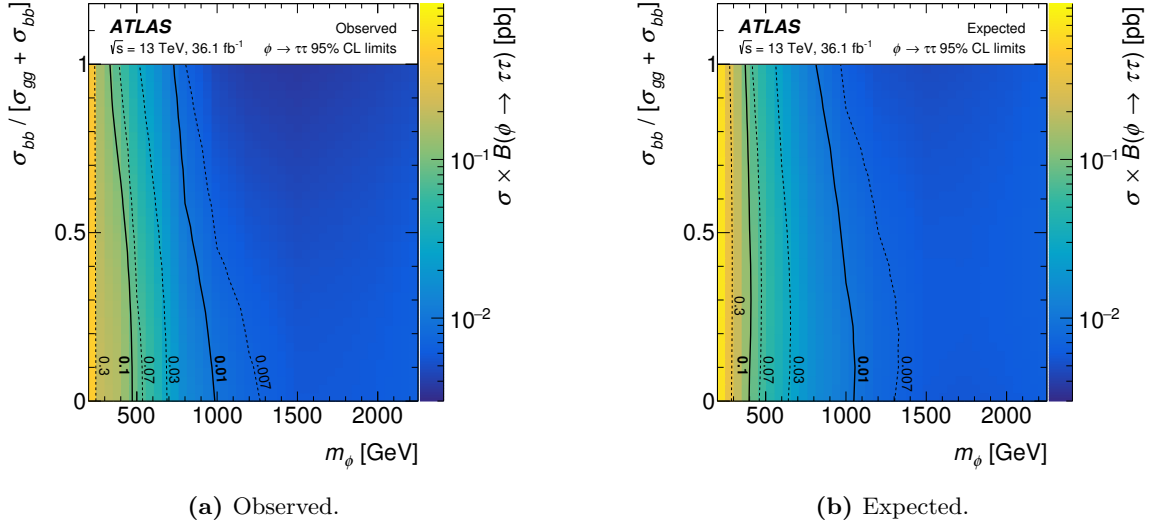
(a) Observed.

(b) Expected.

Figure 8. The (a) observed and (b) expected 95% CL upper limit on the production cross section times branching fraction for $\phi \to \tau\tau$ as a function of the fractional contribution from b-associated production and the scalar boson mass. The solid and dashed lines represent contours of fixed $\sigma \times B$.
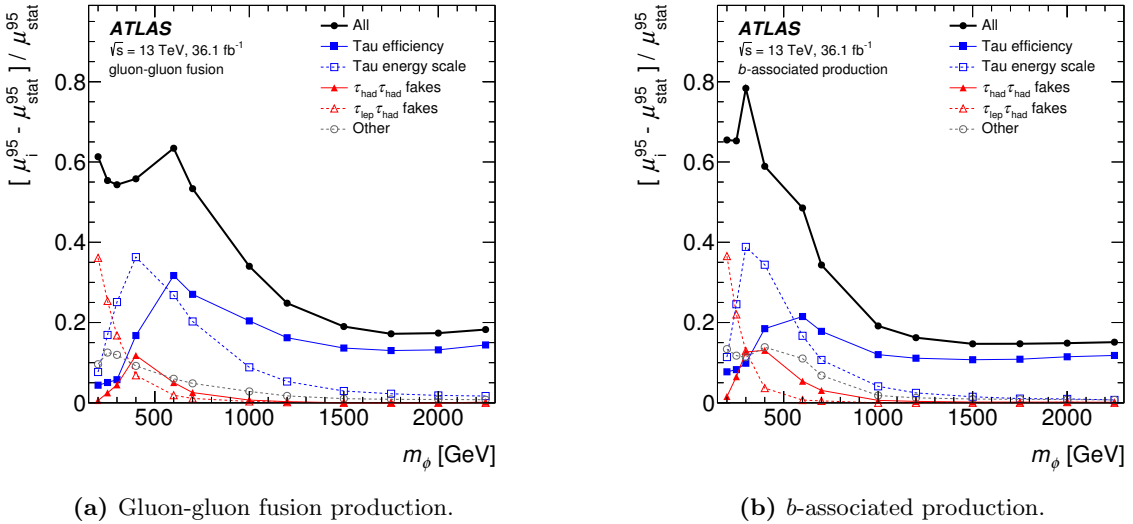

(a) Gluon-gluon fusion production.

(b) b-associated production.

Figure 9. Impact of major groups of systematic uncertainties on the $\phi \to \tau\tau$ 95% CL cross section upper limits as a function of the scalar boson mass, separately for the (a) gluon-gluon fusion and (b) b-associated production mechanisms.
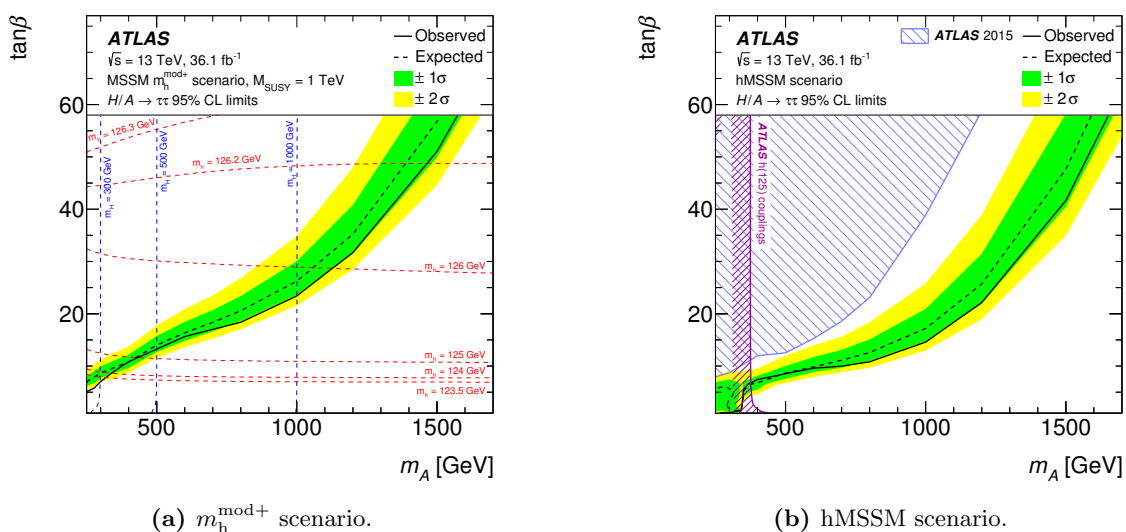
(a) $m_{\rm h}^{\rm mod+}$ scenario.

(b) hMSSM scenario.

Figure 10. The observed and expected 95% CL upper limits on $\tan\beta$ as a function of m_A in the MSSM (a) $m_{\rm h}^{\rm mod+}$ and (b) hMSSM scenarios. For the $m_{\rm h}^{\rm mod+}$ scenario, dashed lines of constant m_h and m_H are shown in red and blue, respectively. For the hMSSM scenario, the exclusion arising from the SM Higgs boson coupling measurements of ref. [143] and the exclusion limit from the ATLAS 2015 $H/A \to \tau\tau$ search result of ref. [29] are shown.

$m_{\rm h}^{\rm mod+}$ scenario, the observed (expected) 95% CL upper limits exclude $\tan\beta > 5.1$ (7.0) for $m_A = 0.25\,\text{TeV}$ and $\tan\beta > 51$ (57) for $m_A = 1.5\,\text{TeV}$. Constraints in the hMSSM scenario are stronger due to the presence of low-mass neutralinos in the $m_{\rm h}^{\rm mod+}$ scenario that reduce the $H/A \to \tau\tau$ branching fraction and which are absent in the hMSSM scenario. In the hMSSM scenario, the most stringent observed (expected) constraints on $\tan\beta$ for the combined search exclude $\tan\beta > 1.0$ (5.5) for $m_A = 0.25\,\text{TeV}$ and $\tan\beta > 42$ (48) for $m_A = 1.5\,\text{TeV}$ at 95% CL. The expected exclusion limit and bands around $m_A = 350\,\text{GeV}$ reflect the behaviour of the $A \to \tau\tau$ branching fraction close to the $A \to t\bar{t}$ kinematic threshold for low $\tan\beta$, allowing for some exclusion in this region. However, when m_A is above the $A \to t\bar{t}$ production threshold, this additional decay mode reduces the sensitivity of the $A \to \tau\tau$ search for low $\tan\beta$.

8.4 Z' interpretations

The data are also interpreted in terms of Z' models. As shown in figure 7(c), the observed (expected) lower limit on the mass of a $Z'_{\rm SSM}$ boson is 2.42 (2.47) TeV at 95% CL. Limits at 95% CL are also placed on $Z'_{\rm NU}$ bosons as a function of $m_{Z'}$ and the mixing angle between the heavy and light SU(2) gauge groups, ϕ, as shown in figure 11. Masses below 2.25–2.60 TeV are excluded in the range $0.03 < \sin^2\phi < 0.5$ assuming no μ–τ mixing.
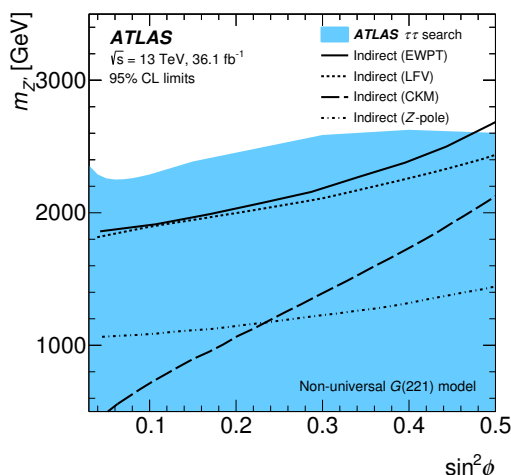
Figure 11. The 95% CL exclusion in the non-universal $G(221)$ parameter space overlaid with indirect upper limits at 95% CL from fits to electroweak precision measurements [144], lepton flavour violation [145], CKM unitarity [146] and Z-pole measurements [36].

9 Conclusion

A search for neutral Higgs bosons as predicted in the Minimal Supersymmetric Standard Model and Z' bosons decaying to a pair of τ-leptons is performed using a data sample from proton-proton collisions at $\sqrt{s} = 13$ TeV recorded by the ATLAS detector at the LHC, corresponding to an integrated luminosity of $36.1\,\mathrm{fb}^{-1}$. The $\tau_e\tau_{\mathrm{had}}$, $\tau_\mu\tau_{\mathrm{had}}$ and $\tau_{\mathrm{had}}\tau_{\mathrm{had}}$ channels are analysed and no indication of an excess over the expected SM background is found. Upper limits on the cross section for the production of scalar and Z' bosons times the branching fraction to ditau final states are set at 95% CL, significantly increasing the sensitivity and the explored mass range compared to previous searches. They are in the range 0.78–$0.0058\,\mathrm{pb}$ (0.70–$0.0037\,\mathrm{pb}$) for gluon-gluon fusion (b-associated) production of scalar bosons with masses of 0.2–$2.25\,\mathrm{TeV}$ and 1.56–$0.0072\,\mathrm{pb}$ for Drell-Yan production of Z' bosons with masses of 0.2–$4\,\mathrm{TeV}$. In the context of the hMSSM scenario, the most stringent limits for the combined search exclude $\tan\beta > 1.0$ for $m_A = 0.25\,\mathrm{TeV}$ and $\tan\beta > 42$ for $m_A = 1.5\,\mathrm{TeV}$ at 95% CL. In the context of the Sequential Standard Model, Z'_{SSM} bosons with masses less than $2.42\,\mathrm{TeV}$ are excluded at 95% CL, while $m_{Z'_{\mathrm{NU}}} < 2.25$–$2.60\,\mathrm{TeV}$ is excluded in the range $0.03 < \sin^2\phi < 0.5$ in the non-universal $G(221)$ model.

References

[1] ATLAS collaboration, *Observation of a new particle in the search for the Standard Model Higgs boson with the ATLAS detector at the LHC*, *Phys. Lett.* **B 716** (2012) 1 [arXiv:1207.7214] [INSPIRE].

[2] CMS collaboration, *Observation of a new boson at a mass of* 125 *GeV with the CMS experiment at the LHC*, *Phys. Lett.* **B 716** (2012) 30 [arXiv:1207.7235] [INSPIRE].

[3] L. Evans and P. Bryant, *LHC machine*, 2008 *JINST* **3** S08001 [INSPIRE].

[4] ATLAS collaboration, *Study of the spin and parity of the Higgs boson in diboson decays with the ATLAS detector*, *Eur. Phys. J.* **C 75** (2015) 476 [arXiv:1506.05669] [INSPIRE].

[5] ATLAS collaboration, *Measurements of the Higgs boson production and decay rates and coupling strengths using pp collision data at* $\sqrt{s} = 7$ *and* 8 *TeV in the ATLAS experiment*, *Eur. Phys. J.* **C 76** (2016) 6 [arXiv:1507.04548] [INSPIRE].

[6] CMS collaboration, *Precise determination of the mass of the Higgs boson and tests of compatibility of its couplings with the Standard Model predictions using proton collisions at* 7 *and* 8 *TeV*, *Eur. Phys. J.* **C 75** (2015) 212 [arXiv:1412.8662] [INSPIRE].

[7] CMS collaboration, *Constraints on the spin-parity and anomalous HVV couplings of the Higgs boson in proton collisions at 7 and 8 TeV*, *Phys. Rev.* **D 92** (2015) 012004 [arXiv:1411.3441] [InSPIRE].

[8] ATLAS and CMS collaborations, *Measurements of the Higgs boson production and decay rates and constraints on its couplings from a combined ATLAS and CMS analysis of the LHC pp collision data at $\sqrt{s} = 7$ and 8 TeV*, *JHEP* **08** (2016) 045 [arXiv:1606.02266] [InSPIRE].

[9] F. Englert and R. Brout, *Broken symmetry and the mass of gauge vector mesons*, *Phys. Rev. Lett.* **13** (1964) 321 [InSPIRE].

[10] P.W. Higgs, *Broken symmetries, massless particles and gauge fields*, *Phys. Lett.* **12** (1964) 132 [InSPIRE].

[11] P.W. Higgs, *Broken symmetries and the masses of gauge bosons*, *Phys. Rev. Lett.* **13** (1964) 508 [InSPIRE].

[12] P.W. Higgs, *Spontaneous symmetry breakdown without massless bosons*, *Phys. Rev.* **145** (1966) 1156 [InSPIRE].

[13] G.S. Guralnik, C.R. Hagen and T.W.B. Kibble, *Global conservation laws and massless particles*, *Phys. Rev. Lett.* **13** (1964) 585 [InSPIRE].

[14] T.W.B. Kibble, *Symmetry breaking in non-Abelian gauge theories*, *Phys. Rev.* **155** (1967) 1554 [InSPIRE].

[15] A. Djouadi, *The anatomy of electro-weak symmetry breaking II. The Higgs bosons in the minimal supersymmetric model*, *Phys. Rept.* **459** (2008) 1 [hep-ph/0503173] [InSPIRE].

[16] G.C. Branco, P.M. Ferreira, L. Lavoura, M.N. Rebelo, M. Sher and J.P. Silva, *Theory and phenomenology of two-Higgs-doublet models*, *Phys. Rept.* **516** (2012) 1 [arXiv:1106.0034] [InSPIRE].

[17] P. Fayet, *Supersymmetry and weak, electromagnetic and strong interactions*, *Phys. Lett.* **B 64** (1976) 159 [InSPIRE].

[18] P. Fayet, *Spontaneously broken supersymmetric theories of weak, electromagnetic and strong interactions*, *Phys. Lett.* **B 69** (1977) 489 [InSPIRE].

[19] M. Carena, S. Heinemeyer, O. Stål, C.E.M. Wagner and G. Weiglein, *MSSM Higgs boson searches at the LHC: benchmark scenarios after the discovery of a Higgs-like particle*, *Eur. Phys. J.* **C 73** (2013) 2552 [arXiv:1302.7033] [InSPIRE].

[20] A. Djouadi, L. Maiani, G. Moreau, A. Polosa, J. Quevillon and V. Riquer, *The post-Higgs MSSM scenario: habemus MSSM?*, *Eur. Phys. J.* **C 73** (2013) 2650 [arXiv:1307.5205] [InSPIRE].

[21] E. Bagnaschi et al., *Benchmark scenarios for low* $\tan\beta$ *in the MSSM*, LHCHXSWG-2015-002, CERN, Geneva Switzerland, (2015).

[22] DELPHI, OPAL, ALEPH, LEP Working Group for Higgs Boson Searches and L3 collaborations, S. Schael et al., *Search for neutral MSSM Higgs bosons at LEP*, *Eur. Phys. J.* **C 47** (2006) 547 [hep-ex/0602042] [InSPIRE].

[23] Tevatron New Phenomena & Higgs Working Group collaboration, D. Benjamin et al., *Combined CDF and D0 upper limits on MSSM Higgs boson production in* $\tau\tau$ *final states with up to* $2.2\,fb^{-1}$, arXiv:1003.3363 [InSPIRE].

[24] CDF collaboration, T. Aaltonen et al., *Search for Higgs bosons predicted in two-Higgs-doublet models via decays to τ lepton pairs in 1.96 TeV $p\bar{p}$ collisions*, *Phys. Rev. Lett.* **103** (2009) 201801 [arXiv:0906.1014] [INSPIRE].

[25] D0 collaboration, V.M. Abazov et al., *Search for Higgs bosons decaying to τ pairs in $p\bar{p}$ collisions with the D0 detector*, *Phys. Rev. Lett.* **101** (2008) 071804 [arXiv:0805.2491] [INSPIRE].

[26] CMS collaboration, *Search for neutral MSSM Higgs bosons decaying to a pair of τ leptons in pp collisions*, *JHEP* **10** (2014) 160 [arXiv:1408.3316] [INSPIRE].

[27] CMS collaboration, *Search for neutral MSSM Higgs bosons decaying into a pair of bottom quarks*, *JHEP* **11** (2015) 071 [arXiv:1506.08329] [INSPIRE].

[28] LHCb collaboration, *Limits on neutral Higgs boson production in the forward region in pp collisions at $\sqrt{s} = 7$ TeV*, *JHEP* **05** (2013) 132 [arXiv:1304.2591] [INSPIRE].

[29] ATLAS collaboration, *Search for minimal supersymmetric Standard Model Higgs bosons H/A and for a Z' boson in the $\tau\tau$ final state produced in pp collisions at $\sqrt{s} = 13$ TeV with the ATLAS detector*, *Eur. Phys. J.* **C 76** (2016) 585 [arXiv:1608.00890] [INSPIRE].

[30] J.L. Hewett and T.G. Rizzo, *Low-energy phenomenology of superstring inspired E_6 models*, *Phys. Rept.* **183** (1989) 193 [INSPIRE].

[31] M. Cvetič and S. Godfrey, *Discovery and identification of extra gauge bosons*, hep-ph/9504216 [INSPIRE].

[32] A. Leike, *The phenomenology of extra neutral gauge bosons*, *Phys. Rept.* **317** (1999) 143 [hep-ph/9805494] [INSPIRE].

[33] R. Diener, S. Godfrey and T.A.W. Martin, *Unravelling an extra neutral gauge boson at the LHC using third generation fermions*, *Phys. Rev.* **D 83** (2011) 115008 [arXiv:1006.2845] [INSPIRE].

[34] P. Langacker, *The physics of heavy Z' gauge bosons*, *Rev. Mod. Phys.* **81** (2009) 1199 [arXiv:0801.1345] [INSPIRE].

[35] K.R. Lynch, E.H. Simmons, M. Narain and S. Mrenna, *Finding Z' bosons coupled preferentially to the third family at LEP and the Tevatron*, *Phys. Rev.* **D 63** (2001) 035006 [hep-ph/0007286] [INSPIRE].

[36] E. Malkawi, T.M.P. Tait and C.-P. Yuan, *A model of strong flavor dynamics for the top quark*, *Phys. Lett.* **B 385** (1996) 304 [hep-ph/9603349] [INSPIRE].

[37] K. Hsieh, K. Schmitz, J.-H. Yu and C.-P. Yuan, *Global analysis of general $SU(2) \times SU(2) \times U(1)$ models with precision data*, *Phys. Rev.* **D 82** (2010) 035011 [arXiv:1003.3482] [INSPIRE].

[38] D.J. Muller and S. Nandi, *Top flavor: a separate $SU(2)$ for the third family*, *Phys. Lett.* **B 383** (1996) 345 [hep-ph/9602390] [INSPIRE].

[39] D.A. Faroughy, A. Greljo and J.F. Kamenik, *Confronting lepton flavor universality violation in B decays with high-p_T tau lepton searches at LHC*, *Phys. Lett.* **B 764** (2017) 126 [arXiv:1609.07138] [INSPIRE].

[40] R.S. Chivukula and E.H. Simmons, *Electroweak limits on nonuniversal Z' bosons*, *Phys. Rev.* **D 66** (2002) 015006 [hep-ph/0205064] [INSPIRE].

[41] ATLAS collaboration, *A search for high-mass resonances decaying to $\tau^+\tau^-$ in pp collisions at $\sqrt{s} = 8$ TeV with the ATLAS detector*, *JHEP* **07** (2015) 157 [arXiv:1502.07177] [INSPIRE].

[42] CMS collaboration, *Search for heavy resonances decaying to tau lepton pairs in proton-proton collisions at $\sqrt{s} = 13$ TeV*, *JHEP* **02** (2017) 048 [arXiv:1611.06594] [INSPIRE].

[43] ATLAS collaboration, *The ATLAS experiment at the CERN Large Hadron Collider*, 2008 *JINST* **3** S08003 [INSPIRE].

[44] ATLAS collaboration, *ATLAS insertable B-layer technical design report*, ATLAS-TDR-19, CERN, Geneva Switzerland, (2010) [*Addendum* ATLAS-TDR-19-ADD-1].

[45] ATLAS collaboration, *Performance of the ATLAS trigger system in* 2015, *Eur. Phys. J.* **C 77** (2017) 317 [arXiv:1611.09661] [INSPIRE].

[46] ATLAS collaboration, *Trigger menu in* 2016, ATL-DAQ-PUB-2017-001, CERN, Geneva Switzerland, (2017).

[47] ATLAS collaboration, *Selection of jets produced in* 13 *TeV proton-proton collisions with the ATLAS detector*, ATLAS-CONF-2015-029, CERN, Geneva Switzerland, (2015).

[48] P. Nason, *A new method for combining NLO QCD with shower Monte Carlo algorithms*, *JHEP* **11** (2004) 040 [hep-ph/0409146] [INSPIRE].

[49] S. Frixione, P. Nason and C. Oleari, *Matching NLO QCD computations with parton shower simulations: the POWHEG method*, *JHEP* **11** (2007) 070 [arXiv:0709.2092] [INSPIRE].

[50] S. Alioli, P. Nason, C. Oleari and E. Re, *A general framework for implementing NLO calculations in shower Monte Carlo programs: the POWHEG BOX*, *JHEP* **06** (2010) 043 [arXiv:1002.2581] [INSPIRE].

[51] J. Alwall et al., *The automated computation of tree-level and next-to-leading order differential cross sections and their matching to parton shower simulations*, *JHEP* **07** (2014) 079 [arXiv:1405.0301] [INSPIRE].

[52] M. Wiesemann, R. Frederix, S. Frixione, V. Hirschi, F. Maltoni and P. Torrielli, *Higgs production in association with bottom quarks*, *JHEP* **02** (2015) 132 [arXiv:1409.5301] [INSPIRE].

[53] H.-L. Lai et al., *New parton distributions for collider physics*, *Phys. Rev.* **D 82** (2010) 074024 [arXiv:1007.2241] [INSPIRE].

[54] S. Dulat et al., *New parton distribution functions from a global analysis of quantum chromodynamics*, *Phys. Rev.* **D 93** (2016) 033006 [arXiv:1506.07443] [INSPIRE].

[55] T. Sjöstrand et al., *An introduction to PYTHIA* 8.2, *Comput. Phys. Commun.* **191** (2015) 159 [arXiv:1410.3012] [INSPIRE].

[56] ATLAS collaboration, *Measurement of the Z/γ^* boson transverse momentum distribution in pp collisions at $\sqrt{s} = 7$ TeV with the ATLAS detector*, *JHEP* **09** (2014) 145 [arXiv:1406.3660] [INSPIRE].

[57] ATLAS collaboration, *ATLAS run* 1 *PYTHIA*8 *tunes*, ATL-PHYS-PUB-2014-021, CERN, Geneva Switzerland, (2014).

[58] J. Pumplin, D.R. Stump, J. Huston, H.L. Lai, P.M. Nadolsky and W.K. Tung, *New generation of parton distributions with uncertainties from global QCD analysis*, *JHEP* **07** (2002) 012 [hep-ph/0201195] [INSPIRE].

[59] R.D. Ball et al., *Parton distributions with LHC data*, *Nucl. Phys.* **B 867** (2013) 244 [arXiv:1207.1303] [INSPIRE].

[60] LHC HIGGS CROSS SECTION WORKING GROUP collaboration, D. de Florian et al., *Handbook of LHC Higgs cross sections: 4. Deciphering the nature of the Higgs sector*, arXiv:1610.07922 [INSPIRE].

[61] R.V. Harlander, S. Liebler and H. Mantler, *SusHi: a program for the calculation of Higgs production in gluon fusion and bottom-quark annihilation in the Standard Model and the MSSM*, *Comput. Phys. Commun.* **184** (2013) 1605 [arXiv:1212.3249] [INSPIRE].

[62] M. Spira, A. Djouadi, D. Graudenz and P.M. Zerwas, *Higgs boson production at the LHC*, *Nucl. Phys.* **B 453** (1995) 17 [hep-ph/9504378] [INSPIRE].

[63] R.V. Harlander and M. Steinhauser, *Supersymmetric Higgs production in gluon fusion at next-to-leading order*, *JHEP* **09** (2004) 066 [hep-ph/0409010] [INSPIRE].

[64] R. Harlander and P. Kant, *Higgs production and decay: analytic results at next-to-leading order QCD*, *JHEP* **12** (2005) 015 [hep-ph/0509189] [INSPIRE].

[65] G. Degrassi and P. Slavich, *NLO QCD bottom corrections to Higgs boson production in the MSSM*, *JHEP* **11** (2010) 044 [arXiv:1007.3465] [INSPIRE].

[66] G. Degrassi, S. Di Vita and P. Slavich, *NLO QCD corrections to pseudoscalar Higgs production in the MSSM*, *JHEP* **08** (2011) 128 [arXiv:1107.0914] [INSPIRE].

[67] G. Degrassi, S. Di Vita and P. Slavich, *On the NLO QCD corrections to the production of the heaviest neutral Higgs scalar in the MSSM*, *Eur. Phys. J.* **C 72** (2012) 2032 [arXiv:1204.1016] [INSPIRE].

[68] R.V. Harlander and W.B. Kilgore, *Next-to-next-to-leading order Higgs production at hadron colliders*, *Phys. Rev. Lett.* **88** (2002) 201801 [hep-ph/0201206] [INSPIRE].

[69] C. Anastasiou and K. Melnikov, *Higgs boson production at hadron colliders in NNLO QCD*, *Nucl. Phys.* **B 646** (2002) 220 [hep-ph/0207004] [INSPIRE].

[70] V. Ravindran, J. Smith and W.L. van Neerven, *NNLO corrections to the total cross-section for Higgs boson production in hadron hadron collisions*, *Nucl. Phys.* **B 665** (2003) 325 [hep-ph/0302135] [INSPIRE].

[71] R.V. Harlander and W.B. Kilgore, *Production of a pseudoscalar Higgs boson at hadron colliders at next-to-next-to leading order*, *JHEP* **10** (2002) 017 [hep-ph/0208096] [INSPIRE].

[72] C. Anastasiou and K. Melnikov, *Pseudoscalar Higgs boson production at hadron colliders in NNLO QCD*, *Phys. Rev.* **D 67** (2003) 037501 [hep-ph/0208115] [INSPIRE].

[73] U. Aglietti, R. Bonciani, G. Degrassi and A. Vicini, *Two loop light fermion contribution to Higgs production and decays*, *Phys. Lett.* **B 595** (2004) 432 [hep-ph/0404071] [INSPIRE].

[74] R. Bonciani, G. Degrassi and A. Vicini, *On the generalized harmonic polylogarithms of one complex variable*, *Comput. Phys. Commun.* **182** (2011) 1253 [arXiv:1007.1891] [INSPIRE].

[75] R.V. Harlander and W.B. Kilgore, *Higgs boson production in bottom quark fusion at next-to-next-to leading order*, *Phys. Rev.* **D 68** (2003) 013001 [hep-ph/0304035] [INSPIRE].

[76] S. Dittmaier, M. Krämer and M. Spira, *Higgs radiation off bottom quarks at the Tevatron and the CERN LHC*, *Phys. Rev.* **D 70** (2004) 074010 [hep-ph/0309204] [INSPIRE].

[77] S. Dawson, C.B. Jackson, L. Reina and D. Wackeroth, *Exclusive Higgs boson production with bottom quarks at hadron colliders*, *Phys. Rev.* **D 69** (2004) 074027 [hep-ph/0311067] [INSPIRE].

[78] R. Harlander, M. Krämer and M. Schumacher, *Bottom-quark associated Higgs-boson production: reconciling the four- and five-flavour scheme approach*, arXiv:1112.3478 [INSPIRE].

[79] S. Heinemeyer, W. Hollik and G. Weiglein, *FeynHiggs: a program for the calculation of the masses of the neutral CP even Higgs bosons in the MSSM*, *Comput. Phys. Commun.* **124** (2000) 76 [hep-ph/9812320] [INSPIRE].

[80] S. Heinemeyer, W. Hollik and G. Weiglein, *The masses of the neutral CP-even Higgs bosons in the MSSM: accurate analysis at the two loop level*, *Eur. Phys. J.* **C 9** (1999) 343 [hep-ph/9812472] [INSPIRE].

[81] G. Degrassi, S. Heinemeyer, W. Hollik, P. Slavich and G. Weiglein, *Towards high precision predictions for the MSSM Higgs sector*, *Eur. Phys. J.* **C 28** (2003) 133 [hep-ph/0212020] [INSPIRE].

[82] M. Frank, T. Hahn, S. Heinemeyer, W. Hollik, H. Rzehak and G. Weiglein, *The Higgs boson masses and mixings of the complex MSSM in the Feynman-diagrammatic approach*, *JHEP* **02** (2007) 047 [hep-ph/0611326] [INSPIRE].

[83] T. Hahn, S. Heinemeyer, W. Hollik, H. Rzehak and G. Weiglein, *High-precision predictions for the light CP-even Higgs boson mass of the minimal supersymmetric Standard Model*, *Phys. Rev. Lett.* **112** (2014) 141801 [arXiv:1312.4937] [INSPIRE].

[84] K.E. Williams, H. Rzehak and G. Weiglein, *Higher order corrections to Higgs boson decays in the MSSM with complex parameters*, *Eur. Phys. J.* **C 71** (2011) 1669 [arXiv:1103.1335] [INSPIRE].

[85] A. Djouadi, J. Kalinowski and M. Spira, *HDECAY: a program for Higgs boson decays in the Standard Model and its supersymmetric extension*, *Comput. Phys. Commun.* **108** (1998) 56 [hep-ph/9704448] [INSPIRE].

[86] A. Djouadi, M.M. Muhlleitner and M. Spira, *Decays of supersymmetric particles: the program SUSY-HIT (SUspect-SdecaY-HDECAY-InTerface)*, *Acta Phys. Polon.* **B 38** (2007) 635 [hep-ph/0609292] [INSPIRE].

[87] A. Bredenstein, A. Denner, S. Dittmaier and M.M. Weber, *Precise predictions for the Higgs-boson decay $H \to WW/ZZ \to 4$ leptons*, *Phys. Rev.* **D 74** (2006) 013004 [hep-ph/0604011] [INSPIRE].

[88] A. Bredenstein, A. Denner, S. Dittmaier and M.M. Weber, *Radiative corrections to the semileptonic and hadronic Higgs-boson decays $H \to WW/ZZ \to 4$ fermions*, *JHEP* **02** (2007) 080 [hep-ph/0611234] [INSPIRE].

[89] Z. Czyczula, T. Przedzinski and Z. Was, *TauSpinner program for studies on spin effect in tau production at the LHC*, *Eur. Phys. J.* **C 72** (2012) 1988 [arXiv:1201.0117] [INSPIRE].

[90] A. Kaczmarska, J. Piatlicki, T. Przedzinski, E. Richter-Was and Z. Was, *Application of TauSpinner for studies on τ-lepton polarization and spin correlations in Z, W and H decays at the LHC*, *Acta Phys. Polon.* **B 45** (2014) 1921 [arXiv:1402.2068] [INSPIRE].

[91] S. Banerjee, J. Kalinowski, W. Kotlarski, T. Przedzinski and Z. Was, *Ascertaining the spin for new resonances decaying into $\tau^+\tau^-$ at hadron colliders*, *Eur. Phys. J.* **C 73** (2013) 2313 [arXiv:1212.2873] [InSPIRE].

[92] T. Sjöstrand, S. Mrenna and P.Z. Skands, *A brief introduction to PYTHIA 8.1*, *Comput. Phys. Commun.* **178** (2008) 852 [arXiv:0710.3820] [InSPIRE].

[93] T. Sjöstrand, S. Mrenna and P.Z. Skands, *PYTHIA 6.4 physics and manual*, *JHEP* **05** (2006) 026 [hep-ph/0603175] [InSPIRE].

[94] C. Anastasiou, L.J. Dixon, K. Melnikov and F. Petriello, *High precision QCD at hadron colliders: electroweak gauge boson rapidity distributions at NNLO*, *Phys. Rev.* **D 69** (2004) 094008 [hep-ph/0312266] [InSPIRE].

[95] S. Alioli, P. Nason, C. Oleari and E. Re, *NLO Higgs boson production via gluon fusion matched with shower in POWHEG*, *JHEP* **04** (2009) 002 [arXiv:0812.0578] [InSPIRE].

[96] N. Davidson, T. Przedzinski and Z. Was, *PHOTOS interface in C++: technical and physics documentation*, *Comput. Phys. Commun.* **199** (2016) 86 [arXiv:1011.0937] [InSPIRE].

[97] S.G. Bondarenko and A.A. Sapronov, *NLO EW and QCD proton-proton cross section calculations with mcsanc-v1.01*, *Comput. Phys. Commun.* **184** (2013) 2343 [arXiv:1301.3687] [InSPIRE].

[98] A.D. Martin, R.G. Roberts, W.J. Stirling and R.S. Thorne, *Parton distributions incorporating QED contributions*, *Eur. Phys. J.* **C 39** (2005) 155 [hep-ph/0411040] [InSPIRE].

[99] T. Gleisberg et al., *Event generation with SHERPA 1.1*, *JHEP* **02** (2009) 007 [arXiv:0811.4622] [InSPIRE].

[100] T. Gleisberg and S. Höche, *Comix, a new matrix element generator*, *JHEP* **12** (2008) 039 [arXiv:0808.3674] [InSPIRE].

[101] F. Cascioli, P. Maierhofer and S. Pozzorini, *Scattering amplitudes with open loops*, *Phys. Rev. Lett.* **108** (2012) 111601 [arXiv:1111.5206] [InSPIRE].

[102] S. Schumann and F. Krauss, *A parton shower algorithm based on Catani-Seymour dipole factorisation*, *JHEP* **03** (2008) 038 [arXiv:0709.1027] [InSPIRE].

[103] S. Höche, F. Krauss, M. Schönherr and F. Siegert, *QCD matrix elements + parton showers: the NLO case*, *JHEP* **04** (2013) 027 [arXiv:1207.5030] [InSPIRE].

[104] K. Melnikov and F. Petriello, *Electroweak gauge boson production at hadron colliders through $O(\alpha_s^2)$*, *Phys. Rev.* **D 74** (2006) 114017 [hep-ph/0609070] [InSPIRE].

[105] R. Gavin, Y. Li, F. Petriello and S. Quackenbush, *FEWZ 2.0: a code for hadronic Z production at next-to-next-to-leading order*, *Comput. Phys. Commun.* **182** (2011) 2388 [arXiv:1011.3540] [InSPIRE].

[106] P. Artoisenet, R. Frederix, O. Mattelaer and R. Rietkerk, *Automatic spin-entangled decays of heavy resonances in Monte Carlo simulations*, *JHEP* **03** (2013) 015 [arXiv:1212.3460] [InSPIRE].

[107] P.Z. Skands, *Tuning Monte Carlo generators: the Perugia tunes*, *Phys. Rev.* **D 82** (2010) 074018 [arXiv:1005.3457] [InSPIRE].

[108] M. Czakon and A. Mitov, *Top++: a program for the calculation of the top-pair cross-section at hadron colliders*, *Comput. Phys. Commun.* **185** (2014) 2930 [arXiv:1112.5675] [INSPIRE].

[109] P. Kant et al., *HatHor for single top-quark production: updated predictions and uncertainty estimates for single top-quark production in hadronic collisions*, *Comput. Phys. Commun.* **191** (2015) 74 [arXiv:1406.4403] [INSPIRE].

[110] M. Aliev, H. Lacker, U. Langenfeld, S. Moch, P. Uwer and M. Wiedermann, *HATHOR: HAdronic Top and Heavy quarks crOss section calculatoR*, *Comput. Phys. Commun.* **182** (2011) 1034 [arXiv:1007.1327] [INSPIRE].

[111] N. Kidonakis, *Two-loop soft anomalous dimensions for single top quark associated production with a W^- or H^-*, *Phys. Rev.* **D 82** (2010) 054018 [arXiv:1005.4451] [INSPIRE].

[112] D.J. Lange, *The EvtGen particle decay simulation package*, *Nucl. Instrum. Meth.* **A 462** (2001) 152 [INSPIRE].

[113] ATLAS collaboration, *Summary of ATLAS PYTHIA 8 tunes*, ATL-PHYS-PUB-2012-003, CERN, Geneva Switzerland, (2012).

[114] A.D. Martin, W.J. Stirling, R.S. Thorne and G. Watt, *Parton distributions for the LHC*, *Eur. Phys. J.* **C 63** (2009) 189 [arXiv:0901.0002] [INSPIRE].

[115] GEANT4 collaboration, S. Agostinelli et al., *GEANT4: a simulation toolkit*, *Nucl. Instrum. Meth.* **A 506** (2003) 250 [INSPIRE].

[116] ATLAS collaboration, *The ATLAS simulation infrastructure*, *Eur. Phys. J.* **C 70** (2010) 823 [arXiv:1005.4568] [INSPIRE].

[117] ATLAS collaboration, *The simulation principle and performance of the ATLAS fast calorimeter simulation FastCaloSim*, ATL-PHYS-PUB-2010-013, CERN, Geneva Switzerland, (2010).

[118] ATLAS collaboration, *Electron reconstruction and identification efficiency measurements with the ATLAS detector using the* 2011 *LHC proton-proton collision data*, *Eur. Phys. J.* **C 74** (2014) 2941 [arXiv:1404.2240] [INSPIRE].

[119] ATLAS collaboration, *Electron and photon energy calibration with the ATLAS detector using LHC run* 1 *data*, *Eur. Phys. J.* **C 74** (2014) 3071 [arXiv:1407.5063] [INSPIRE].

[120] ATLAS collaboration, *Electron efficiency measurements with the ATLAS detector using the* 2015 *LHC proton-proton collision data*, ATLAS-CONF-2016-024, CERN, Geneva Switzerland, (2016).

[121] ATLAS collaboration, *Muon reconstruction performance of the ATLAS detector in proton-proton collision data at $\sqrt{s} = 13$ TeV*, *Eur. Phys. J.* **C 76** (2016) 292 [arXiv:1603.05598] [INSPIRE].

[122] ATLAS collaboration, *Topological cell clustering in the ATLAS calorimeters and its performance in LHC run* 1, *Eur. Phys. J.* **C 77** (2017) 490 [arXiv:1603.02934] [INSPIRE].

[123] M. Cacciari, G.P. Salam and G. Soyez, *The anti-k_t jet clustering algorithm*, *JHEP* **04** (2008) 063 [arXiv:0802.1189] [INSPIRE].

[124] M. Cacciari, G.P. Salam and G. Soyez, *FastJet user manual*, *Eur. Phys. J.* **C 72** (2012) 1896 [arXiv:1111.6097] [INSPIRE].

[125] ATLAS collaboration, *Jet energy scale measurements and their systematic uncertainties in proton-proton collisions at $\sqrt{s} = 13\,TeV$ with the ATLAS detector*, *Phys. Rev.* **D 96** (2017) 072002 [arXiv:1703.09665] [InSPIRE].

[126] ATLAS collaboration, *Performance of pile-up mitigation techniques for jets in pp collisions at $\sqrt{s} = 8\,TeV$ using the ATLAS detector*, *Eur. Phys. J.* **C 76** (2016) 581 [arXiv:1510.03823] [InSPIRE].

[127] ATLAS collaboration, *Performance of b-jet identification in the ATLAS experiment*, 2016 *JINST* **11** P04008 [arXiv:1512.01094] [InSPIRE].

[128] ATLAS collaboration, *Optimisation of the ATLAS b-tagging performance for the* 2016 *LHC run*, ATL-PHYS-PUB-2016-012, CERN, Geneva Switzerland, (2016).

[129] ATLAS collaboration, *Identification and energy calibration of hadronically decaying tau leptons with the ATLAS experiment in pp collisions at $\sqrt{s} = 8\,TeV$*, *Eur. Phys. J.* **C 75** (2015) 303 [arXiv:1412.7086] [InSPIRE].

[130] ATLAS collaboration, *Reconstruction, energy calibration and identification of hadronically decaying tau leptons in the ATLAS experiment for run-2 of the LHC*, ATL-PHYS-PUB-2015-045, CERN, Geneva Switzerland, (2015).

[131] ATLAS collaboration, *Measurement of the tau lepton reconstruction and identification performance in the ATLAS experiment using pp collisions at $\sqrt{s} = 13\,TeV$*, ATLAS-CONF-2017-029, CERN, Geneva Switzerland, (2017).

[132] ATLAS collaboration, *Performance of missing transverse momentum reconstruction for the ATLAS detector in the first proton-proton collisions at at $\sqrt{s} = 13\,TeV$*, ATL-PHYS-PUB-2015-027, CERN, Geneva Switzerland, (2015).

[133] ATLAS collaboration, *Expected performance of missing transverse momentum reconstruction for the ATLAS detector at $\sqrt{s} = 13\,TeV$*, ATL-PHYS-PUB-2015-023, CERN, Geneva Switzerland, (2015).

[134] ATLAS collaboration, *Luminosity determination in pp collisions at $\sqrt{s} = 8\,TeV$ using the ATLAS detector at the LHC*, *Eur. Phys. J.* **C 76** (2016) 653 [arXiv:1608.03953] [InSPIRE].

[135] ATLAS collaboration, *Search for high-mass new phenomena in the dilepton final state using proton-proton collisions at $\sqrt{s} = 13\,TeV$ with the ATLAS detector*, *Phys. Lett.* **B 761** (2016) 372 [arXiv:1607.03669] [InSPIRE].

[136] J.M. Campbell, R.K. Ellis and C. Williams, *Vector boson pair production at the LHC*, *JHEP* **07** (2011) 018 [arXiv:1105.0020] [InSPIRE].

[137] ATLAS collaboration, *Simulation of top quark production for the ATLAS experiment at $\sqrt{s} = 13\,TeV$*, ATL-PHYS-PUB-2016-004, CERN, Geneva Switzerland, (2016).

[138] M. Bahr et al., *HERWIG++ physics and manual*, *Eur. Phys. J.* **C 58** (2008) 639 [arXiv:0803.0883] [InSPIRE].

[139] NNPDF collaboration, R.D. Ball et al., *Parton distributions for the LHC run II*, *JHEP* **04** (2015) 040 [arXiv:1410.8849] [InSPIRE].

[140] G. Choudalakis and D. Casadei, *Plotting the differences between data and expectation*, *Eur. Phys. J. Plus* **127** (2012) 25 [arXiv:1111.2062] [InSPIRE].

[141] G. Cowan, K. Cranmer, E. Gross and O. Vitells, *Asymptotic formulae for likelihood-based tests of new physics*, *Eur. Phys. J.* **C 71** (2011) 1554 [*Erratum ibid.* **C 73** (2013) 2501] [arXiv:1007.1727] [InSPIRE].

[142] A.L. Read, *Presentation of search results: the CL_s technique*, *J. Phys.* **G 28** (2002) 2693 [InSPIRE].

[143] ATLAS collaboration, *Constraints on new phenomena via Higgs boson couplings and invisible decays with the ATLAS detector*, *JHEP* **11** (2015) 206 [arXiv:1509.00672] [InSPIRE].

[144] Q.-H. Cao, Z. Li, J.-H. Yu and C.-P. Yuan, *Discovery and identification of W' and Z' in SU(2) × SU(2) × U(1) models at the LHC*, *Phys. Rev.* **D 86** (2012) 095010 [arXiv:1205.3769] [InSPIRE].

[145] K.Y. Lee, *Lepton flavour violation in a nonuniversal gauge interaction model*, *Phys. Rev.* **D 82** (2010) 097701 [arXiv:1009.0104] [InSPIRE].

[146] K.Y. Lee, *Unitarity of the CKM matrix in a nonuniversal gauge interaction model*, *Phys. Rev.* **D 71** (2005) 115008 [hep-ph/0410381] [InSPIRE].

[147] ATLAS collaboration, *ATLAS computing acknowledgements* 2016–2017, ATL-GEN-PUB-2016-002, CERN, Geneva Switzerland, (2016).

The ATLAS collaboration

M. Aaboud[137d], G. Aad[88], B. Abbott[115], O. Abdinov[12,*], B. Abeloos[119], S.H. Abidi[161],
O.S. AbouZeid[139], N.L. Abraham[151], H. Abramowicz[155], H. Abreu[154], R. Abreu[118],
Y. Abulaiti[148a,148b], B.S. Acharya[167a,167b,a], S. Adachi[157], L. Adamczyk[41a], J. Adelman[110],
M. Adersberger[102], T. Adye[133], A.A. Affolder[139], Y. Afik[154], T. Agatonovic-Jovin[14],
C. Agheorghiesei[28c], J.A. Aguilar-Saavedra[128a,128f], S.P. Ahlen[24], F. Ahmadov[68,b],
G. Aielli[135a,135b], S. Akatsuka[71], H. Akerstedt[148a,148b], T.P.A. Åkesson[84], E. Akilli[52],
A.V. Akimov[98], G.L. Alberghi[22a,22b], J. Albert[172], P. Albicocco[50], M.J. Alconada Verzini[74],
S.C. Alderweireldt[108], M. Aleksa[32], I.N. Aleksandrov[68], C. Alexa[28b], G. Alexander[155],
T. Alexopoulos[10], M. Alhroob[115], B. Ali[130], M. Aliev[76a,76b], G. Alimonti[94a], J. Alison[33],
S.P. Alkire[38], B.M.M. Allbrooke[151], B.W. Allen[118], P.P. Allport[19], A. Aloisio[106a,106b],
A. Alonso[39], F. Alonso[74], C. Alpigiani[140], A.A. Alshehri[56], M.I. Alstaty[88], B. Alvarez Gonzalez[32],
D. Álvarez Piqueras[170], M.G. Alviggi[106a,106b], B.T. Amadio[16], Y. Amaral Coutinho[26a],
C. Amelung[25], D. Amidei[92], S.P. Amor Dos Santos[128a,128c], S. Amoroso[32], G. Amundsen[25],
C. Anastopoulos[141], L.S. Ancu[52], N. Andari[19], T. Andeen[11], C.F. Anders[60b], J.K. Anders[77],
K.J. Anderson[33], A. Andreazza[94a,94b], V. Andrei[60a], S. Angelidakis[37], I. Angelozzi[109],
A. Angerami[38], A.V. Anisenkov[111,c], N. Anjos[13], A. Annovi[126a,126b], C. Antel[60a], M. Antonelli[50],
A. Antonov[100,*], D.J. Antrim[166], F. Anulli[134a], M. Aoki[69], L. Aperio Bella[32], G. Arabidze[93],
Y. Arai[69], J.P. Araque[128a], V. Araujo Ferraz[26a], A.T.H. Arce[48], R.E. Ardell[80], F.A. Arduh[74],
J-F. Arguin[97], S. Argyropoulos[66], M. Arik[20a], A.J. Armbruster[32], L.J. Armitage[79], O. Arnaez[161],
H. Arnold[51], M. Arratia[30], O. Arslan[23], A. Artamonov[99,*], G. Artoni[122], S. Artz[86], S. Asai[157],
N. Asbah[45], A. Ashkenazi[155], L. Asquith[151], K. Assamagan[27], R. Astalos[146a], M. Atkinson[169],
N.B. Atlay[143], K. Augsten[130], G. Avolio[32], B. Axen[16], M.K. Ayoub[35a], G. Azuelos[97,d],
A.E. Baas[60a], M.J. Baca[19], H. Bachacou[138], K. Bachas[76a,76b], M. Backes[122], P. Bagnaia[134a,134b],
M. Bahmani[42], H. Bahrasemani[144], A.J. Bailey[170], J.T. Baines[133], M. Bajic[39], O.K. Baker[179],
P.J. Bakker[109], E.M. Baldin[111,c], P. Balek[175], F. Balli[138], W.K. Balunas[124], E. Banas[42],
A. Bandyopadhyay[23], Sw. Banerjee[176,e], A.A.E. Bannoura[178], L. Barak[155], E.L. Barberio[91],
D. Barberis[53a,53b], M. Barbero[88], T. Barillari[103], M-S Barisits[32], J.T. Barkeloo[118], T. Barklow[145],
N. Barlow[30], S.L. Barnes[36c], B.M. Barnett[133], R.M. Barnett[16], Z. Barnovska-Blenessy[36a],
A. Baroncelli[136a], G. Barone[25], A.J. Barr[122], L. Barranco Navarro[170], F. Barreiro[85],
J. Barreiro Guimarães da Costa[35a], R. Bartoldus[145], A.E. Barton[75], P. Bartos[146a], A. Basalaev[125],
A. Bassalat[119,f], R.L. Bates[56], S.J. Batista[161], J.R. Batley[30], M. Battaglia[139], M. Bauce[134a,134b],
F. Bauer[138], H.S. Bawa[145,g], J.B. Beacham[113], M.D. Beattie[75], T. Beau[83], P.H. Beauchemin[165],
P. Bechtle[23], H.P. Beck[18,h], H.C. Beck[57], K. Becker[122], M. Becker[86], C. Becot[112], A.J. Beddall[20e],
A. Beddall[20b], V.A. Bednyakov[68], M. Bedognetti[109], C.P. Bee[150], T.A. Beermann[32],
M. Begalli[26a], M. Begel[27], J.K. Behr[45], A.S. Bell[81], G. Bella[155], L. Bellagamba[22a], A. Bellerive[31],
M. Bellomo[154], K. Belotskiy[100], O. Beltramello[32], N.L. Belyaev[100], O. Benary[155,*],
D. Benchekroun[137a], M. Bender[102], N. Benekos[10], Y. Benhammou[155], E. Benhar Noccioli[179],
J. Benitez[66], D.P. Benjamin[48], M. Benoit[52], J.R. Bensinger[25], S. Bentvelsen[109], L. Beresford[122],
M. Beretta[50], D. Berge[109], E. Bergeaas Kuutmann[168], N. Berger[5], L.J. Bergsten[25], J. Beringer[16],
S. Berlendis[58], N.R. Bernard[89], G. Bernardi[83], C. Bernius[145], F.U. Bernlochner[23], T. Berry[80],
P. Berta[86], C. Bertella[35a], G. Bertoli[148a,148b], I.A. Bertram[75], C. Bertsche[45], G.J. Besjes[39],
O. Bessidskaia Bylund[148a,148b], M. Bessner[45], N. Besson[138], A. Bethani[87], S. Bethke[103],
A. Betti[23], A.J. Bevan[79], J. Beyer[103], R.M. Bianchi[127], O. Biebel[102], D. Biedermann[17],
R. Bielski[87], K. Bierwagen[86], N.V. Biesuz[126a,126b], M. Biglietti[136a], T.R.V. Billoud[97],
H. Bilokon[50], M. Bindi[57], A. Bingul[20b], C. Bini[134a,134b], S. Biondi[22a,22b], T. Bisanz[57],
C. Bittrich[47], D.M. Bjergaard[48], J.E. Black[145], K.M. Black[24], R.E. Blair[6], T. Blazek[146a],

I. Bloch[45], C. Blocker[25], A. Blue[56], U. Blumenschein[79], S. Blunier[34a], G.J. Bobbink[109],
V.S. Bobrovnikov[111,c], S.S. Bocchetta[84], A. Bocci[48], C. Bock[102], M. Boehler[51], D. Boerner[178],
D. Bogavac[102], A.G. Bogdanchikov[111], C. Bohm[148a], V. Boisvert[80], P. Bokan[168,i], T. Bold[41a],
A.S. Boldyrev[101], A.E. Bolz[60b], M. Bomben[83], M. Bona[79], M. Boonekamp[138], A. Borisov[132],
G. Borissov[75], J. Bortfeldt[32], D. Bortoletto[122], V. Bortolotto[62a], D. Boscherini[22a], M. Bosman[13],
J.D. Bossio Sola[29], J. Boudreau[127], E.V. Bouhova-Thacker[75], D. Boumediene[37], C. Bourdarios[119],
S.K. Boutle[56], A. Boveia[113], J. Boyd[32], I.R. Boyko[68], A.J. Bozson[80], J. Bracinik[19], A. Brandt[8],
G. Brandt[57], O. Brandt[60a], F. Braren[45], U. Bratzler[158], B. Brau[89], J.E. Brau[118],
W.D. Breaden Madden[56], K. Brendlinger[45], A.J. Brennan[91], L. Brenner[109], R. Brenner[168],
S. Bressler[175], D.L. Briglin[19], T.M. Bristow[49], D. Britton[56], D. Britzger[45], F.M. Brochu[30],
I. Brock[23], R. Brock[93], G. Brooijmans[38], T. Brooks[80], W.K. Brooks[34b], J. Brosamer[16],
E. Brost[110], J.H Broughton[19], P.A. Bruckman de Renstrom[42], D. Bruncko[146b], A. Bruni[22a],
G. Bruni[22a], L.S. Bruni[109], S. Bruno[135a,135b], BH Brunt[30], M. Bruschi[22a], N. Bruscino[127],
P. Bryant[33], L. Bryngemark[45], T. Buanes[15], Q. Buat[144], P. Buchholz[143], A.G. Buckley[56],
I.A. Budagov[68], F. Buehrer[51], M.K. Bugge[121], O. Bulekov[100], D. Bullock[8], T.J. Burch[110],
S. Burdin[77], C.D. Burgard[109], A.M. Burger[5], B. Burghgrave[110], K. Burka[42], S. Burke[133],
I. Burmeister[46], J.T.P. Burr[122], D. Büscher[51], V. Büscher[86], P. Bussey[56], J.M. Butler[24],
C.M. Buttar[56], J.M. Butterworth[81], P. Butti[32], W. Buttinger[27], A. Buzatu[153],
A.R. Buzykaev[111,c], C.-Q. Li[36a], S. Cabrera Urbán[170], D. Caforio[130], H. Cai[169],
V.M. Cairo[40a,40b], O. Cakir[4a], N. Calace[52], P. Calafiura[16], A. Calandri[88], G. Calderini[83],
P. Calfayan[64], G. Callea[40a,40b], L.P. Caloba[26a], S. Calvente Lopez[85], D. Calvet[37], S. Calvet[37],
T.P. Calvet[88], R. Camacho Toro[33], S. Camarda[32], P. Camarri[135a,135b], D. Cameron[121],
R. Caminal Armadans[169], C. Camincher[58], S. Campana[32], M. Campanelli[81], A. Camplani[94a,94b],
A. Campoverde[143], V. Canale[106a,106b], M. Cano Bret[36c], J. Cantero[116], T. Cao[155],
M.D.M. Capeans Garrido[32], I. Caprini[28b], M. Caprini[28b], M. Capua[40a,40b], R.M. Carbone[38],
R. Cardarelli[135a], F. Cardillo[51], I. Carli[131], T. Carli[32], G. Carlino[106a], B.T. Carlson[127],
L. Carminati[94a,94b], R.M.D. Carney[148a,148b], S. Caron[108], E. Carquin[34b], S. Carrá[94a,94b],
G.D. Carrillo-Montoya[32], D. Casadei[19], M.P. Casado[13,j], A.F. Casha[161], M. Casolino[13],
D.W. Casper[166], R. Castelijn[109], V. Castillo Gimenez[170], N.F. Castro[128a,k], A. Catinaccio[32],
J.R. Catmore[121], A. Cattai[32], J. Caudron[23], V. Cavaliere[169], E. Cavallaro[13], D. Cavalli[94a],
M. Cavalli-Sforza[13], V. Cavasinni[126a,126b], E. Celebi[20d], F. Ceradini[136a,136b], L. Cerda Alberich[170],
A.S. Cerqueira[26b], A. Cerri[151], L. Cerrito[135a,135b], F. Cerutti[16], A. Cervelli[22a,22b], S.A. Cetin[20d],
A. Chafaq[137a], D. Chakraborty[110], S.K. Chan[59], W.S. Chan[109], Y.L. Chan[62a], P. Chang[169],
J.D. Chapman[30], D.G. Charlton[19], C.C. Chau[31], C.A. Chavez Barajas[151], S. Che[113],
S. Cheatham[167a,167c], A. Chegwidden[93], S. Chekanov[6], S.V. Chekulaev[163a], G.A. Chelkov[68,l],
M.A. Chelstowska[32], C. Chen[36a], C. Chen[67], H. Chen[27], J. Chen[36a], S. Chen[35b], S. Chen[157],
X. Chen[35c,m], Y. Chen[70], H.C. Cheng[92], H.J. Cheng[35a,35d], A. Cheplakov[68],
E. Cheremushkina[132], R. Cherkaoui El Moursli[137e], E. Cheu[7], K. Cheung[63], L. Chevalier[138],
V. Chiarella[50], G. Chiarelli[126a,126b], G. Chiodini[76a], A.S. Chisholm[32], A. Chitan[28b], Y.H. Chiu[172],
M.V. Chizhov[68], K. Choi[64], A.R. Chomont[37], S. Chouridou[156], Y.S. Chow[62a], V. Christodoulou[81],
M.C. Chu[62a], J. Chudoba[129], A.J. Chuinard[90], J.J. Chwastowski[42], L. Chytka[117], A.K. Ciftci[4a],
D. Cinca[46], V. Cindro[78], I.A. Cioara[23], A. Ciocio[16], F. Cirotto[106a,106b], Z.H. Citron[175],
M. Citterio[94a], M. Ciubancan[28b], A. Clark[52], B.L. Clark[59], M.R. Clark[38], P.J. Clark[49],
R.N. Clarke[16], C. Clement[148a,148b], Y. Coadou[88], M. Cobal[167a,167c], A. Coccaro[52], J. Cochran[67],
L. Colasurdo[108], B. Cole[38], A.P. Colijn[109], J. Collot[58], T. Colombo[166], P. Conde Muiño[128a,128b],
E. Coniavitis[51], S.H. Connell[147b], I.A. Connelly[87], S. Constantinescu[28b], G. Conti[32],
F. Conventi[106a,n], M. Cooke[16], A.M. Cooper-Sarkar[122], F. Cormier[171], K.J.R. Cormier[161],
M. Corradi[134a,134b], F. Corriveau[90,o], A. Cortes-Gonzalez[32], G. Costa[94a], M.J. Costa[170],

D. Costanzo[141], G. Cottin[30], G. Cowan[80], B.E. Cox[87], K. Cranmer[112], S.J. Crawley[56],
R.A. Creager[124], G. Cree[31], S. Crépé-Renaudin[58], F. Crescioli[83], W.A. Cribbs[148a,148b],
M. Cristinziani[23], V. Croft[112], G. Crosetti[40a,40b], A. Cueto[85], T. Cuhadar Donszelmann[141],
A.R. Cukierman[145], J. Cummings[179], M. Curatolo[50], J. Cúth[86], S. Czekierda[42], P. Czodrowski[32],
G. D'amen[22a,22b], S. D'Auria[56], L. D'eramo[83], M. D'Onofrio[77],
M.J. Da Cunha Sargedas De Sousa[128a,128b], C. Da Via[87], W. Dabrowski[41a], T. Dado[146a],
T. Dai[92], O. Dale[15], F. Dallaire[97], C. Dallapiccola[89], M. Dam[39], J.R. Dandoy[124], M.F. Daneri[29],
N.P. Dang[176], A.C. Daniells[19], N.S. Dann[87], M. Danninger[171], M. Dano Hoffmann[138], V. Dao[150],
G. Darbo[53a], S. Darmora[8], J. Dassoulas[3], A. Dattagupta[118], T. Daubney[45], W. Davey[23],
C. David[45], T. Davidek[131], D.R. Davis[48], P. Davison[81], E. Dawe[91], I. Dawson[141], K. De[8],
R. de Asmundis[106a], A. De Benedetti[115], S. De Castro[22a,22b], S. De Cecco[83], N. De Groot[108],
P. de Jong[109], H. De la Torre[93], F. De Lorenzi[67], A. De Maria[57], D. De Pedis[134a],
A. De Salvo[134a], U. De Sanctis[135a,135b], A. De Santo[151], K. De Vasconcelos Corga[88],
J.B. De Vivie De Regie[119], R. Debbe[27], C. Debenedetti[139], D.V. Dedovich[68], N. Dehghanian[3],
I. Deigaard[109], M. Del Gaudio[40a,40b], J. Del Peso[85], D. Delgove[119], F. Deliot[138], C.M. Delitzsch[7],
A. Dell'Acqua[32], L. Dell'Asta[24], M. Dell'Orso[126a,126b], M. Della Pietra[106a,106b], d. della Volpe[52],
M. Delmastro[5], C. Delporte[119], P.A. Delsart[58], D.A. DeMarco[161], S. Demers[179], M. Demichev[68],
A. Demilly[83], S.P. Denisov[132], D. Denysiuk[138], D. Derendarz[42], J.E. Derkaoui[137d], F. Derue[83],
P. Dervan[77], K. Desch[23], C. Deterre[45], K. Dette[161], M.R. Devesa[29], P.O. Deviveiros[32],
A. Dewhurst[133], S. Dhaliwal[25], F.A. Di Bello[52], A. Di Ciaccio[135a,135b], L. Di Ciaccio[5],
W.K. Di Clemente[124], C. Di Donato[106a,106b], A. Di Girolamo[32], B. Di Girolamo[32],
B. Di Micco[136a,136b], R. Di Nardo[32], K.F. Di Petrillo[59], A. Di Simone[51], R. Di Sipio[161],
D. Di Valentino[31], C. Diaconu[88], M. Diamond[161], F.A. Dias[39], M.A. Diaz[34a], E.B. Diehl[92],
J. Dietrich[17], S. Díez Cornell[45], A. Dimitrievska[14], J. Dingfelder[23], P. Dita[28b], S. Dita[28b],
F. Dittus[32], F. Djama[88], T. Djobava[54b], J.I. Djuvsland[60a], M.A.B. do Vale[26c], D. Dobos[32],
M. Dobre[28b], D. Dodsworth[25], C. Doglioni[84], J. Dolejsi[131], Z. Dolezal[131], M. Donadelli[26d],
S. Donati[126a,126b], P. Dondero[123a,123b], J. Donini[37], J. Dopke[133], A. Doria[106a], M.T. Dova[74],
A.T. Doyle[56], E. Drechsler[57], M. Dris[10], Y. Du[36b], J. Duarte-Campderros[155], F. Dubinin[98],
A. Dubreuil[52], E. Duchovni[175], G. Duckeck[102], A. Ducourthial[83], O.A. Ducu[97,p], D. Duda[109],
A. Dudarev[32], A.Chr. Dudder[86], E.M. Duffield[16], L. Duflot[119], M. Dührssen[32], C. Dulsen[178],
M. Dumancic[175], A.E. Dumitriu[28b], A.K. Duncan[56], M. Dunford[60a], A. Duperrin[88],
H. Duran Yildiz[4a], M. Düren[55], A. Durglishvili[54b], D. Duschinger[47], B. Dutta[45], D. Duvnjak[1],
M. Dyndal[45], B.S. Dziedzic[42], C. Eckardt[45], K.M. Ecker[103], R.C. Edgar[92], T. Eifert[32], G. Eigen[15],
K. Einsweiler[16], T. Ekelof[168], M. El Kacimi[137c], R. El Kosseifi[88], V. Ellajosyula[88], M. Ellert[168],
S. Elles[5], F. Ellinghaus[178], A.A. Elliot[172], N. Ellis[32], J. Elmsheuser[27], M. Elsing[32],
D. Emeliyanov[133], Y. Enari[157], J.S. Ennis[173], M.B. Epland[48], J. Erdmann[46], A. Ereditato[18],
M. Ernst[27], S. Errede[169], M. Escalier[119], C. Escobar[170], B. Esposito[50], O. Estrada Pastor[170],
A.I. Etienvre[138], E. Etzion[155], H. Evans[64], A. Ezhilov[125], M. Ezzi[137e], F. Fabbri[22a,22b],
L. Fabbri[22a,22b], V. Fabiani[108], G. Facini[81], R.M. Fakhrutdinov[132], S. Falciano[134a], R.J. Falla[81],
J. Faltova[32], Y. Fang[35a], M. Fanti[94a,94b], A. Farbin[8], A. Farilla[136a], C. Farina[127],
E.M. Farina[123a,123b], T. Farooque[93], S. Farrell[16], S.M. Farrington[173], P. Farthouat[32], F. Fassi[137e],
P. Fassnacht[32], D. Fassouliotis[9], M. Faucci Giannelli[49], A. Favareto[53a,53b], W.J. Fawcett[122],
L. Fayard[119], O.L. Fedin[125,q], W. Fedorko[171], S. Feigl[121], L. Feligioni[88], C. Feng[36b], E.J. Feng[32],
M.J. Fenton[56], A.B. Fenyuk[132], L. Feremenga[8], P. Fernandez Martinez[170], J. Ferrando[45],
A. Ferrari[168], P. Ferrari[109], R. Ferrari[123a], D.E. Ferreira de Lima[60b], A. Ferrer[170], D. Ferrere[52],
C. Ferretti[92], F. Fiedler[86], A. Filipčič[78], M. Filipuzzi[45], F. Filthaut[108], M. Fincke-Keeler[172],
K.D. Finelli[24], M.C.N. Fiolhais[128a,128c,r], L. Fiorini[170], A. Fischer[2], C. Fischer[13], J. Fischer[178],
W.C. Fisher[93], N. Flaschel[45], I. Fleck[143], P. Fleischmann[92], R.R.M. Fletcher[124], T. Flick[178],

B.M. Flierl[102], L.R. Flores Castillo[62a], M.J. Flowerdew[103], G.T. Forcolin[87], A. Formica[138],
F.A. Förster[13], A. Forti[87], A.G. Foster[19], D. Fournier[119], H. Fox[75], S. Fracchia[141],
P. Francavilla[126a,126b], M. Franchini[22a,22b], S. Franchino[60a], D. Francis[32], L. Franconi[121],
M. Franklin[59], M. Frate[166], M. Fraternali[123a,123b], D. Freeborn[81], S.M. Fressard-Batraneanu[32],
B. Freund[97], D. Froidevaux[32], J.A. Frost[122], C. Fukunaga[158], T. Fusayasu[104], J. Fuster[170],
O. Gabizon[154], A. Gabrielli[22a,22b], A. Gabrielli[16], G.P. Gach[41a], S. Gadatsch[32], S. Gadomski[80],
G. Gagliardi[53a,53b], L.G. Gagnon[97], C. Galea[108], B. Galhardo[128a,128c], E.J. Gallas[122],
B.J. Gallop[133], P. Gallus[130], G. Galster[39], K.K. Gan[113], S. Ganguly[37], Y. Gao[77], Y.S. Gao[145,g],
F.M. Garay Walls[34a], C. García[170], J.E. García Navarro[170], J.A. García Pascual[35a],
M. Garcia-Sciveres[16], R.W. Gardner[33], N. Garelli[145], V. Garonne[121], A. Gascon Bravo[45],
K. Gasnikova[45], C. Gatti[50], A. Gaudiello[53a,53b], G. Gaudio[123a], I.L. Gavrilenko[98], C. Gay[171],
G. Gaycken[23], E.N. Gazis[10], C.N.P. Gee[133], J. Geisen[57], M. Geisen[86], M.P. Geisler[60a],
K. Gellerstedt[148a,148b], C. Gemme[53a], M.H. Genest[58], C. Geng[92], S. Gentile[134a,134b],
C. Gentsos[156], S. George[80], D. Gerbaudo[13], G. Geßner[46], S. Ghasemi[143], M. Ghneimat[23],
B. Giacobbe[22a], S. Giagu[134a,134b], N. Giangiacomi[22a,22b], P. Giannetti[126a,126b], S.M. Gibson[80],
M. Gignac[171], M. Gilchriese[16], D. Gillberg[31], G. Gilles[178], D.M. Gingrich[3,d],
M.P. Giordani[167a,167c], F.M. Giorgi[22a], P.F. Giraud[138], P. Giromini[59], G. Giugliarelli[167a,167c],
D. Giugni[94a], F. Giuli[122], C. Giuliani[103], M. Giulini[60b], B.K. Gjelsten[121], S. Gkaitatzis[156],
I. Gkialas[9,s], E.L. Gkougkousis[13], P. Gkountoumis[10], L.K. Gladilin[101], C. Glasman[85],
J. Glatzer[13], P.C.F. Glaysher[45], A. Glazov[45], M. Goblirsch-Kolb[25], J. Godlewski[42], S. Goldfarb[91],
T. Golling[52], D. Golubkov[132], A. Gomes[128a,128b,128d], R. Gonçalo[128a], R. Goncalves Gama[26a],
J. Goncalves Pinto Firmino Da Costa[138], G. Gonella[51], L. Gonella[19], A. Gongadze[68],
J.L. Gonski[59], S. González de la Hoz[170], S. Gonzalez-Sevilla[52], L. Goossens[32], P.A. Gorbounov[99],
H.A. Gordon[27], I. Gorelov[107], B. Gorini[32], E. Gorini[76a,76b], A. Gorišek[78], A.T. Goshaw[48],
C. Gössling[46], M.I. Gostkin[68], C.A. Gottardo[23], C.R. Goudet[119], D. Goujdami[137c],
A.G. Goussiou[140], N. Govender[147b,t], E. Gozani[154], I. Grabowska-Bold[41a], P.O.J. Gradin[168],
J. Gramling[166], E. Gramstad[121], S. Grancagnolo[17], V. Gratchev[125], P.M. Gravila[28f], C. Gray[56],
H.M. Gray[16], Z.D. Greenwood[82,u], C. Grefe[23], K. Gregersen[81], I.M. Gregor[45], P. Grenier[145],
K. Grevtsov[5], J. Griffiths[8], A.A. Grillo[139], K. Grimm[75], S. Grinstein[13,v], Ph. Gris[37],
J.-F. Grivaz[119], S. Groh[86], E. Gross[175], J. Grosse-Knetter[57], G.C. Grossi[82], Z.J. Grout[81],
A. Grummer[107], L. Guan[92], W. Guan[176], J. Guenther[32], F. Guescini[163a], D. Guest[166],
O. Gueta[155], B. Gui[113], E. Guido[53a,53b], T. Guillemin[5], S. Guindon[32], U. Gul[56], C. Gumpert[32],
J. Guo[36c], W. Guo[92], Y. Guo[36a,w], R. Gupta[43], S. Gurbuz[20a], G. Gustavino[115], B.J. Gutelman[154],
P. Gutierrez[115], N.G. Gutierrez Ortiz[81], C. Gutschow[81], C. Guyot[138], M.P. Guzik[41a],
C. Gwenlan[122], C.B. Gwilliam[77], A. Haas[112], C. Haber[16], H.K. Hadavand[8], N. Haddad[137e],
A. Hadef[88], S. Hageböck[23], M. Hagihara[164], H. Hakobyan[180,*], M. Haleem[45], J. Haley[116],
G. Halladjian[93], G.D. Hallewell[88], K. Hamacher[178], P. Hamal[117], K. Hamano[172], A. Hamilton[147a],
G.N. Hamity[141], P.G. Hamnett[45], L. Han[36a], S. Han[35a,35d], K. Hanagaki[69,x], K. Hanawa[157],
M. Hance[139], D.M. Handl[102], B. Haney[124], P. Hanke[60a], J.B. Hansen[39], J.D. Hansen[39],
M.C. Hansen[23], P.H. Hansen[39], K. Hara[164], A.S. Hard[176], T. Harenberg[178], F. Hariri[119],
S. Harkusha[95], P.F. Harrison[173], N.M. Hartmann[102], Y. Hasegawa[142], A. Hasib[49], S. Hassani[138],
S. Haug[18], R. Hauser[93], L. Hauswald[47], L.B. Havener[38], M. Havranek[130], C.M. Hawkes[19],
R.J. Hawkings[32], D. Hayakawa[159], D. Hayden[93], C.P. Hays[122], J.M. Hays[79], H.S. Hayward[77],
S.J. Haywood[133], S.J. Head[19], T. Heck[86], V. Hedberg[84], L. Heelan[8], S. Heer[23], K.K. Heidegger[51],
S. Heim[45], T. Heim[16], B. Heinemann[45,y], J.J. Heinrich[102], L. Heinrich[112], C. Heinz[55],
J. Hejbal[129], L. Helary[32], A. Held[171], S. Hellman[148a,148b], C. Helsens[32], R.C.W. Henderson[75],
Y. Heng[176], S. Henkelmann[171], A.M. Henriques Correia[32], S. Henrot-Versille[119], G.H. Herbert[17],
H. Herde[25], V. Herget[177], Y. Hernández Jiménez[147c], H. Herr[86], G. Herten[51], R. Hertenberger[102],

L. Hervas[32], T.C. Herwig[124], G.G. Hesketh[81], N.P. Hessey[163a], J.W. Hetherly[43], S. Higashino[69], E. Higón-Rodriguez[170], K. Hildebrand[33], E. Hill[172], J.C. Hill[30], K.H. Hiller[45], S.J. Hillier[19], M. Hils[47], I. Hinchliffe[16], M. Hirose[51], D. Hirschbuehl[178], B. Hiti[78], O. Hladik[129], D.R. Hlaluku[147c], X. Hoad[49], J. Hobbs[150], N. Hod[163a], M.C. Hodgkinson[141], P. Hodgson[141], A. Hoecker[32], M.R. Hoeferkamp[107], F. Hoenig[102], D. Hohn[23], T.R. Holmes[33], M. Homann[46], S. Honda[164], T. Honda[69], T.M. Hong[127], B.H. Hooberman[169], W.H. Hopkins[118], Y. Horii[105], A.J. Horton[144], J-Y. Hostachy[58], A. Hostiuc[140], S. Hou[153], A. Hoummada[137a], J. Howarth[87], J. Hoya[74], M. Hrabovsky[117], J. Hrdinka[32], I. Hristova[17], J. Hrivnac[119], T. Hryn'ova[5], A. Hrynevich[96], P.J. Hsu[63], S.-C. Hsu[140], Q. Hu[27], S. Hu[36c], Y. Huang[35a], Z. Hubacek[130], F. Hubaut[88], F. Huegging[23], T.B. Huffman[122], E.W. Hughes[38], M. Huhtinen[32], R.F.H. Hunter[31], P. Huo[150], N. Huseynov[68,b], J. Huston[93], J. Huth[59], R. Hyneman[92], G. Iacobucci[52], G. Iakovidis[27], I. Ibragimov[143], L. Iconomidou-Fayard[119], Z. Idrissi[137e], P. Iengo[32], O. Igonkina[109,z], T. Iizawa[174], Y. Ikegami[69], M. Ikeno[69], Y. Ilchenko[11,aa], D. Iliadis[156], N. Ilic[145], F. Iltzsche[47], G. Introzzi[123a,123b], P. Ioannou[9,*], M. Iodice[136a], K. Iordanidou[38], V. Ippolito[59], M.F. Isacson[168], N. Ishijima[120], M. Ishino[157], M. Ishitsuka[159], C. Issever[122], S. Istin[20a], F. Ito[164], J.M. Iturbe Ponce[62a], R. Iuppa[162a,162b], H. Iwasaki[69], J.M. Izen[44], V. Izzo[106a], S. Jabbar[3], P. Jackson[1], R.M. Jacobs[23], V. Jain[2], K.B. Jakobi[86], K. Jakobs[51], S. Jakobsen[65], T. Jakoubek[129], D.O. Jamin[116], D.K. Jana[82], R. Jansky[52], J. Janssen[23], M. Janus[57], P.A. Janus[41a], G. Jarlskog[84], N. Javadov[68,b], T. Javůrek[51], M. Javurkova[51], F. Jeanneau[138], L. Jeanty[16], J. Jejelava[54a,ab], A. Jelinskas[173], P. Jenni[51,ac], C. Jeske[173], S. Jézéquel[5], H. Ji[176], J. Jia[150], H. Jiang[67], Y. Jiang[36a], Z. Jiang[145], S. Jiggins[81], J. Jimenez Pena[170], S. Jin[35b], A. Jinaru[28b], O. Jinnouchi[159], H. Jivan[147c], P. Johansson[141], K.A. Johns[7], C.A. Johnson[64], W.J. Johnson[140], K. Jon-And[148a,148b], R.W.L. Jones[75], S.D. Jones[151], S. Jones[7], T.J. Jones[77], J. Jongmanns[60a], P.M. Jorge[128a,128b], J. Jovicevic[163a], X. Ju[176], A. Juste Rozas[13,v], M.K. Köhler[175], A. Kaczmarska[42], M. Kado[119], H. Kagan[113], M. Kagan[145], S.J. Kahn[88], T. Kaji[174], E. Kajomovitz[154], C.W. Kalderon[84], A. Kaluza[86], S. Kama[43], A. Kamenshchikov[132], N. Kanaya[157], L. Kanjir[78], V.A. Kantserov[100], J. Kanzaki[69], B. Kaplan[112], L.S. Kaplan[176], D. Kar[147c], K. Karakostas[10], N. Karastathis[10], M.J. Kareem[163b], E. Karentzos[10], S.N. Karpov[68], Z.M. Karpova[68], K. Karthik[112], V. Kartvelishvili[75], A.N. Karyukhin[132], K. Kasahara[164], L. Kashif[176], R.D. Kass[113], A. Kastanas[149], Y. Kataoka[157], C. Kato[157], A. Katre[52], J. Katzy[45], K. Kawade[70], K. Kawagoe[73], T. Kawamoto[157], G. Kawamura[57], E.F. Kay[77], V.F. Kazanin[111,c], R. Keeler[172], R. Kehoe[43], J.S. Keller[31], E. Kellermann[84], J.J. Kempster[80], J Kendrick[19], H. Keoshkerian[161], O. Kepka[129], B.P. Kerševan[78], S. Kersten[178], R.A. Keyes[90], M. Khader[169], F. Khalil-zada[12], A. Khanov[116], A.G. Kharlamov[111,c], T. Kharlamova[111,c], A. Khodinov[160], T.J. Khoo[52], V. Khovanskiy[99,*], E. Khramov[68], J. Khubua[54b,ad], S. Kido[70], C.R. Kilby[80], H.Y. Kim[8], S.H. Kim[164], Y.K. Kim[33], N. Kimura[156], O.M. Kind[17], B.T. King[77], D. Kirchmeier[47], J. Kirk[133], A.E. Kiryunin[103], T. Kishimoto[157], D. Kisielewska[41a], V. Kitali[45], O. Kivernyk[5], E. Kladiva[146b], T. Klapdor-Kleingrothaus[51], M.H. Klein[92], M. Klein[77], U. Klein[77], K. Kleinknecht[86], P. Klimek[110], A. Klimentov[27], R. Klingenberg[46,*], T. Klingl[23], T. Klioutchnikova[32], F.F. Klitzner[102], E.-E. Kluge[60a], P. Kluit[109], S. Kluth[103], E. Kneringer[65], E.B.F.G. Knoops[88], A. Knue[103], A. Kobayashi[157], D. Kobayashi[73], T. Kobayashi[157], M. Kobel[47], M. Kocian[145], P. Kodys[131], T. Koffas[31], E. Koffeman[109], N.M. Köhler[103], T. Koi[145], M. Kolb[60b], I. Koletsou[5], T. Kondo[69], N. Kondrashova[36c], K. Köneke[51], A.C. König[108], T. Kono[69,ae], R. Konoplich[112,af], N. Konstantinidis[81], B. Konya[84], R. Kopeliansky[64], S. Koperny[41a], A.K. Kopp[51], K. Korcyl[42], K. Kordas[156], A. Korn[81], A.A. Korol[111,c], I. Korolkov[13], E.V. Korolkova[141], O. Kortner[103], S. Kortner[103], T. Kosek[131], V.V. Kostyukhin[23], A. Kotwal[48], A. Koulouris[10], A. Kourkoumeli-Charalampidi[123a,123b], C. Kourkoumelis[9], E. Kourlitis[141], V. Kouskoura[27], A.B. Kowalewska[42], R. Kowalewski[172], T.Z. Kowalski[41a], C. Kozakai[157],

W. Kozanecki[138], A.S. Kozhin[132], V.A. Kramarenko[101], G. Kramberger[78], D. Krasnopevtsev[100],
M.W. Krasny[83], A. Krasznahorkay[32], D. Krauss[103], J.A. Kremer[41a], J. Kretzschmar[77],
K. Kreutzfeldt[55], P. Krieger[161], K. Krizka[16], K. Kroeninger[46], H. Kroha[103], J. Kroll[129],
J. Kroll[124], J. Kroseberg[23], J. Krstic[14], U. Kruchonak[68], H. Krüger[23], N. Krumnack[67],
M.C. Kruse[48], T. Kubota[91], H. Kucuk[81], S. Kuday[4b], J.T. Kuechler[178], S. Kuehn[32], A. Kugel[60a],
F. Kuger[177], T. Kuhl[45], V. Kukhtin[68], R. Kukla[88], Y. Kulchitsky[95], S. Kuleshov[34b],
Y.P. Kulinich[169], M. Kuna[134a,134b], T. Kunigo[71], A. Kupco[129], T. Kupfer[46], O. Kuprash[155],
H. Kurashige[70], L.L. Kurchaninov[163a], Y.A. Kurochkin[95], M.G. Kurth[35a,35d], E.S. Kuwertz[172],
M. Kuze[159], J. Kvita[117], T. Kwan[172], D. Kyriazopoulos[141], A. La Rosa[103],
J.L. La Rosa Navarro[26d], L. La Rotonda[40a,40b], F. La Ruffa[40a,40b], C. Lacasta[170],
F. Lacava[134a,134b], J. Lacey[45], D.P.J. Lack[87], H. Lacker[17], D. Lacour[83], E. Ladygin[68], R. Lafaye[5],
B. Laforge[83], T. Lagouri[179], S. Lai[57], S. Lammers[64], W. Lampl[7], E. Lançon[27], U. Landgraf[51],
M.P.J. Landon[79], M.C. Lanfermann[52], V.S. Lang[45], J.C. Lange[13], R.J. Langenberg[32],
A.J. Lankford[166], F. Lanni[27], K. Lantzsch[23], A. Lanza[123a], A. Lapertosa[53a,53b], S. Laplace[83],
J.F. Laporte[138], T. Lari[94a], F. Lasagni Manghi[22a,22b], M. Lassnig[32], T.S. Lau[62a], P. Laurelli[50],
W. Lavrijsen[16], A.T. Law[139], P. Laycock[77], T. Lazovich[59], M. Lazzaroni[94a,94b], B. Le[91],
O. Le Dortz[83], E. Le Guirriec[88], E.P. Le Quilleuc[138], M. LeBlanc[172], T. LeCompte[6],
F. Ledroit-Guillon[58], C.A. Lee[27], G.R. Lee[34a], S.C. Lee[153], L. Lee[59], B. Lefebvre[90], G. Lefebvre[83],
M. Lefebvre[172], F. Legger[102], C. Leggett[16], G. Lehmann Miotto[32], X. Lei[7], W.A. Leight[45],
M.A.L. Leite[26d], R. Leitner[131], D. Lellouch[175], B. Lemmer[57], K.J.C. Leney[81], T. Lenz[23],
B. Lenzi[32], R. Leone[7], S. Leone[126a,126b], C. Leonidopoulos[49], G. Lerner[151], C. Leroy[97], R. Les[161],
A.A.J. Lesage[138], C.G. Lester[30], M. Levchenko[125], J. Levêque[5], D. Levin[92], L.J. Levinson[175],
M. Levy[19], D. Lewis[79], B. Li[36a,w], H. Li[150], L. Li[36c], Q. Li[35a,35d], Q. Li[36a], S. Li[48], X. Li[36c],
Y. Li[143], Z. Liang[35a], B. Liberti[135a], A. Liblong[161], K. Lie[62c], J. Liebal[23], W. Liebig[15],
A. Limosani[152], C.Y. Lin[30], K. Lin[93], S.C. Lin[182], T.H. Lin[86], R.A. Linck[64], B.E. Lindquist[150],
A.E. Lionti[52], E. Lipeles[124], A. Lipniacka[15], M. Lisovyi[60b], T.M. Liss[169,ag], A. Lister[171],
A.M. Litke[139], B. Liu[67], H. Liu[92], H. Liu[27], J.K.K. Liu[122], J. Liu[36b], J.B. Liu[36a], K. Liu[88],
L. Liu[169], M. Liu[36a], Y.L. Liu[36a], Y. Liu[36a], M. Livan[123a,123b], A. Lleres[58], J. Llorente Merino[35a],
S.L. Lloyd[79], C.Y. Lo[62b], F. Lo Sterzo[43], E.M. Lobodzinska[45], P. Loch[7], F.K. Loebinger[87],
A. Loesle[51], K.M. Loew[25], T. Lohse[17], K. Lohwasser[141], M. Lokajicek[129], B.A. Long[24],
J.D. Long[169], R.E. Long[75], L. Longo[76a,76b], K.A. Looper[113], J.A. Lopez[34b], I. Lopez Paz[13],
A. Lopez Solis[83], J. Lorenz[102], N. Lorenzo Martinez[5], M. Losada[21], P.J. Lösel[102], X. Lou[35a],
A. Lounis[119], J. Love[6], P.A. Love[75], H. Lu[62a], N. Lu[92], Y.J. Lu[63], H.J. Lubatti[140],
C. Luci[134a,134b], A. Lucotte[58], C. Luedtke[51], F. Luehring[64], W. Lukas[65], L. Luminari[134a],
O. Lundberg[148a,148b], B. Lund-Jensen[149], M.S. Lutz[89], P.M. Luzi[83], D. Lynn[27], R. Lysak[129],
E. Lytken[84], F. Lyu[35a], V. Lyubushkin[68], H. Ma[27], L.L. Ma[36b], Y. Ma[36b], G. Maccarrone[50],
A. Macchiolo[103], C.M. Macdonald[141], B. Maček[78], J. Machado Miguens[124,128b], D. Madaffari[170],
R. Madar[37], W.F. Mader[47], A. Madsen[45], N. Madysa[47], J. Maeda[70], S. Maeland[15], T. Maeno[27],
A.S. Maevskiy[101], V. Magerl[51], C. Maiani[119], C. Maidantchik[26a], T. Maier[102],
A. Maio[128a,128b,128d], O. Majersky[146a], S. Majewski[118], Y. Makida[69], N. Makovec[119],
B. Malaescu[83], Pa. Malecki[42], V.P. Maleev[125], F. Malek[58], U. Mallik[66], D. Malon[6], C. Malone[30],
S. Maltezos[10], S. Malyukov[32], J. Mamuzic[170], G. Mancini[50], I. Mandić[78], J. Maneira[128a,128b],
L. Manhaes de Andrade Filho[26b], J. Manjarres Ramos[47], K.H. Mankinen[84], A. Mann[102],
A. Manousos[32], B. Mansoulie[138], J.D. Mansour[35a], R. Mantifel[90], M. Mantoani[57],
S. Manzoni[94a,94b], L. Mapelli[32], G. Marceca[29], L. March[52], L. Marchese[122], G. Marchiori[83],
M. Marcisovsky[129], C.A. Marin Tobon[32], M. Marjanovic[37], D.E. Marley[92], F. Marroquim[26a],
S.P. Marsden[87], Z. Marshall[16], M.U.F Martensson[168], S. Marti-Garcia[170], C.B. Martin[113],
T.A. Martin[173], V.J. Martin[49], B. Martin dit Latour[15], M. Martinez[13,v],

V.I. Martinez Outschoorn[169], S. Martin-Haugh[133], V.S. Martoiu[28b], A.C. Martyniuk[81],
A. Marzin[32], L. Masetti[86], T. Mashimo[157], R. Mashinistov[98], J. Masik[87], A.L. Maslennikov[111,c],
L.H. Mason[91], L. Massa[135a,135b], P. Mastrandrea[5], A. Mastroberardino[40a,40b], T. Masubuchi[157],
P. Mättig[178], J. Maurer[28b], S.J. Maxfield[77], D.A. Maximov[111,c], R. Mazini[153], I. Maznas[156],
S.M. Mazza[94a,94b], N.C. Mc Fadden[107], G. Mc Goldrick[161], S.P. Mc Kee[92], A. McCarn[92],
R.L. McCarthy[150], T.G. McCarthy[103], L.I. McClymont[81], E.F. McDonald[91], J.A. Mcfayden[32],
G. Mchedlidze[57], S.J. McMahon[133], P.C. McNamara[91], C.J. McNicol[173], R.A. McPherson[172,o],
S. Meehan[140], T.J. Megy[51], S. Mehlhase[102], A. Mehta[77], T. Meideck[58], K. Meier[60a], B. Meirose[44],
D. Melini[170,ah], B.R. Mellado Garcia[147c], J.D. Mellenthin[57], M. Melo[146a], F. Meloni[18],
A. Melzer[23], S.B. Menary[87], L. Meng[77], X.T. Meng[92], A. Mengarelli[22a,22b], S. Menke[103],
E. Meoni[40a,40b], S. Mergelmeyer[17], C. Merlassino[18], P. Mermod[52], L. Merola[106a,106b],
C. Meroni[94a], F.S. Merritt[33], A. Messina[134a,134b], J. Metcalfe[6], A.S. Mete[166], C. Meyer[124],
J-P. Meyer[138], J. Meyer[109], H. Meyer Zu Theenhausen[60a], F. Miano[151], R.P. Middleton[133],
S. Miglioranzi[53a,53b], L. Mijović[49], G. Mikenberg[175], M. Mikestikova[129], M. Mikuž[78], M. Milesi[91],
A. Milic[161], D.A. Millar[79], D.W. Miller[33], C. Mills[49], A. Milov[175], D.A. Milstead[148a,148b],
A.A. Minaenko[132], Y. Minami[157], I.A. Minashvili[54b], A.I. Mincer[112], B. Mindur[41a], M. Mineev[68],
Y. Minegishi[157], Y. Ming[176], L.M. Mir[13], A. Mirto[76a,76b], K.P. Mistry[124], T. Mitani[174],
J. Mitrevski[102], V.A. Mitsou[170], A. Miucci[18], P.S. Miyagawa[141], A. Mizukami[69],
J.U. Mjörnmark[84], T. Mkrtchyan[180], M. Mlynarikova[131], T. Moa[148a,148b], K. Mochizuki[97],
P. Mogg[51], S. Mohapatra[38], S. Molander[148a,148b], R. Moles-Valls[23], M.C. Mondragon[93],
K. Mönig[45], J. Monk[39], E. Monnier[88], A. Montalbano[150], J. Montejo Berlingen[32], F. Monticelli[74],
S. Monzani[94a,94b], R.W. Moore[3], N. Morange[119], D. Moreno[21], M. Moreno Llácer[32],
P. Morettini[53a], S. Morgenstern[32], D. Mori[144], T. Mori[157], M. Morii[59], M. Morinaga[174],
V. Morisbak[121], A.K. Morley[32], G. Mornacchi[32], J.D. Morris[79], L. Morvaj[150], P. Moschovakos[10],
M. Mosidze[54b], H.J. Moss[141], J. Moss[145,ai], K. Motohashi[159], R. Mount[145], E. Mountricha[27],
E.J.W. Moyse[89], S. Muanza[88], V.E. Muckhoff[23], F. Mueller[103], J. Mueller[127], R.S.P. Mueller[102],
D. Muenstermann[75], P. Mullen[56], G.A. Mullier[18], F.J. Munoz Sanchez[87], W.J. Murray[173,133],
H. Musheghyan[32], M. Muškinja[78], A.G. Myagkov[132,aj], M. Myska[130], B.P. Nachman[16],
O. Nackenhorst[52], K. Nagai[122], R. Nagai[69,ae], K. Nagano[69], Y. Nagasaka[61], K. Nagata[164],
M. Nagel[51], E. Nagy[88], A.M. Nairz[32], Y. Nakahama[105], K. Nakamura[69], T. Nakamura[157],
I. Nakano[114], R.F. Naranjo Garcia[45], R. Narayan[11], D.I. Narrias Villar[60a], I. Naryshkin[125],
T. Naumann[45], G. Navarro[21], R. Nayyar[7], H.A. Neal[92], P.Yu. Nechaeva[98], T.J. Neep[138],
A. Negri[123a,123b], M. Negrini[22a], S. Nektarijevic[108], C. Nellist[57], A. Nelson[166], M.E. Nelson[122],
S. Nemecek[129], P. Nemethy[112], M. Nessi[32,ak], M.S. Neubauer[169], M. Neumann[178],
P.R. Newman[19], T.Y. Ng[62c], Y.S. Ng[17], T. Nguyen Manh[97], R.B. Nickerson[122], R. Nicolaidou[138],
J. Nielsen[139], N. Nikiforou[11], V. Nikolaenko[132,aj], I. Nikolic-Audit[83], K. Nikolopoulos[19],
P. Nilsson[27], Y. Ninomiya[69], A. Nisati[134a], N. Nishu[36c], R. Nisius[103], I. Nitsche[46], T. Nitta[174],
T. Nobe[157], Y. Noguchi[71], M. Nomachi[120], I. Nomidis[31], M.A. Nomura[27], T. Nooney[79],
M. Nordberg[32], N. Norjoharuddeen[122], O. Novgorodova[47], M. Nozaki[69], L. Nozka[117],
K. Ntekas[166], E. Nurse[81], F. Nuti[91], K. O'connor[25], D.C. O'Neil[144], A.A. O'Rourke[45],
V. O'Shea[56], F.G. Oakham[31,d], H. Oberlack[103], T. Obermann[23], J. Ocariz[83], A. Ochi[70],
I. Ochoa[38], J.P. Ochoa-Ricoux[34a], S. Oda[73], S. Odaka[69], A. Oh[87], S.H. Oh[48], C.C. Ohm[149],
H. Ohman[168], H. Oide[53a,53b], H. Okawa[164], Y. Okumura[157], T. Okuyama[69], A. Olariu[28b],
L.F. Oleiro Seabra[128a], S.A. Olivares Pino[34a], D. Oliveira Damazio[27], M.J.R. Olsson[33],
A. Olszewski[42], J. Olszowska[42], A. Onofre[128a,128e], K. Onogi[105], P.U.E. Onyisi[11,aa], H. Oppen[121],
M.J. Oreglia[33], Y. Oren[155], D. Orestano[136a,136b], N. Orlando[62b], R.S. Orr[161], B. Osculati[53a,53b,*],
R. Ospanov[36a], G. Otero y Garzon[29], H. Otono[73], M. Ouchrif[137d], F. Ould-Saada[121],
A. Ouraou[138], K.P. Oussoren[109], Q. Ouyang[35a], M. Owen[56], R.E. Owen[19], V.E. Ozcan[20a],

N. Ozturk[8], K. Pachal[144], A. Pacheco Pages[13], L. Pacheco Rodriguez[138], C. Padilla Aranda[13],
S. Pagan Griso[16], M. Paganini[179], F. Paige[27], G. Palacino[64], S. Palazzo[40a,40b], S. Palestini[32],
M. Palka[41b], D. Pallin[37], E.St. Panagiotopoulou[10], I. Panagoulias[10], C.E. Pandini[52],
J.G. Panduro Vazquez[80], P. Pani[32], S. Panitkin[27], D. Pantea[28b], L. Paolozzi[52],
Th.D. Papadopoulou[10], K. Papageorgiou[9,s], A. Paramonov[6], D. Paredes Hernandez[179],
A.J. Parker[75], M.A. Parker[30], K.A. Parker[45], F. Parodi[53a,53b], J.A. Parsons[38], U. Parzefall[51],
V.R. Pascuzzi[161], J.M. Pasner[139], E. Pasqualucci[134a], S. Passaggio[53a], Fr. Pastore[80],
S. Pataraia[86], J.R. Pater[87], T. Pauly[32], B. Pearson[103], S. Pedraza Lopez[170], R. Pedro[128a,128b],
S.V. Peleganchuk[111,c], O. Penc[129], C. Peng[35a,35d], H. Peng[36a], J. Penwell[64], B.S. Peralva[26b],
M.M. Perego[138], D.V. Perepelitsa[27], F. Peri[17], L. Perini[94a,94b], H. Pernegger[32],
S. Perrella[106a,106b], R. Peschke[45], V.D. Peshekhonov[68,*], K. Peters[45], R.F.Y. Peters[87],
B.A. Petersen[32], T.C. Petersen[39], E. Petit[58], A. Petridis[1], C. Petridou[156], P. Petroff[119],
E. Petrolo[134a], M. Petrov[122], F. Petrucci[136a,136b], N.E. Pettersson[89], A. Peyaud[138], R. Pezoa[34b],
F.H. Phillips[93], P.W. Phillips[133], G. Piacquadio[150], E. Pianori[173], A. Picazio[89], M.A. Pickering[122],
R. Piegaia[29], J.E. Pilcher[33], A.D. Pilkington[87], M. Pinamonti[135a,135b], J.L. Pinfold[3],
H. Pirumov[45], M. Pitt[175], L. Plazak[146a], M.-A. Pleier[27], V. Pleskot[86], E. Plotnikova[68],
D. Pluth[67], P. Podberezko[111], R. Poettgen[84], R. Poggi[123a,123b], L. Poggioli[119], I. Pogrebnyak[93],
D. Pohl[23], I. Pokharel[57], G. Polesello[123a], A. Poley[45], A. Policicchio[40a,40b], R. Polifka[32],
A. Polini[22a], C.S. Pollard[56], V. Polychronakos[27], K. Pommès[32], D. Ponomarenko[100],
L. Pontecorvo[134a], G.A. Popeneciu[28d], D.M. Portillo Quintero[83], S. Pospisil[130], K. Potamianos[45],
I.N. Potrap[68], C.J. Potter[30], H. Potti[11], T. Poulsen[84], J. Poveda[32], M.E. Pozo Astigarraga[32],
P. Pralavorio[88], A. Pranko[16], S. Prell[67], D. Price[87], M. Primavera[76a], S. Prince[90], N. Proklova[100],
K. Prokofiev[62c], F. Prokoshin[34b], S. Protopopescu[27], J. Proudfoot[6], M. Przybycien[41a], A. Puri[169],
P. Puzo[119], J. Qian[92], G. Qin[56], Y. Qin[87], A. Quadt[57], M. Queitsch-Maitland[45], D. Quilty[56],
S. Raddum[121], V. Radeka[27], V. Radescu[122], S.K. Radhakrishnan[150], P. Radloff[118], P. Rados[91],
F. Ragusa[94a,94b], G. Rahal[181], J.A. Raine[87], S. Rajagopalan[27], C. Rangel-Smith[168], T. Rashid[119],
S. Raspopov[5], M.G. Ratti[94a,94b], D.M. Rauch[45], F. Rauscher[102], S. Rave[86], I. Ravinovich[175],
J.H. Rawling[87], M. Raymond[32], A.L. Read[121], N.P. Readioff[58], M. Reale[76a,76b],
D.M. Rebuzzi[123a,123b], A. Redelbach[177], G. Redlinger[27], R. Reece[139], R.G. Reed[147c], K. Reeves[44],
L. Rehnisch[17], J. Reichert[124], A. Reiss[86], C. Rembser[32], H. Ren[35a,35d], M. Rescigno[134a],
S. Resconi[94a], E.D. Resseguie[124], S. Rettie[171], E. Reynolds[19], O.L. Rezanova[111,c], P. Reznicek[131],
R. Rezvani[97], R. Richter[103], S. Richter[81], E. Richter-Was[41b], O. Ricken[23], M. Ridel[83], P. Rieck[103],
C.J. Riegel[178], J. Rieger[57], O. Rifki[115], M. Rijssenbeek[150], A. Rimoldi[123a,123b], M. Rimoldi[18],
L. Rinaldi[22a], G. Ripellino[149], B. Ristić[32], E. Ritsch[32], I. Riu[13], F. Rizatdinova[116], E. Rizvi[79],
C. Rizzi[13], R.T. Roberts[87], S.H. Robertson[90,o], A. Robichaud-Veronneau[90], D. Robinson[30],
J.E.M. Robinson[45], A. Robson[56], E. Rocco[86], C. Roda[126a,126b], Y. Rodina[88,al],
S. Rodriguez Bosca[170], A. Rodriguez Perez[13], D. Rodriguez Rodriguez[170], S. Roe[32], C.S. Rogan[59],
O. Røhne[121], J. Roloff[59], A. Romaniouk[100], M. Romano[22a,22b], S.M. Romano Saez[37],
E. Romero Adam[170], N. Rompotis[77], M. Ronzani[51], L. Roos[83], S. Rosati[134a], K. Rosbach[51],
P. Rose[139], N.-A. Rosien[57], E. Rossi[106a,106b], L.P. Rossi[53a], J.H.N. Rosten[30], R. Rosten[140],
M. Rotaru[28b], J. Rothberg[140], D. Rousseau[119], A. Rozanov[88], Y. Rozen[154], X. Ruan[147c],
F. Rubbo[145], F. Rühr[51], A. Ruiz-Martinez[31], Z. Rurikova[51], N.A. Rusakovich[68], H.L. Russell[90],
J.P. Rutherfoord[7], N. Ruthmann[32], E.M. Rüttinger[45], Y.F. Ryabov[125], M. Rybar[169],
G. Rybkin[119], S. Ryu[6], A. Ryzhov[132], G.F. Rzehorz[57], A.F. Saavedra[152], G. Sabato[109],
S. Sacerdoti[29], H.F-W. Sadrozinski[139], R. Sadykov[68], F. Safai Tehrani[134a], P. Saha[110],
M. Sahinsoy[60a], M. Saimpert[45], M. Saito[157], T. Saito[157], H. Sakamoto[157], Y. Sakurai[174],
G. Salamanna[136a,136b], J.E. Salazar Loyola[34b], D. Salek[109], P.H. Sales De Bruin[168],
D. Salihagic[103], A. Salnikov[145], J. Salt[170], D. Salvatore[40a,40b], F. Salvatore[151],

A. Salvucci[62a,62b,62c], A. Salzburger[32], D. Sammel[51], D. Sampsonidis[156], D. Sampsonidou[156],
J. Sánchez[170], V. Sanchez Martinez[170], A. Sanchez Pineda[167a,167c], H. Sandaker[121],
R.L. Sandbach[79], C.O. Sander[45], M. Sandhoff[178], C. Sandoval[21], D.P.C. Sankey[133],
M. Sannino[53a,53b], Y. Sano[105], A. Sansoni[50], C. Santoni[37], H. Santos[128a], I. Santoyo Castillo[151],
A. Sapronov[68], J.G. Saraiva[128a,128d], B. Sarrazin[23], O. Sasaki[69], K. Sato[164], E. Sauvan[5],
G. Savage[80], P. Savard[161,d], C. Sawyer[133], L. Sawyer[82,u], J. Saxon[33], C. Sbarra[22a],
A. Sbrizzi[22a,22b], T. Scanlon[81], D.A. Scannicchio[166], J. Schaarschmidt[140], P. Schacht[103],
B.M. Schachtner[102], D. Schaefer[33], L. Schaefer[124], R. Schaefer[45], J. Schaeffer[86], S. Schaepe[32],
S. Schaetzel[60b], U. Schäfer[86], A.C. Schaffer[119], D. Schaile[102], R.D. Schamberger[150],
V.A. Schegelsky[125], D. Scheirich[131], F. Schenck[17], M. Schernau[166], C. Schiavi[53a,53b], S. Schier[139],
L.K. Schildgen[23], C. Schillo[51], M. Schioppa[40a,40b], S. Schlenker[32], K.R. Schmidt-Sommerfeld[103],
K. Schmieden[32], C. Schmitt[86], S. Schmitt[45], S. Schmitz[86], U. Schnoor[51], L. Schoeffel[138],
A. Schoening[60b], B.D. Schoenrock[93], E. Schopf[23], M. Schott[86], J.F.P. Schouwenberg[108],
J. Schovancova[32], S. Schramm[52], N. Schuh[86], A. Schulte[86], M.J. Schultens[23],
H.-C. Schultz-Coulon[60a], H. Schulz[17], M. Schumacher[51], B.A. Schumm[139], Ph. Schune[138],
A. Schwartzman[145], T.A. Schwarz[92], H. Schweiger[87], Ph. Schwemling[138], R. Schwienhorst[93],
J. Schwindling[138], A. Sciandra[23], G. Sciolla[25], M. Scornajenghi[40a,40b], F. Scuri[126a,126b],
F. Scutti[91], J. Searcy[92], P. Seema[23], S.C. Seidel[107], A. Seiden[139], J.M. Seixas[26a],
G. Sekhniaidze[106a], K. Sekhon[92], S.J. Sekula[43], N. Semprini-Cesari[22a,22b], S. Senkin[37],
C. Serfon[121], L. Serin[119], L. Serkin[167a,167b], M. Sessa[136a,136b], R. Seuster[172], H. Severini[115],
T. Sfiligoj[78], F. Sforza[165], A. Sfyrla[52], E. Shabalina[57], N.W. Shaikh[148a,148b], L.Y. Shan[35a],
R. Shang[169], J.T. Shank[24], M. Shapiro[16], P.B. Shatalov[99], K. Shaw[167a,167b], S.M. Shaw[87],
A. Shcherbakova[148a,148b], C.Y. Shehu[151], Y. Shen[115], N. Sherafati[31], A.D. Sherman[24],
P. Sherwood[81], L. Shi[153,am], S. Shimizu[70], C.O. Shimmin[179], M. Shimojima[104], I.P.J. Shipsey[122],
S. Shirabe[73], M. Shiyakova[68,an], J. Shlomi[175], A. Shmeleva[98], D. Shoaleh Saadi[97], M.J. Shochet[33],
S. Shojaii[94a,94b], D.R. Shope[115], S. Shrestha[113], E. Shulga[100], M.A. Shupe[7], P. Sicho[129],
A.M. Sickles[169], P.E. Sidebo[149], E. Sideras Haddad[147c], O. Sidiropoulou[177], A. Sidoti[22a,22b],
F. Siegert[47], Dj. Sijacki[14], J. Silva[128a,128d], S.B. Silverstein[148a], V. Simak[130], L. Simic[68],
S. Simion[119], E. Simioni[86], B. Simmons[81], M. Simon[86], P. Sinervo[161], N.B. Sinev[118],
M. Sioli[22a,22b], G. Siragusa[177], I. Siral[92], S.Yu. Sivoklokov[101], J. Sjölin[148a,148b], M.B. Skinner[75],
P. Skubic[115], M. Slater[19], T. Slavicek[130], M. Slawinska[42], K. Sliwa[165], R. Slovak[131],
V. Smakhtin[175], B.H. Smart[5], J. Smiesko[146a], N. Smirnov[100], S.Yu. Smirnov[100], Y. Smirnov[100],
L.N. Smirnova[101,ao], O. Smirnova[84], J.W. Smith[57], M.N.K. Smith[38], R.W. Smith[38],
M. Smizanska[75], K. Smolek[130], A.A. Snesarev[98], I.M. Snyder[118], S. Snyder[27], R. Sobie[172,o],
F. Socher[47], A. Soffer[155], A. Søgaard[49], D.A. Soh[153], G. Sokhrannyi[78], C.A. Solans Sanchez[32],
M. Solar[130], E.Yu. Soldatov[100], U. Soldevila[170], A.A. Solodkov[132], A. Soloshenko[68],
O.V. Solovyanov[132], V. Solovyev[125], P. Sommer[141], H. Son[165], A. Sopczak[130], D. Sosa[60b],
C.L. Sotiropoulou[126a,126b], S. Sottocornola[123a,123b], R. Soualah[167a,167c], A.M. Soukharev[111,c],
D. South[45], B.C. Sowden[80], S. Spagnolo[76a,76b], M. Spalla[126a,126b], M. Spangenberg[173],
F. Spanò[80], D. Sperlich[17], F. Spettel[103], T.M. Spieker[60a], R. Spighi[22a], G. Spigo[32], L.A. Spiller[91],
M. Spousta[131], R.D. St. Denis[56,*], A. Stabile[94a,94b], R. Stamen[60a], S. Stamm[17], E. Stanecka[42],
R.W. Stanek[6], C. Stanescu[136a], M.M. Stanitzki[45], B.S. Stapf[109], S. Stapnes[121],
E.A. Starchenko[132], G.H. Stark[33], J. Stark[58], S.H Stark[39], P. Staroba[129], P. Starovoitov[60a],
S. Stärz[32], R. Staszewski[42], M. Stegler[45], P. Steinberg[27], B. Stelzer[144], H.J. Stelzer[32],
O. Stelzer-Chilton[163a], H. Stenzel[55], T.J. Stevenson[79], G.A. Stewart[56], M.C. Stockton[118],
M. Stoebe[90], G. Stoicea[28b], P. Stolte[57], S. Stonjek[103], A.R. Stradling[8], A. Straessner[47],
M.E. Stramaglia[18], J. Strandberg[149], S. Strandberg[148a,148b], M. Strauss[115], P. Strizenec[146b],
R. Ströhmer[177], D.M. Strom[118], R. Stroynowski[43], A. Strubig[49], S.A. Stucci[27], B. Stugu[15],

N.A. Styles[45], D. Su[145], J. Su[127], S. Suchek[60a], Y. Sugaya[120], M. Suk[130], V.V. Sulin[98],
DMS Sultan[162a,162b], S. Sultansoy[4c], T. Sumida[71], S. Sun[59], X. Sun[3], K. Suruliz[151],
C.J.E. Suster[152], M.R. Sutton[151], S. Suzuki[69], M. Svatos[129], M. Swiatlowski[33], S.P. Swift[2],
I. Sykora[146a], T. Sykora[131], D. Ta[51], K. Tackmann[45], J. Taenzer[155], A. Taffard[166],
R. Tafirout[163a], E. Tahirovic[79], N. Taiblum[155], H. Takai[27], R. Takashima[72], E.H. Takasugi[103],
K. Takeda[70], T. Takeshita[142], Y. Takubo[69], M. Talby[88], A.A. Talyshev[111,c], J. Tanaka[157],
M. Tanaka[159], R. Tanaka[119], S. Tanaka[69], R. Tanioka[70], B.B. Tannenwald[113], S. Tapia Araya[34b],
S. Tapprogge[86], S. Tarem[154], G.F. Tartarelli[94a], P. Tas[131], M. Tasevsky[129], T. Tashiro[71],
E. Tassi[40a,40b], A. Tavares Delgado[128a,128b], Y. Tayalati[137e], A.C. Taylor[107], A.J. Taylor[49],
G.N. Taylor[91], P.T.E. Taylor[91], W. Taylor[163b], P. Teixeira-Dias[80], D. Temple[144], H. Ten Kate[32],
P.K. Teng[153], J.J. Teoh[120], F. Tepel[178], S. Terada[69], K. Terashi[157], J. Terron[85], S. Terzo[13],
M. Testa[50], R.J. Teuscher[161,o], S.J. Thais[179], T. Theveneaux-Pelzer[88], F. Thiele[39],
J.P. Thomas[19], J. Thomas-Wilsker[80], P.D. Thompson[19], A.S. Thompson[56], L.A. Thomsen[179],
E. Thomson[124], Y. Tian[38], M.J. Tibbetts[16], R.E. Ticse Torres[57], V.O. Tikhomirov[98,ap],
Yu.A. Tikhonov[111,c], S. Timoshenko[100], P. Tipton[179], S. Tisserant[88], K. Todome[159],
S. Todorova-Nova[5], S. Todt[47], J. Tojo[73], S. Tokár[146a], K. Tokushuku[69], E. Tolley[113],
L. Tomlinson[87], M. Tomoto[105], L. Tompkins[145,aq], K. Toms[107], B. Tong[59], P. Tornambe[51],
E. Torrence[118], H. Torres[47], E. Torró Pastor[140], J. Toth[88,ar], F. Touchard[88], D.R. Tovey[141],
C.J. Treado[112], T. Trefzger[177], F. Tresoldi[151], A. Tricoli[27], I.M. Trigger[163a], S. Trincaz-Duvoid[83],
M.F. Tripiana[13], W. Trischuk[161], B. Trocmé[58], A. Trofymov[45], C. Troncon[94a],
M. Trottier-McDonald[16], M. Trovatelli[172], L. Truong[147b], M. Trzebinski[42], A. Trzupek[42],
K.W. Tsang[62a], J.C-L. Tseng[122], P.V. Tsiareshka[95], N. Tsirintanis[9], S. Tsiskaridze[13],
V. Tsiskaridze[51], E.G. Tskhadadze[54a], I.I. Tsukerman[99], V. Tsulaia[16], S. Tsuno[69],
D. Tsybychev[150], Y. Tu[62b], A. Tudorache[28b], V. Tudorache[28b], T.T. Tulbure[28a], A.N. Tuna[59],
S. Turchikhin[68], D. Turgeman[175], I. Turk Cakir[4b,as], R. Turra[94a], P.M. Tuts[38], G. Ucchielli[22a,22b],
I. Ueda[69], M. Ughetto[148a,148b], F. Ukegawa[164], G. Unal[32], A. Undrus[27], G. Unel[166],
F.C. Ungaro[91], Y. Unno[69], K. Uno[157], C. Unverdorben[102], J. Urban[146b], P. Urquijo[91],
P. Urrejola[86], G. Usai[8], J. Usui[69], L. Vacavant[88], V. Vacek[130], B. Vachon[90], K.O.H. Vadla[121],
A. Vaidya[81], C. Valderanis[102], E. Valdes Santurio[148a,148b], M. Valente[52], S. Valentinetti[22a,22b],
A. Valero[170], L. Valéry[13], S. Valkar[131], A. Vallier[5], J.A. Valls Ferrer[170],
W. Van Den Wollenberg[109], H. van der Graaf[109], P. van Gemmeren[6], J. Van Nieuwkoop[144],
I. van Vulpen[109], M.C. van Woerden[109], M. Vanadia[135a,135b], W. Vandelli[32], A. Vaniachine[160],
P. Vankov[109], G. Vardanyan[180], R. Vari[134a], E.W. Varnes[7], C. Varni[53a,53b], T. Varol[43],
D. Varouchas[119], A. Vartapetian[8], K.E. Varvell[152], J.G. Vasquez[179], G.A. Vasquez[34b],
F. Vazeille[37], D. Vazquez Furelos[13], T. Vazquez Schroeder[90], J. Veatch[57], V. Veeraraghavan[7],
L.M. Veloce[161], F. Veloso[128a,128c], S. Veneziano[134a], A. Ventura[76a,76b], M. Venturi[172],
N. Venturi[32], A. Venturini[25], V. Vercesi[123a], M. Verducci[136a,136b], W. Verkerke[109],
A.T. Vermeulen[109], J.C. Vermeulen[109], M.C. Vetterli[144,d], N. Viaux Maira[34b], O. Viazlo[84],
I. Vichou[169,*], T. Vickey[141], O.E. Vickey Boeriu[141], G.H.A. Viehhauser[122], S. Viel[16], L. Vigani[122],
M. Villa[22a,22b], M. Villaplana Perez[94a,94b], E. Vilucchi[50], M.G. Vincter[31], V.B. Vinogradov[68],
A. Vishwakarma[45], C. Vittori[22a,22b], I. Vivarelli[151], S. Vlachos[10], M. Vogel[178], P. Vokac[130],
G. Volpi[13], H. von der Schmitt[103], E. von Toerne[23], V. Vorobel[131], K. Vorobev[100], M. Vos[170],
R. Voss[32], J.H. Vossebeld[77], N. Vranjes[14], M. Vranjes Milosavljevic[14], V. Vrba[130],
M. Vreeswijk[109], R. Vuillermet[32], I. Vukotic[33], P. Wagner[23], W. Wagner[178], J. Wagner-Kuhr[102],
H. Wahlberg[74], S. Wahrmund[47], K. Wakamiya[70], J. Walder[75], R. Walker[102], W. Walkowiak[143],
V. Wallangen[148a,148b], C. Wang[35b], C. Wang[36b,at], F. Wang[176], H. Wang[16], H. Wang[3], J. Wang[45],
J. Wang[152], Q. Wang[115], R.-J. Wang[83], R. Wang[6], S.M. Wang[153], T. Wang[38], W. Wang[153,au],
W. Wang[36a,av], Z. Wang[36c], C. Wanotayaroj[45], A. Warburton[90], C.P. Ward[30], D.R. Wardrope[81],

A. Washbrook[49], P.M. Watkins[19], A.T. Watson[19], M.F. Watson[19], G. Watts[140], S. Watts[87], B.M. Waugh[81], A.F. Webb[11], S. Webb[86], M.S. Weber[18], S.M. Weber[60a], S.W. Weber[177], S.A. Weber[31], J.S. Webster[6], A.R. Weidberg[122], B. Weinert[64], J. Weingarten[57], M. Weirich[86], C. Weiser[51], H. Weits[109], P.S. Wells[32], T. Wenaus[27], T. Wengler[32], S. Wenig[32], N. Wermes[23], M.D. Werner[67], P. Werner[32], M. Wessels[60a], T.D. Weston[18], K. Whalen[118], N.L. Whallon[140], A.M. Wharton[75], A.S. White[92], A. White[8], M.J. White[1], R. White[34b], D. Whiteson[166], B.W. Whitmore[75], F.J. Wickens[133], W. Wiedenmann[176], M. Wielers[133], C. Wiglesworth[39], L.A.M. Wiik-Fuchs[51], A. Wildauer[103], F. Wilk[87], H.G. Wilkens[32], H.H. Williams[124], S. Williams[109], C. Willis[93], S. Willocq[89], J.A. Wilson[19], I. Wingerter-Seez[5], E. Winkels[151], F. Winklmeier[118], O.J. Winston[151], B.T. Winter[23], M. Wittgen[145], M. Wobisch[82,u], A. Wolf[86], T.M.H. Wolf[109], R. Wolff[88], M.W. Wolter[42], H. Wolters[128a,128c], V.W.S. Wong[171], N.L. Woods[139], S.D. Worm[19], B.K. Wosiek[42], J. Wotschack[32], K.W. Wozniak[42], M. Wu[33], S.L. Wu[176], X. Wu[52], Y. Wu[92], T.R. Wyatt[87], B.M. Wynne[49], S. Xella[39], Z. Xi[92], L. Xia[35c], D. Xu[35a], L. Xu[27], T. Xu[138], W. Xu[92], B. Yabsley[152], S. Yacoob[147a], D. Yamaguchi[159], Y. Yamaguchi[159], A. Yamamoto[69], S. Yamamoto[157], T. Yamanaka[157], F. Yamane[70], M. Yamatani[157], T. Yamazaki[157], Y. Yamazaki[70], Z. Yan[24], H. Yang[36c], H. Yang[16], Y. Yang[153], Z. Yang[15], W-M. Yao[16], Y.C. Yap[45], Y. Yasu[69], E. Yatsenko[5], K.H. Yau Wong[23], J. Ye[43], S. Ye[27], I. Yeletskikh[68], E. Yigitbasi[24], E. Yildirim[86], K. Yorita[174], K. Yoshihara[124], C. Young[145], C.J.S. Young[32], J. Yu[8], J. Yu[67], S.P.Y. Yuen[23], I. Yusuff[30,aw], B. Zabinski[42], G. Zacharis[10], R. Zaidan[13], A.M. Zaitsev[132,aj], N. Zakharchuk[45], J. Zalieckas[15], A. Zaman[150], S. Zambito[59], D. Zanzi[91], C. Zeitnitz[178], G. Zemaityte[122], A. Zemla[41a], J.C. Zeng[169], Q. Zeng[145], O. Zenin[132], T. Ženiš[146a], D. Zerwas[119], D. Zhang[36b], D. Zhang[92], F. Zhang[176], G. Zhang[36a,av], H. Zhang[119], J. Zhang[6], L. Zhang[51], L. Zhang[36a], M. Zhang[169], P. Zhang[35b], R. Zhang[23], R. Zhang[36a,at], X. Zhang[36b], Y. Zhang[35a,35d], Z. Zhang[119], X. Zhao[43], Y. Zhao[36b,ax], Z. Zhao[36a], A. Zhemchugov[68], B. Zhou[92], C. Zhou[176], L. Zhou[43], M. Zhou[35a,35d], M. Zhou[150], N. Zhou[36c], Y. Zhou[7], C.G. Zhu[36b], H. Zhu[35a], J. Zhu[92], Y. Zhu[36a], X. Zhuang[35a], K. Zhukov[98], A. Zibell[177], D. Zieminska[64], N.I. Zimine[68], C. Zimmermann[86], S. Zimmermann[51], Z. Zinonos[103], M. Zinser[86], M. Ziolkowski[143], L. Živković[14], G. Zobernig[176], A. Zoccoli[22a,22b], T.G. Zorbas[141], R. Zou[33], M. zur Nedden[17] and L. Zwalinski[32]

1 Department of Physics, University of Adelaide, Adelaide, Australia
2 Physics Department, SUNY Albany, Albany NY, United States of America
3 Department of Physics, University of Alberta, Edmonton AB, Canada
4 (a) Department of Physics, Ankara University, Ankara; (b) Istanbul Aydin University, Istanbul; (c) Division of Physics, TOBB University of Economics and Technology, Ankara, Turkey
5 LAPP, CNRS/IN2P3 and Université Savoie Mont Blanc, Annecy-le-Vieux, France
6 High Energy Physics Division, Argonne National Laboratory, Argonne IL, United States of America
7 Department of Physics, University of Arizona, Tucson AZ, United States of America
8 Department of Physics, The University of Texas at Arlington, Arlington TX, United States of America
9 Physics Department, National and Kapodistrian University of Athens, Athens, Greece
10 Physics Department, National Technical University of Athens, Zografou, Greece
11 Department of Physics, The University of Texas at Austin, Austin TX, United States of America
12 Institute of Physics, Azerbaijan Academy of Sciences, Baku, Azerbaijan
13 Institut de Física d'Altes Energies (IFAE), The Barcelona Institute of Science and Technology, Barcelona, Spain
14 Institute of Physics, University of Belgrade, Belgrade, Serbia
15 Department for Physics and Technology, University of Bergen, Bergen, Norway
16 Physics Division, Lawrence Berkeley National Laboratory and University of California, Berkeley CA, United States of America

[17] *Department of Physics, Humboldt University, Berlin, Germany*

[18] *Albert Einstein Center for Fundamental Physics and Laboratory for High Energy Physics, University of Bern, Bern, Switzerland*

[19] *School of Physics and Astronomy, University of Birmingham, Birmingham, United Kingdom*

[20] [a] *Department of Physics, Bogazici University, Istanbul;* [b] *Department of Physics Engineering, Gaziantep University, Gaziantep;* [d] *Istanbul Bilgi University, Faculty of Engineering and Natural Sciences, Istanbul;* [e] *Bahcesehir University, Faculty of Engineering and Natural Sciences, Istanbul, Turkey*

[21] *Centro de Investigaciones, Universidad Antonio Narino, Bogota, Colombia*

[22] [a] *INFN Sezione di Bologna;* [b] *Dipartimento di Fisica e Astronomia, Università di Bologna, Bologna, Italy*

[23] *Physikalisches Institut, University of Bonn, Bonn, Germany*

[24] *Department of Physics, Boston University, Boston MA, United States of America*

[25] *Department of Physics, Brandeis University, Waltham MA, United States of America*

[26] [a] *Universidade Federal do Rio De Janeiro COPPE/EE/IF, Rio de Janeiro;* [b] *Electrical Circuits Department, Federal University of Juiz de Fora (UFJF), Juiz de Fora;* [c] *Federal University of Sao Joao del Rei (UFSJ), Sao Joao del Rei;* [d] *Instituto de Fisica, Universidade de Sao Paulo, Sao Paulo, Brazil*

[27] *Physics Department, Brookhaven National Laboratory, Upton NY, United States of America*

[28] [a] *Transilvania University of Brasov, Brasov;* [b] *Horia Hulubei National Institute of Physics and Nuclear Engineering, Bucharest;* [c] *Department of Physics, Alexandru Ioan Cuza University of Iasi, Iasi;* [d] *National Institute for Research and Development of Isotopic and Molecular Technologies, Physics Department, Cluj Napoca;* [e] *University Politehnica Bucharest, Bucharest;* [f] *West University in Timisoara, Timisoara, Romania*

[29] *Departamento de Física, Universidad de Buenos Aires, Buenos Aires, Argentina*

[30] *Cavendish Laboratory, University of Cambridge, Cambridge, United Kingdom*

[31] *Department of Physics, Carleton University, Ottawa ON, Canada*

[32] *CERN, Geneva, Switzerland*

[33] *Enrico Fermi Institute, University of Chicago, Chicago IL, United States of America*

[34] [a] *Departamento de Física, Pontificia Universidad Católica de Chile, Santiago;* [b] *Departamento de Física, Universidad Técnica Federico Santa María, Valparaíso, Chile*

[35] [a] *Institute of High Energy Physics, Chinese Academy of Sciences, Beijing;* [b] *Department of Physics, Nanjing University, Jiangsu;* [c] *Physics Department, Tsinghua University, Beijing 100084;* [d] *University of Chinese Academy of Science (UCAS), Beijing, China*

[36] [a] *Department of Modern Physics and State Key Laboratory of Particle Detection and Electronics, University of Science and Technology of China, Anhui;* [b] *School of Physics, Shandong University, Shandong;* [c] *Department of Physics and Astronomy, Key Laboratory for Particle Physics, Astrophysics and Cosmology, Ministry of Education; Shanghai Key Laboratory for Particle Physics and Cosmology, Shanghai Jiao Tong University, Tsung-Dao Lee Institute, China*

[37] *Université Clermont Auvergne, CNRS/IN2P3, LPC, Clermont-Ferrand, France*

[38] *Nevis Laboratory, Columbia University, Irvington NY, United States of America*

[39] *Niels Bohr Institute, University of Copenhagen, Kobenhavn, Denmark*

[40] [a] *INFN Gruppo Collegato di Cosenza, Laboratori Nazionali di Frascati;* [b] *Dipartimento di Fisica, Università della Calabria, Rende, Italy*

[41] [a] *AGH University of Science and Technology, Faculty of Physics and Applied Computer Science, Krakow;* [b] *Marian Smoluchowski Institute of Physics, Jagiellonian University, Krakow, Poland*

[42] *Institute of Nuclear Physics Polish Academy of Sciences, Krakow, Poland*

[43] *Physics Department, Southern Methodist University, Dallas TX, United States of America*

[44] *Physics Department, University of Texas at Dallas, Richardson TX, United States of America*

[45] *DESY, Hamburg and Zeuthen, Germany*

[46] *Lehrstuhl für Experimentelle Physik IV, Technische Universität Dortmund, Dortmund, Germany*

[47] *Institut für Kern- und Teilchenphysik, Technische Universität Dresden, Dresden, Germany*

[48] *Department of Physics, Duke University, Durham NC, United States of America*

[49] *SUPA - School of Physics and Astronomy, University of Edinburgh, Edinburgh, United Kingdom*

[50] *INFN e Laboratori Nazionali di Frascati, Frascati, Italy*

[51] *Fakultät für Mathematik und Physik, Albert-Ludwigs-Universität, Freiburg, Germany*

[52] *Departement de Physique Nucleaire et Corpusculaire, Université de Genève, Geneva, Switzerland*

[53] *[a] INFN Sezione di Genova; [b] Dipartimento di Fisica, Università di Genova, Genova, Italy*

[54] *[a] E. Andronikashvili Institute of Physics, Iv. Javakhishvili Tbilisi State University, Tbilisi; [b] High Energy Physics Institute, Tbilisi State University, Tbilisi, Georgia*

[55] *II Physikalisches Institut, Justus-Liebig-Universität Giessen, Giessen, Germany*

[56] *SUPA - School of Physics and Astronomy, University of Glasgow, Glasgow, United Kingdom*

[57] *II Physikalisches Institut, Georg-August-Universität, Göttingen, Germany*

[58] *Laboratoire de Physique Subatomique et de Cosmologie, Université Grenoble-Alpes, CNRS/IN2P3, Grenoble, France*

[59] *Laboratory for Particle Physics and Cosmology, Harvard University, Cambridge MA, United States of America*

[60] *[a] Kirchhoff-Institut für Physik, Ruprecht-Karls-Universität Heidelberg, Heidelberg; [b] Physikalisches Institut, Ruprecht-Karls-Universität Heidelberg, Heidelberg, Germany*

[61] *Faculty of Applied Information Science, Hiroshima Institute of Technology, Hiroshima, Japan*

[62] *[a] Department of Physics, The Chinese University of Hong Kong, Shatin, N.T., Hong Kong; [b] Department of Physics, The University of Hong Kong, Hong Kong; [c] Department of Physics and Institute for Advanced Study, The Hong Kong University of Science and Technology, Clear Water Bay, Kowloon, Hong Kong, China*

[63] *Department of Physics, National Tsing Hua University, Taiwan, Taiwan*

[64] *Department of Physics, Indiana University, Bloomington IN, United States of America*

[65] *Institut für Astro- und Teilchenphysik, Leopold-Franzens-Universität, Innsbruck, Austria*

[66] *University of Iowa, Iowa City IA, United States of America*

[67] *Department of Physics and Astronomy, Iowa State University, Ames IA, United States of America*

[68] *Joint Institute for Nuclear Research, JINR Dubna, Dubna, Russia*

[69] *KEK, High Energy Accelerator Research Organization, Tsukuba, Japan*

[70] *Graduate School of Science, Kobe University, Kobe, Japan*

[71] *Faculty of Science, Kyoto University, Kyoto, Japan*

[72] *Kyoto University of Education, Kyoto, Japan*

[73] *Research Center for Advanced Particle Physics and Department of Physics, Kyushu University, Fukuoka, Japan*

[74] *Instituto de Física La Plata, Universidad Nacional de La Plata and CONICET, La Plata, Argentina*

[75] *Physics Department, Lancaster University, Lancaster, United Kingdom*

[76] *[a] INFN Sezione di Lecce; [b] Dipartimento di Matematica e Fisica, Università del Salento, Lecce, Italy*

[77] *Oliver Lodge Laboratory, University of Liverpool, Liverpool, United Kingdom*

[78] *Department of Experimental Particle Physics, Jožef Stefan Institute and Department of Physics, University of Ljubljana, Ljubljana, Slovenia*

[79] *School of Physics and Astronomy, Queen Mary University of London, London, United Kingdom*

[80] *Department of Physics, Royal Holloway University of London, Surrey, United Kingdom*

[81] *Department of Physics and Astronomy, University College London, London, United Kingdom*

[82] *Louisiana Tech University, Ruston LA, United States of America*

[83] *Laboratoire de Physique Nucléaire et de Hautes Energies, UPMC and Université Paris-Diderot and CNRS/IN2P3, Paris, France*

[84] *Fysiska institutionen, Lunds universitet, Lund, Sweden*

[85] *Departamento de Fisica Teorica C-15, Universidad Autonoma de Madrid, Madrid, Spain*

[86] *Institut für Physik, Universität Mainz, Mainz, Germany*

[87] *School of Physics and Astronomy, University of Manchester, Manchester, United Kingdom*

[88] *CPPM, Aix-Marseille Université and CNRS/IN2P3, Marseille, France*

89   *Department of Physics, University of Massachusetts, Amherst MA, United States of America*

90   *Department of Physics, McGill University, Montreal QC, Canada*

91   *School of Physics, University of Melbourne, Victoria, Australia*

92   *Department of Physics, The University of Michigan, Ann Arbor MI, United States of America*

93   *Department of Physics and Astronomy, Michigan State University, East Lansing MI, United States of America*

94   *[a] INFN Sezione di Milano; [b] Dipartimento di Fisica, Università di Milano, Milano, Italy*

95   *B.I. Stepanov Institute of Physics, National Academy of Sciences of Belarus, Minsk, Republic of Belarus*

96   *Research Institute for Nuclear Problems of Byelorussian State University, Minsk, Republic of Belarus*

97   *Group of Particle Physics, University of Montreal, Montreal QC, Canada*

98   *P.N. Lebedev Physical Institute of the Russian Academy of Sciences, Moscow, Russia*

99   *Institute for Theoretical and Experimental Physics (ITEP), Moscow, Russia*

100   *National Research Nuclear University MEPhI, Moscow, Russia*

101   *D.V. Skobeltsyn Institute of Nuclear Physics, M.V. Lomonosov Moscow State University, Moscow, Russia*

102   *Fakultät für Physik, Ludwig-Maximilians-Universität München, München, Germany*

103   *Max-Planck-Institut für Physik (Werner-Heisenberg-Institut), München, Germany*

104   *Nagasaki Institute of Applied Science, Nagasaki, Japan*

105   *Graduate School of Science and Kobayashi-Maskawa Institute, Nagoya University, Nagoya, Japan*

106   *[a] INFN Sezione di Napoli; [b] Dipartimento di Fisica, Università di Napoli, Napoli, Italy*

107   *Department of Physics and Astronomy, University of New Mexico, Albuquerque NM, United States of America*

108   *Institute for Mathematics, Astrophysics and Particle Physics, Radboud University Nijmegen/Nikhef, Nijmegen, Netherlands*

109   *Nikhef National Institute for Subatomic Physics and University of Amsterdam, Amsterdam, Netherlands*

110   *Department of Physics, Northern Illinois University, DeKalb IL, United States of America*

111   *Budker Institute of Nuclear Physics, SB RAS, Novosibirsk, Russia*

112   *Department of Physics, New York University, New York NY, United States of America*

113   *Ohio State University, Columbus OH, United States of America*

114   *Faculty of Science, Okayama University, Okayama, Japan*

115   *Homer L. Dodge Department of Physics and Astronomy, University of Oklahoma, Norman OK, United States of America*

116   *Department of Physics, Oklahoma State University, Stillwater OK, United States of America*

117   *Palacký University, RCPTM, Olomouc, Czech Republic*

118   *Center for High Energy Physics, University of Oregon, Eugene OR, United States of America*

119   *LAL, Univ. Paris-Sud, CNRS/IN2P3, Université Paris-Saclay, Orsay, France*

120   *Graduate School of Science, Osaka University, Osaka, Japan*

121   *Department of Physics, University of Oslo, Oslo, Norway*

122   *Department of Physics, Oxford University, Oxford, United Kingdom*

123   *[a] INFN Sezione di Pavia; [b] Dipartimento di Fisica, Università di Pavia, Pavia, Italy*

124   *Department of Physics, University of Pennsylvania, Philadelphia PA, United States of America*

125   *National Research Centre "Kurchatov Institute" B.P.Konstantinov Petersburg Nuclear Physics Institute, St. Petersburg, Russia*

126   *[a] INFN Sezione di Pisa; [b] Dipartimento di Fisica E. Fermi, Università di Pisa, Pisa, Italy*

127   *Department of Physics and Astronomy, University of Pittsburgh, Pittsburgh PA, United States of America*

128   *[a] Laboratório de Instrumentação e Física Experimental de Partículas - LIP, Lisboa; [b] Faculdade de Ciências, Universidade de Lisboa, Lisboa; [c] Department of Physics, University of Coimbra, Coimbra; [d] Centro de Física Nuclear da Universidade de Lisboa, Lisboa; [e] Departamento de*

Fisica, Universidade do Minho, Braga; ^(f) Departamento de Fisica Teorica y del Cosmos, Universidad de Granada, Granada; ^(g) Dep Fisica and CEFITEC of Faculdade de Ciencias e Tecnologia, Universidade Nova de Lisboa, Caparica, Portugal

129   *Institute of Physics, Academy of Sciences of the Czech Republic, Praha, Czech Republic*

130   *Czech Technical University in Prague, Praha, Czech Republic*

131   *Charles University, Faculty of Mathematics and Physics, Prague, Czech Republic*

132   *State Research Center Institute for High Energy Physics (Protvino), NRC KI, Russia*

133   *Particle Physics Department, Rutherford Appleton Laboratory, Didcot, United Kingdom*

134   ^(a) *INFN Sezione di Roma;* ^(b) *Dipartimento di Fisica, Sapienza Università di Roma, Roma, Italy*

135   ^(a) *INFN Sezione di Roma Tor Vergata;* ^(b) *Dipartimento di Fisica, Università di Roma Tor Vergata, Roma, Italy*

136   ^(a) *INFN Sezione di Roma Tre;* ^(b) *Dipartimento di Matematica e Fisica, Università Roma Tre, Roma, Italy*

137   ^(a) *Faculté des Sciences Ain Chock, Réseau Universitaire de Physique des Hautes Energies - Université Hassan II, Casablanca;* ^(b) *Centre National de l'Energie des Sciences Techniques Nucleaires, Rabat;* ^(c) *Faculté des Sciences Semlalia, Université Cadi Ayyad, LPHEA-Marrakech;* ^(d) *Faculté des Sciences, Université Mohamed Premier and LPTPM, Oujda;* ^(e) *Faculté des sciences, Université Mohammed V, Rabat, Morocco*

138   *DSM/IRFU (Institut de Recherches sur les Lois Fondamentales de l'Univers), CEA Saclay (Commissariat à l'Energie Atomique et aux Energies Alternatives), Gif-sur-Yvette, France*

139   *Santa Cruz Institute for Particle Physics, University of California Santa Cruz, Santa Cruz CA, United States of America*

140   *Department of Physics, University of Washington, Seattle WA, United States of America*

141   *Department of Physics and Astronomy, University of Sheffield, Sheffield, United Kingdom*

142   *Department of Physics, Shinshu University, Nagano, Japan*

143   *Department Physik, Universität Siegen, Siegen, Germany*

144   *Department of Physics, Simon Fraser University, Burnaby BC, Canada*

145   *SLAC National Accelerator Laboratory, Stanford CA, United States of America*

146   ^(a) *Faculty of Mathematics, Physics & Informatics, Comenius University, Bratislava;* ^(b) *Department of Subnuclear Physics, Institute of Experimental Physics of the Slovak Academy of Sciences, Kosice, Slovak Republic*

147   ^(a) *Department of Physics, University of Cape Town, Cape Town;* ^(b) *Department of Physics, University of Johannesburg, Johannesburg;* ^(c) *School of Physics, University of the Witwatersrand, Johannesburg, South Africa*

148   ^(a) *Department of Physics, Stockholm University;* ^(b) *The Oskar Klein Centre, Stockholm, Sweden*

149   *Physics Department, Royal Institute of Technology, Stockholm, Sweden*

150   *Departments of Physics & Astronomy and Chemistry, Stony Brook University, Stony Brook NY, United States of America*

151   *Department of Physics and Astronomy, University of Sussex, Brighton, United Kingdom*

152   *School of Physics, University of Sydney, Sydney, Australia*

153   *Institute of Physics, Academia Sinica, Taipei, Taiwan*

154   *Department of Physics, Technion: Israel Institute of Technology, Haifa, Israel*

155   *Raymond and Beverly Sackler School of Physics and Astronomy, Tel Aviv University, Tel Aviv, Israel*

156   *Department of Physics, Aristotle University of Thessaloniki, Thessaloniki, Greece*

157   *International Center for Elementary Particle Physics and Department of Physics, The University of Tokyo, Tokyo, Japan*

158   *Graduate School of Science and Technology, Tokyo Metropolitan University, Tokyo, Japan*

159   *Department of Physics, Tokyo Institute of Technology, Tokyo, Japan*

160   *Tomsk State University, Tomsk, Russia*

161   *Department of Physics, University of Toronto, Toronto ON, Canada*

162   ^(a) *INFN-TIFPA;* ^(b) *University of Trento, Trento, Italy*

163 (a) *TRIUMF, Vancouver BC;* (b) *Department of Physics and Astronomy, York University, Toronto ON, Canada*

164 *Faculty of Pure and Applied Sciences, and Center for Integrated Research in Fundamental Science and Engineering, University of Tsukuba, Tsukuba, Japan*

165 *Department of Physics and Astronomy, Tufts University, Medford MA, United States of America*

166 *Department of Physics and Astronomy, University of California Irvine, Irvine CA, United States of America*

167 (a) *INFN Gruppo Collegato di Udine, Sezione di Trieste, Udine;* (b) *ICTP, Trieste;* (c) *Dipartimento di Chimica, Fisica e Ambiente, Università di Udine, Udine, Italy*

168 *Department of Physics and Astronomy, University of Uppsala, Uppsala, Sweden*

169 *Department of Physics, University of Illinois, Urbana IL, United States of America*

170 *Instituto de Fisica Corpuscular (IFIC), Centro Mixto Universidad de Valencia - CSIC, Spain*

171 *Department of Physics, University of British Columbia, Vancouver BC, Canada*

172 *Department of Physics and Astronomy, University of Victoria, Victoria BC, Canada*

173 *Department of Physics, University of Warwick, Coventry, United Kingdom*

174 *Waseda University, Tokyo, Japan*

175 *Department of Particle Physics, The Weizmann Institute of Science, Rehovot, Israel*

176 *Department of Physics, University of Wisconsin, Madison WI, United States of America*

177 *Fakultät für Physik und Astronomie, Julius-Maximilians-Universität, Würzburg, Germany*

178 *Fakultät für Mathematik und Naturwissenschaften, Fachgruppe Physik, Bergische Universität Wuppertal, Wuppertal, Germany*

179 *Department of Physics, Yale University, New Haven CT, United States of America*

180 *Yerevan Physics Institute, Yerevan, Armenia*

181 *Centre de Calcul de l'Institut National de Physique Nucléaire et de Physique des Particules (IN2P3), Villeurbanne, France*

182 *Academia Sinica Grid Computing, Institute of Physics, Academia Sinica, Taipei, Taiwan*

a *Also at Department of Physics, King's College London, London, United Kingdom*

b *Also at Institute of Physics, Azerbaijan Academy of Sciences, Baku, Azerbaijan*

c *Also at Novosibirsk State University, Novosibirsk, Russia*

d *Also at TRIUMF, Vancouver BC, Canada*

e *Also at Department of Physics & Astronomy, University of Louisville, Louisville, KY, United States of America*

f *Also at Physics Department, An-Najah National University, Nablus, Palestine*

g *Also at Department of Physics, California State University, Fresno CA, United States of America*

h *Also at Department of Physics, University of Fribourg, Fribourg, Switzerland*

i *Also at II Physikalisches Institut, Georg-August-Universität, Göttingen, Germany*

j *Also at Departament de Fisica de la Universitat Autonoma de Barcelona, Barcelona, Spain*

k *Also at Departamento de Fisica e Astronomia, Faculdade de Ciencias, Universidade do Porto, Portugal*

l *Also at Tomsk State University, Tomsk, and Moscow Institute of Physics and Technology State University, Dolgoprudny, Russia*

m *Also at The Collaborative Innovation Center of Quantum Matter (CICQM), Beijing, China*

n *Also at Universita di Napoli Parthenope, Napoli, Italy*

o *Also at Institute of Particle Physics (IPP), Canada*

p *Also at Horia Hulubei National Institute of Physics and Nuclear Engineering, Bucharest, Romania*

q *Also at Department of Physics, St. Petersburg State Polytechnical University, St. Petersburg, Russia*

r *Also at Borough of Manhattan Community College, City University of New York, New York City, United States of America*

s *Also at Department of Financial and Management Engineering, University of the Aegean, Chios, Greece*

[t] Also at Centre for High Performance Computing, CSIR Campus, Rosebank, Cape Town, South Africa

[u] Also at Louisiana Tech University, Ruston LA, United States of America

[v] Also at Institucio Catalana de Recerca i Estudis Avancats, ICREA, Barcelona, Spain

[w] Also at Department of Physics, The University of Michigan, Ann Arbor MI, United States of America

[x] Also at Graduate School of Science, Osaka University, Osaka, Japan

[y] Also at Fakultät für Mathematik und Physik, Albert-Ludwigs-Universität, Freiburg, Germany

[z] Also at Institute for Mathematics, Astrophysics and Particle Physics, Radboud University Nijmegen/Nikhef, Nijmegen, Netherlands

[aa] Also at Department of Physics, The University of Texas at Austin, Austin TX, United States of America

[ab] Also at Institute of Theoretical Physics, Ilia State University, Tbilisi, Georgia

[ac] Also at CERN, Geneva, Switzerland

[ad] Also at Georgian Technical University (GTU),Tbilisi, Georgia

[ae] Also at Ochadai Academic Production, Ochanomizu University, Tokyo, Japan

[af] Also at Manhattan College, New York NY, United States of America

[ag] Also at The City College of New York, New York NY, United States of America

[ah] Also at Departamento de Fisica Teorica y del Cosmos, Universidad de Granada, Granada, Portugal

[ai] Also at Department of Physics, California State University, Sacramento CA, United States of America

[aj] Also at Moscow Institute of Physics and Technology State University, Dolgoprudny, Russia

[ak] Also at Departement de Physique Nucleaire et Corpusculaire, Université de Genève, Geneva, Switzerland

[al] Also at Institut de Física d'Altes Energies (IFAE), The Barcelona Institute of Science and Technology, Barcelona, Spain

[am] Also at School of Physics, Sun Yat-sen University, Guangzhou, China

[an] Also at Institute for Nuclear Research and Nuclear Energy (INRNE) of the Bulgarian Academy of Sciences, Sofia, Bulgaria

[ao] Also at Faculty of Physics, M.V.Lomonosov Moscow State University, Moscow, Russia

[ap] Also at National Research Nuclear University MEPhI, Moscow, Russia

[aq] Also at Department of Physics, Stanford University, Stanford CA, United States of America

[ar] Also at Institute for Particle and Nuclear Physics, Wigner Research Centre for Physics, Budapest, Hungary

[as] Also at Giresun University, Faculty of Engineering, Turkey

[at] Also at CPPM, Aix-Marseille Université and CNRS/IN2P3, Marseille, France

[au] Also at Department of Physics, Nanjing University, Jiangsu, China

[av] Also at Institute of Physics, Academia Sinica, Taipei, Taiwan

[aw] Also at University of Malaya, Department of Physics, Kuala Lumpur, Malaysia

[ax] Also at LAL, Univ. Paris-Sud, CNRS/IN2P3, Université Paris-Saclay, Orsay, France

[*] Deceased